Climate Classification Preprocessing Algorithm

by

Nicole Latrice Campbell

A dissertation submitted in partial fulfillment
of the requirements for the degree of
Doctor of Philosophy
(Applied Physics)
in The University of Michigan
2012

Doctorial Committee:
Professor Marc Ross, Chairman
Professor Roy Clarke
Professor Jennifer Jamison, University of Arkansas
Professor Jean Krisch
Melvin Williams Jr., Associate Deputy Secretary of the US Department of Energy

---

“I shall be telling this with a sigh somewhere ages and ages hence: Two roads diverged in a wood, and I— I took the one less traveled by, And that has made all the difference.”
--- Robert Frost

“Triumph is born out of struggle. Faith is the alchemist. If you want to paint portraits of victory you have to use some dark colors.”
--- God, Portrayed by Morgan Freeman in the film Bruce Almighty

“I hate how God makes me a success when I deserved to fail then I try to repay him but he cancels my debt & accepts only the sacrifice of praise which is a small price to pay for all that I owe.”---Author unknown

“Our deepest fear is not that we are inadequate.
Our deepest fear is that we are powerful beyond measure.
It is our light, not our darkness that frightens us most.
We ask ourselves, 'Who am I to be brilliant, gorgeous, talented, and famous?'
Actually, who are you not to be?
You are a child of God. Your playing small does not serve the world.
We were born to make manifest the glory of God that is within us.
It's not just in some of us; it's in all of us.
And when we let our own light shine,
we unconsciously give other people permission to do the same.
As we are liberated from our own fear, our presence automatically liberates others.”
---Nelson Mandela in his 1994 Inaugural Speech

For
My Mother Shirley M. Williams-Jones and Stepfather Roger Jones
Sisters Melody Williams-Bussey and Jacqueline Williams
Brother Anthony Williams
My Aunts: Ola Mae Tennant, Mary Lou Hayes, Charlene Williams, DeWanda Gail Anderson, Shirley Williams and Daisy Harris,
My Uncles: Ray Williams, Jr., Wesley Williams, Kenneth Lane Moore, Henry Williams, and Jimmy Lee Brown,
My Professors and Mentors: Professor L. D. Swift, Professor Charles Vincent Smith, Professor Ron Carter, Professor Joan Reinhardt, Professor Abigail Reid Mechtenburg, Professor Marc Ross
And finally to my 8^{th} and 9^{th} grade Math teacher, Mr. Thomas Ngar

Table of Contents

LIST OF TABLES

LIST OF FIGURES

LIST OF APPENDICES

ABSTRACT

Remote sensing has numerous applications in the fields of defense, medical imaging and environmental research. The Climate Classification Preprocessing algorithm (CPA) combines the areas of remote sensing, data mining and climate research in the development of a neural fuzzy-logic algorithm. CPA identifies atmospheric targets utilizing data from the Atmospheric Radiation and Measurement Program (ARM) Tropical Western Pacific site (TWP) without using computational global model data. CPA is a true multi-sensor data mining algorithm that provides key preprocessing figures and graphs necessary to climate research.

This research explores multi-sensor responses to random and/or complex atmospheric targets. Through the utilization of CPA, the classification of atmospheric target properties at the ARM observation sites in the TWP is performed through the process of data mining. Data mining is the process of finding patterns or relationships in large data sets. CPA provides and/or identifies reflectivity, velocity and spectral width diagrams, Contour Frequency by Altitude Diagrams (M-CFAD), condensed water content, and mapping of the data on the same time height grid as the radar by utilization of multiple instruments, which results in the graphical classification of atmospheric targets at the ARM TWP site. Consequently, a fully robust classifier for targets based on several dif-

ferent instruments at the TWP site is achieved with an error rate between 3-10 %. CPA is the first step in achieving one of ARM's long term goals for the program.

Since CPA is a robust atmospheric phase classifier, the algorithm has possible applications such as utilization of the algorithm for possible tracking of insects particularly mosquitoes to track the spread of West Nile Virus and Malaria. Future Research in this area includes the possibility of creating a true multi-retrieval algorithm with CPA at the core of the multi-retrieval algorithm, as well as altering CPA to be a genetic optimization algorithm.

.

CHAPTER I:

Introduction

In 2011, *Science* dedicated an entire special edition issue to the "Dealing with Data". In the issue the importance, relevance and difficulty of the utilization of large data sets is explored across various fields. This dissertation encompasses the development of a data mining algorithm, known as the Climate Classification Preprocessing Algorithm (CPA). Data mining can be defined as a process of utilizing a large sum of data for patterns of recognition. In the case of CPA, the patterns of recognition are the classification of ice, supercooled droplets, drizzle/rain, liquid droplets, insects, melting ice and other particulates or targets found in the atmosphere [1, 2].

The advancement of the application and development of retrieval algorithms, the parameterization of clouds, particulates, hydrometers, and other atmospheric targets is one of the chief goals of the Department of Energy's Atmospheric Radiation and Measurement program (ARM). By developing CPA this dissertation is the first step in creating a multi-retrieval algorithm, which is a long term aspiration of the ARM program. In addition, an objective of this research is to make multi-sensor data utilization convenient for the climate physics scientific community. To that end, an analysis of data provided by the ARM Tropical Western Pacific site (TWP) is performed.

Typically, when research scientists attempt to identify targets in the atmosphere they utilize one frequency of radar and one frequency of lidar data. Though this method is an efficient method for identifying targets in the atmosphere, there are several frequencies of radars, lidars and other instrumentation that can be utilized to identify targets in the atmosphere. The difficulties involved in utilizing several different instruments are numerous. The first difficulty in utilizing data from all relevant instruments is that the data for each instrument has its own time-height grid, and different units. Second, the

amount of data quickly becomes enormous which can complicate manipulation of data. Third, all of the instruments are not utilized at the same time. Fourth, instrument sensitivity must be tracked and accounted. CPA performs multi-sensor analysis by utilizing the data from millimeter cloud radars, micropulse lidar, radar wind profilers, radiosondes and various other relevant instruments at the ARM TWP sites.

CPA produces reflectivity, velocity and spectral width graphs along with the corresponding distribution graphs, modified contour frequency by altitude diagrams (M-CFAD)for user defined periods of time and the condensed water content graphs for the TWP. By utilizing neural fuzzy-logic and multiple instrumentation data classification of ice, supercooled droplets, drizzle/rain, liquid droplets, melting and other particulates or targets found in the atmosphere, CPA is the first step in the creation of a multi-retrieval algorithm. CPA provides a truly robust classification algorithm. CPA advances the field of climate physics research by first analyzing multi-sensor data to identify atmospheric targets in the TWP as well as enabling the utilization of multi-sensor data.

Clouds are controlled by diverse dynamics involving dissimilar microphysical properties, resulting in singular radiative properties. Climate changes can result in shifting frequency and changing characteristics of clouds. These transformations clarify the influence of clouds in the energy cycles. Unless climatic models efficiently embody the processes and feedbacks of diverse cloud types, the climate physics community will continue facing obstacles that will interfere with accurate predictions of future climate changes. Categorizing atmospheric targets into class types is a crucial undertaking in remote sensing of atmospheric targets and the study of global cloud climatology. One of the objectives of this research is to improve climate circulation models, application of

retrieval algorithms and the parameterization of clouds. To that end, an analysis of the data provided by the Tropical Western Pacific (TWP) Atmospheric Radiation Measurement (ARM) located off the coast of Papua New Guinea is performed. In addition, this project improves parameterization of several atmospheric cloud types and improves the description of their characteristics. This is achieved by comparing several measurements including doppler velocity, spectral width, reflectivity, modified contour frequency by altitude diagrams (CFAD), and the condensed water content. The classification states being utilized are Clear Sky, Warm Cloud, Warm Precipitation, Melting, Super Cooled Liquid, Ice, Ice and supercooled droplets, melting ice, drizzle and/or heavy rain, cloud droplets and/or precipitation, etc. The frequency distribution of each class is also demonstrated. The data will also be analyzed for any new identification markers of cloud or atmospheric target types. The results can be applied towards future development of a product that will seamlessly transition from one retrieval algorithm to another based on a given condition, thereby fulfilling one the long term goals of the ARM program.

Why Study the Climate?

The Tropical Western Pacific site (TWP) was instituted in 1996, consisting of the three locations, shown in Figure 1. The locations are the Manus facility in Negros Island of Papua New Guinea; the facility on Nauru Island, and the Darwin facility in Australia. The locality of these three sites encompasses an expanse that has a significant function in the inter-annual variability of the global climate. Moreover, the area boasts the warmest surface temperatures in the Pacific. This warm body of water provides moisture and heat to the atmosphere causing the deep atmospheric convection that produces high altitude

cirrus clouds. These cirrus clouds have a direct effect on the amount of solar energy entering and exiting the earth's surface. These facilities collect atmospheric data continuously. The data collected aids in recognition of the relationships between clouds and energy. It will be used to improve the circulation models in the climate study, and ultimately used to improve broad circulation models used in climate studies [3, 4, 5, 6, 7].

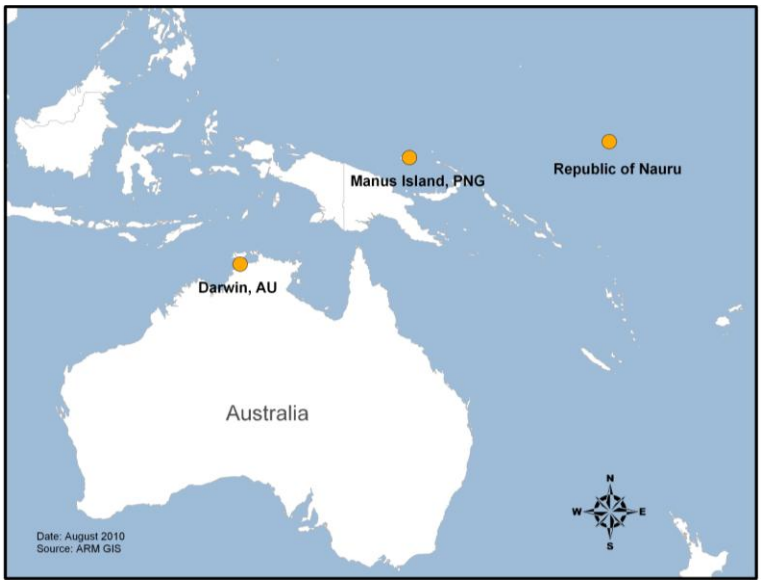

Figure 1: Darwin, Australia, Manus Island and Nauru Island comprise the ARM Tropical Western Pacific site. These locations were chosen because of their warm sea temperatures, high rain rates, atmospheric convection and strong coupling between the atmosphere and the ocean [3].

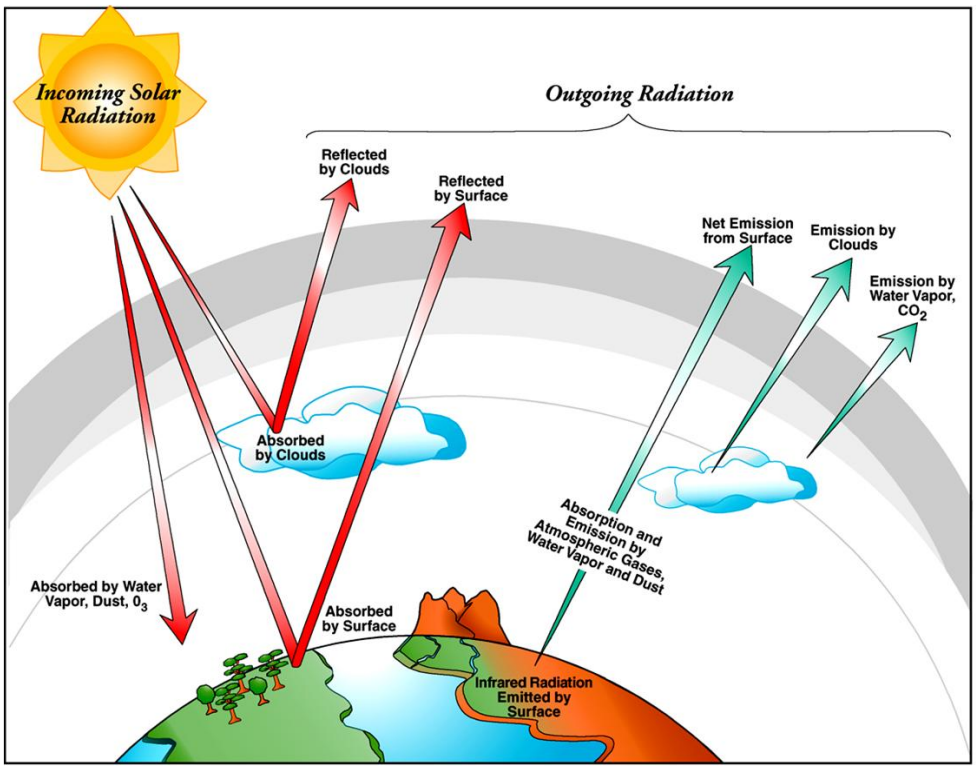

Figure 2: This a figure of the earth's radiative budget which is directly affected by the production of high altitude cirrus clouds in the Tropical Western Pacific (TWP) Atmospheric Radiation and Measurement Program(ARM) sites. An increase in high altitude cirrus clouds, as a result of deep convection in the region, prevents solar energy from leaving the earth and prevents solar energy from entering the earth [8].

Figure 2 shows the earth's radiative budget. The radiative budget is directly affected by the production of high altitude cirrus clouds in the TWP. An increase in high altitude clouds results in solar radiation being prevented from leaving the earth. Conversely, the high altitude cirrus clouds prevent solar energy from leaving the earth. Radiation emitted from the sun is absorbed by water vapor, dust, O_3 O_3,the earth's surface, and by clouds. The Earth then emits infrared radiation which is absorbed and emitted by atmospheric gases, water vapor and dust. The increase in the atmospheric clouds in the TWP region prevents the radiation from leaving the atmosphere.

Figure 3 shows the effect of the .2°C to 1°C temperature differences that occur in the Pacific Ocean. This figure demonstrates the effect of deep mixing of the ocean near

Antarctica. These changes in temperature reveal the global warming resulting from greenhouse gases in the second half of the 20th Century. This is a three dimensional representation of the rise in temperature of the ocean warming due to global warming. Moreover, the year 1998 had the highest temperatures in a thousand years. [9, 3, 10, 11, 6, 110].

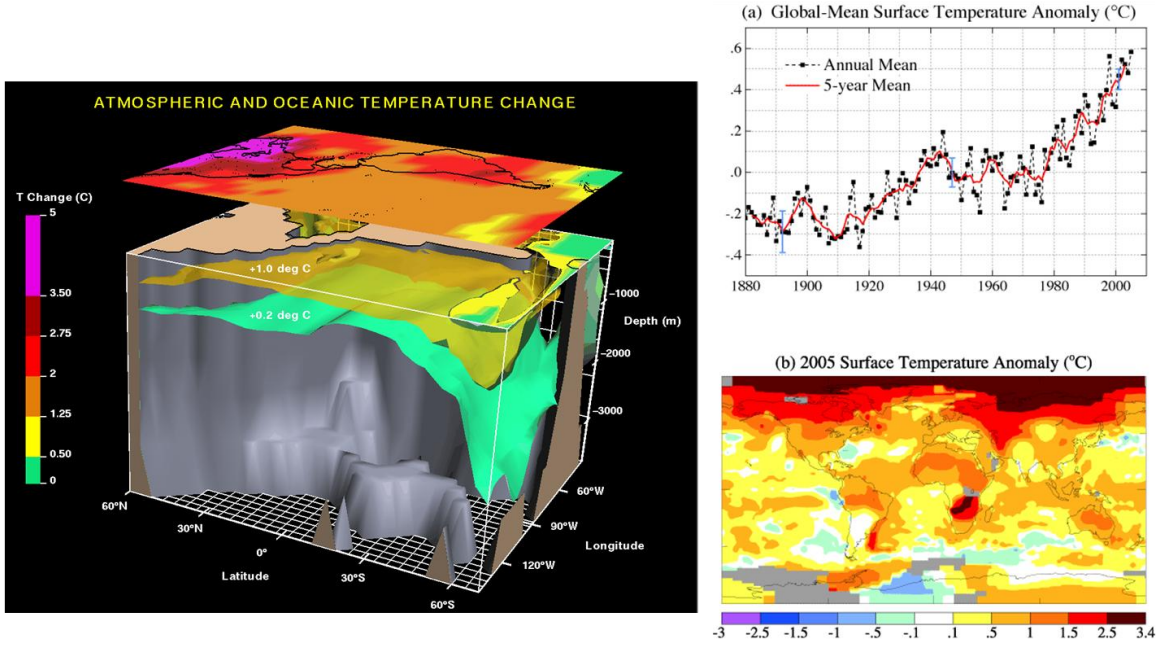

Figure 3: Why Study climate? This is a 3D outlook of the ocean temperature rise due to global warming. The top panel shows the change in temperature for North and South America. The 3D box illustrates how a 1°C to .2°C increase in temperature penetrates the Pacific Ocean [2, 9, 110].

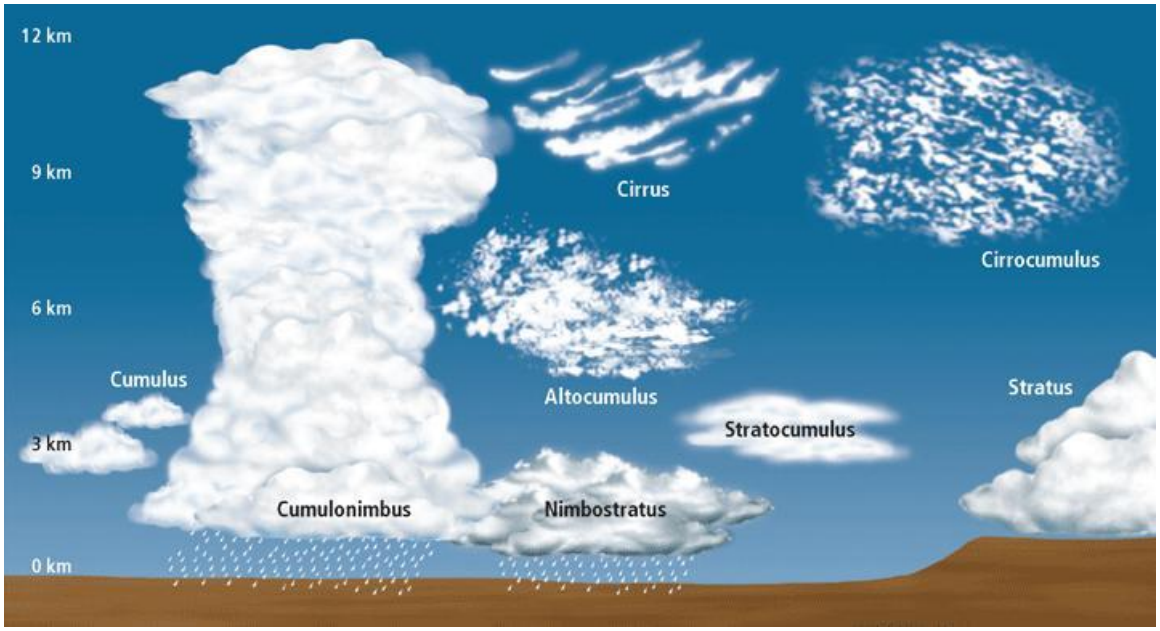

Figure 4: In this figure are some of the clouds stratified by height that are detected and studied at the ARM site [3].

Figure 4 shows a stratified by height representation of the cloud types and cloud formations studied at the Atmospheric Radiation and Measurement Program (ARM). The types of clouds include altocumulus, altostratus, cirrus, cumulus and status. Altocumulus clouds, a principal cloud, is white or grey in color and appears as a wavy patch or layers with rounded masses. Altostratus clouds are another principal cloud and are gray or bluish in color. They appear as a uniform sheet of striated or fibrous in appearance. Cirrus clouds are composed of small particles that are widely dispersed, usually resulting in a transparency and whiteness. This cloud produces a halo phenomenon not found in other cloud formations. Cumulous clouds are a comprised of dense individual detached elements with sharp outlines. Stratus clouds are usually high altitude clouds characterized by horizontal layering with a uniform base. This type of cloud is flat and varies in appearance from grey to white[3, 12, 13, 6, 14].

Clouds consist of tiny drops of water and/or ice crystals and other atmospheric targets. These are a result of condensation of water vapor in the atmosphere. A fully formed cloud is capable of dispersing its contents in the form of precipitation like hail, rain or snow. Classification of clouds or atmospheric targets is performed in reference to specific characteristics in question.

The classification of clouds and other atmospheric targets is based on their height, shape, appearance, temperature and other characteristics. The most commonly seen cloud formations include stratiform and cumuliform or large layered clouds which occupy greater heights. However, some stratiform and cumulus clouds reside at lower altitudes, approximately 2 km. Clouds of similar shape in the top region of the atmosphere are given the prefix cirro before their names. Intermediate altitude clouds are identified with the prefix 'alto' preceding their names. While the cirrus cloud is only found in the highest parts of the troposphere (shaped like light brush strokes), the cumulonimbus cloud colonizes all the heights of the atmosphere from the above ground level to the tropopause. [3, 12, 13, 15, 16].

Hydrometeor or precipitation is defined as any type of water descending from the clouds to the ground. Various forms of precipitation include hail, rain, snow and sleet. The fresh water on the planet is a result of precipitation. Hydrometeors are caused by the cooling of warm humid air forming water vapor which then condenses to form clouds. At this point the precipitation will either coalesce into rain droplets, or ice. Subsequently, the Bagerone process, which involves the acquisition of water molecules from supercooled water droplets resulting in an increase in mass. This increase in mass leads to

the process of falling. The falling ice may melt and become precipitation before coming into contact with the ground. [3,2,1,5]

The three common modes of precipitation are Convective, Stratiform and Orographic. Convective is from clouds like cumulus or cumulonimbus. This type of precipitation is common in the tropics. It is characterized by showers of varying intensity. Hail and Graupel are results of convective rainfall. Stratiform, a larger form of precipitation, occurs when air slowly ascends long cold-fronts. Orographic precipitation is caused by large scale flow of most air over a mountain resulting in condensation. This type of precipitation ensures that the windward side of the mountain is wetter than the leeward side. The reason this occurs is because moisture from the leeward side is moved to the wind ward side [5, 13, 17, 3, 10].

Atmospheric Radiation and Measurement Program (ARM)

The Atmospheric Radiation and measurement program (ARM) is the largest atmospheric research facility funded by the United States. ARM is a key contributor to the international effort to track the effects of global warming. ARM was developed in 1989 by the Department of Energy's Office of Science to create several ground based stations to study cloud formation and the effect it has on radiative transfer. ARM consists of two mobile facilities, three permanent facilities which are the North Slope of Alaska, the Southern Great Plains, and the Tropical Western Pacific (TWP) sites, an aerial facility, and a database archive. These facilities conduct research on climate alterations; oceans and water bodies, ecological systems and atmospheric chemistry. Measurements at the TWP sites include the launching of radiosondes, microwave radiometers, broadband sur-

face radiative fluxes, surface meteorology, millimeter wavelength cloud radar (MMCR), micropulse lidar (ML), and ceilometers. The latter provide information for cloud detection and measurement of the height of cloud bases and the vertical distributions of hydrometeors [3, 17, 19, 20, 14]

There are a variety of measurements that are beneficial to the categorization and classification of clouds and other atmospheric targets. Though water and ice clouds are relatively unproblematic to identify clouds, and other atmospheric targets which have a mixture of ice and water content are much more difficult to identify. These types of clouds, known as mixed-phase clouds, are an area of intense study in the climate physics community. The strong interest in mixed-phased clouds is based upon the scientific community's lack of knowledge of how or to what extent these clouds affect cloud formation or other hydrometeors in the atmosphere. Mixed-phase clouds, along with Cirrocumulus, Cirrus, Anvil, and other types of clouds can be investigated. The measurements can provide data that can be analyzed to obtain detailed microphysical properties of clouds. The accumulation of large in-situ data sets adequate for analysis is cost prohibitive. It is for this reason, along with the desire to provide the scientific community with large datasets to analyze the effects of global warming, that the Atmospheric Radiation and Measurement program was created and funded by the United States. The core research themes of ARM are the aerosol life cycle, cloud life cycle, cloud aerosol interactions and radiative processes [3, 4, 109, 5].

Atmospheric Radiation and Measurement Program (ARM) Objectives

ARM's vision is to provide provision accurate and detailed depiction of the different climate system, the determination and accounting for climatic uncertainties and models of the earth system so as to develop lasting solutions for environmental challenges. From the Climate Research Facility, the research community can access strategically sited in-situ and remote sensing observatories that have been designed for improving the representation and understanding of climate and earth system models. The facilities also improve the understanding of clouds and aerosols and their interactions and coupling with the Earth's surface.[3]

The ARM Climate Research Facility carries out field research across the globe through its numerous field research sites. Three primary locations, Southern Great Plains, Tropical Western Pacific, North Slope of Alaska, are well equipped to collect the enormous amounts of atmospheric measurements needed to create data files. Scientists utilize the data for various studies such as the effects of dense cloud and aerosols cover on radiant energy as well as interdisciplinary research involving weather forecasting, global climate modeling, and ecology. Included in this process is the value added processing carried out by the ARM staff and scientists, where new data streams are created from the collected ones. The analysis of products is done through software provided by the facility. [3]

ARM Database, Data Processing and Value Added Products

Cloud and radiation measurements gathered from ground instruments, and from aircraft are then stored and distributed through the ARM data archive. Instrumentation data from the ARM sites are taken 24 hours a day and approximately 340 days a year. This enables ARM to furnish the scientific community with decades of radar, lidar, ceilometer, and other equipment data that can be analyzed to determine the balance of the atmospheric radiation and cloud feedback processes which are crucial components of global climate change. The data can then be utilized to research the cloud feedback process, atmospheric radiation balance, and their effects on global and region temperature and rain rates which are critical to understanding global climate change[1, 5, 4, 3, 8].

The measurements provided encompass data essential to the analysis of everything from aerosols and atmospheric carbon to cloud properties. Even with extensive data retrieval at ARM sites all parameters that are of interest to scientists cannot be economically or practically measured. This is another reason that value added products (VAP) are utilized by ARM. Once created, a VAP to analyze mixed-phased clouds is available to scientists worldwide. This type of data archival and data analysis eases the process of identification of new characteristics in climate research and verification of scientific results. Therefore, there are internal and external VAPs as well as unique data precuts available to the scientific community through the ARM archive and website. Some of the most well known VAPs are the Active Remote Sensing Cloud Relocation (ARSCL), (Clothiaux 1998, 2000), the Merge Sounding (MERGESONDE), (Wang 2005), the Microwave Radiometer Statistical Retrieval (MWRRET), and the Microphysical Baseline (MICROBASE) [3, 18, 12, 13, 14].

ARSCL, the Active Remote Sensing Cloud Relocation, value added product (VAP), (Clothiaux 1998, 2000), is utilized in the analysis of cloud properties. ARSCL combines data from millimeter cloud radars (MMCR), laser ceilometers (LC), microwave radiometers (MR), and Micropulse lidars (ML). This VAP combines data resources to generate a determination of precipitation height distributions and approximation of their radar reflectivities, vertical velocities, and Doppler spectral widths. This VAP provides essential information for retrieving cloud microphysical properties and the analysis of radiative effects of clouds on climate [3, 17, 19, 20, 12].

Merge Sounding (MERGESONDE) is a VAP, which produces the best estimate of the atmospheric state of column above to the ARM research sites. It is a derivative of the operational amplifier product produce by [5] which was modified to conform to ARM Line by Line Radiative Transfer Model (LBLRTM) grid spacing. This VAP utilizes observations from Radiosondes sounding, microwave radiometers, surface meteorological instruments [3, 18, 17, 4, 13].

Microwave Radiometer Statistical Retrieval (MWRRET) measures the atmospheric brightness at 31.4 and 23.8 GHz. These two microwave radiometers (MWR) observe brightness and are converted into precipitable water vapor (PWV) and cloud liquid water path (LWP). Both values are critical variables for discernment of radiative transfer in the atmosphere. MWRRET is based upon a statistical methodology that utilizes site-dependent monthly retrieval coefficients developed by [37]. The statistical retrieval is constructed by taking over 10 years of the radiosondes profiles of temperature and relative humidity (RH) and adding different amounts of the liquid water when the RH reaches a particular threshold, usually 95-98%. The resulting ensemble is used to compute

brightness temperatures. The results of which are transformed into opacity, which has a more linear relationship with LWP and integrated water vapor. After the multiple linear regressions, the regression values are utilized to calculate LWP and integrated water content. As a consequence, if the observed atmospheric conditions vary considerably from the mean atmospheric conditions than the PWV and LWP retrievals will not give the user an accurate assessment. Compensation for the effect of the clear-bias in the LWP calculations and that the bias has a monthly and site dependence was first noted by [37]. This effect is compensated for by the VAP by attempts to decrease the extent of the LWP bias by eliminating small offsets from the observed brightness temperatures [3, 17, 12, 37, 38, 19, 13, 21].

The Microphysical Baseline (MICROBASE) VAP is a broadband heating rate profile project (BBHRP) conducted within ARM. The BBHRP produces two heat rate profiles, an instantaneous heat rate profile (PI) and an average heat rate profile for the site (PA). This VAP involves continuous survey of the cloud microphysical properties above the column above the site and over the entire Cloud and Radiation Testbed. It provides detailed information of cloud ice water and cloud liquid water [3, 12, 22, 23].

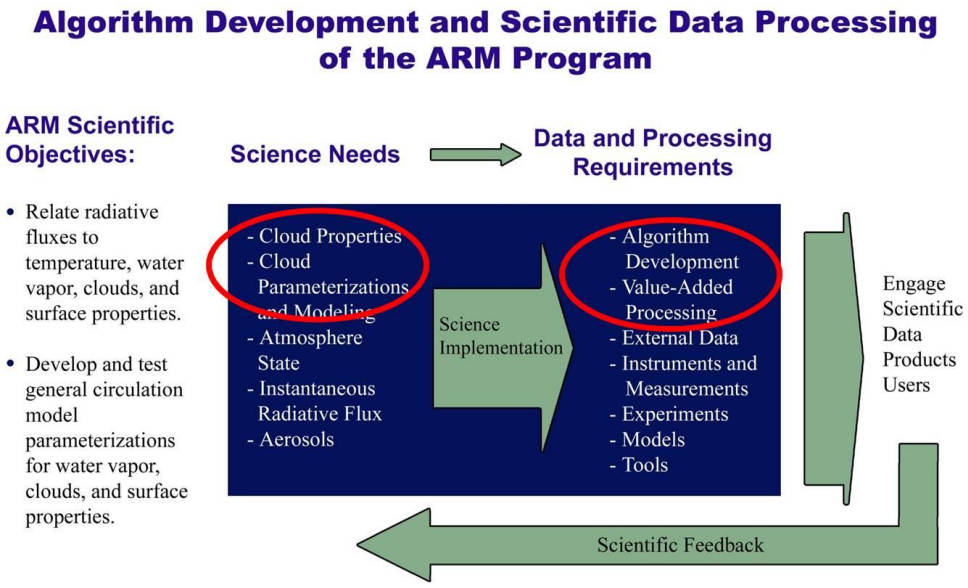

Figure 5: ARM's scientific objectives and scientific needs, which include the development and testing of general circulation models, characterization of cloud, aerosol and atmospheric properties. These needs lead to algorithm development, which ARM calls Value Added Products or Processing (VAPS)[3]

Many of ARM's scientific objectives are achieved through the development of available data into value added products, or best estimate VAPs. Global change research aims at increasing the scientific community's understanding of the interaction between physical, chemical, and biological processes of the Earth, and transformations in the environment. The three sites of the ARM program are detailed in figures 6 and 7 [3].

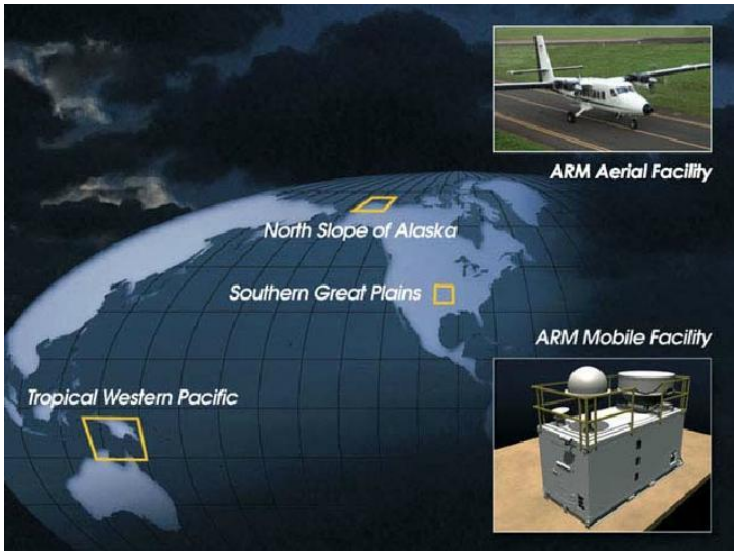

Figure 6: The Atmospheric Radiation and Measurement Program (ARM) has three permanent sites along with the aerial facility [3].

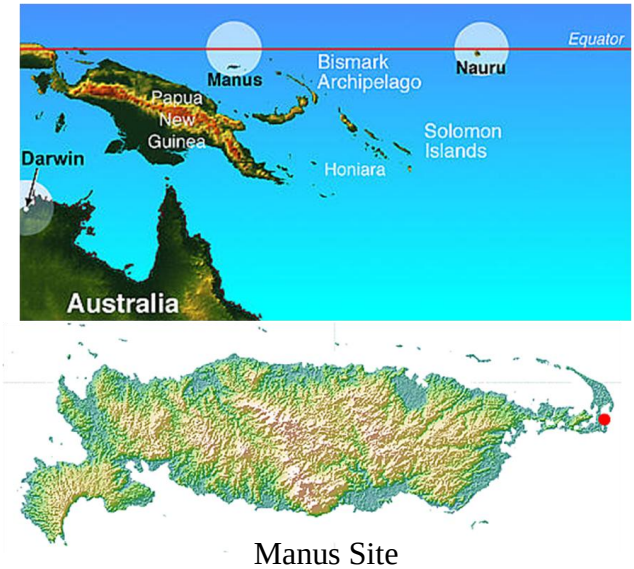

Manus Site

Figure 7: The Tropical Western Pacific (TWP) site is made of the three instrument sites, at Manus, Nauru Island and Darwin, Australia. These sites were chosen for their warm sea temperatures, frequent atmospheric convection, high rain rates, and strong coupling between the atmosphere and the ocean [3].

Radar and Lidar Utilization in Climate Research

RADAR can be utilized to measure and analyze atmospheric targets. In radar, electromagnetic waves are emitted from a transmitter. The transmitted electromagnetic waves attenuate, scatter, diffract, and are absorbed by targets in the atmosphere. A receiver, which usually is at the same location as the transmitter, monostatic, monitors the returned signal from reflecting hydrometeors such as raindrop within clouds. Radar can determine the range, altitude, direction and speed of cloud hydrometeors. The manner in which radar waves scatter depends on the wavelength of the radar signal and the target's shape. When the wavelength is less than the target's size the wave will bounce off the object thereby sending a signal back to the receiver. The opposite is true in that when the wavelength of the signal exceeds the target size, the target will not be visible to the receiver due to a lack of signal bounce back from the target.

In the case of ARM, the radar systems are 35 and 94 GHz that are sensitive to large elements such as ice and light rain. Radar can detect the cloud top and penetrate ice clouds as shown in Figure 8. Radar is unable to detect super-cooled liquid water drops. Liquid water has a significant effect on the attenuation of radar.

LIDAR, the acronym for light detection and ranging, is a way of remote sensing characteristics of a target by illuminating the target with ultraviolet, near infrared or visible light. Lidar systems can be used to detect aerosols, clouds and even single molecules. The wavelengths used can detect targets sizes from 10 micrometers to 250 nanometers. Lidar detection can be incoherent or coherent, combined with the type of lidar system being utilized. The most common types of lidar systems are Raman lidar, Rayleigh lidar, and Mie lidar. The primary measurements that lidar is used for include aerosol scattering,

cloud base height detection, backscattering depolarization ratio, and atmospheric moisture. The Raman Lidar at ARM is a remote sensing instrument used to measure the perpendicular profile of water-vapor mixing ratio and several cloud- and aerosol-related quantities. [3]

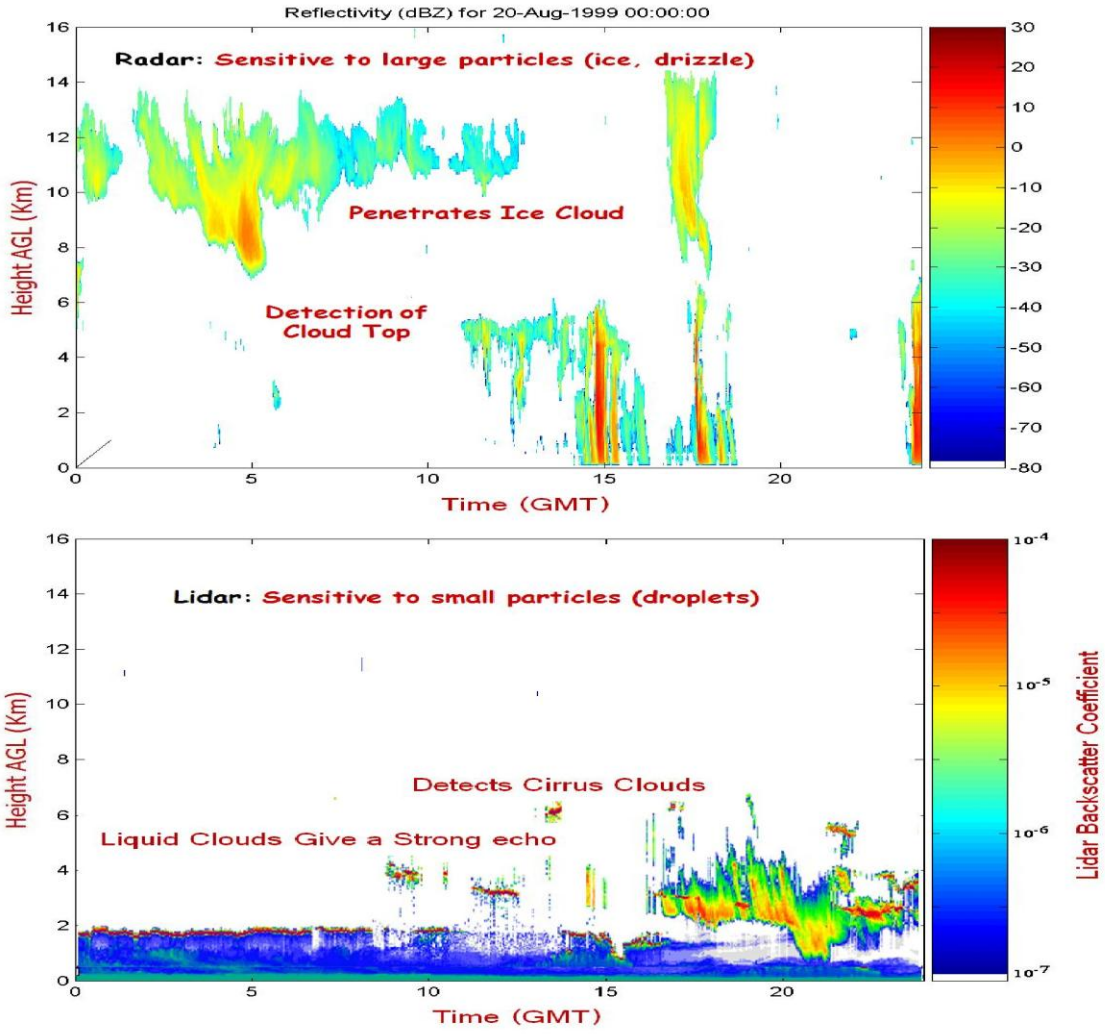

Figure 8: Radar and Lidar at ARM is used for the remote sensing of meteorological phenomena. Radar is more sensitive to large particles such as ice and drizzle, while the lidar is more sensitive to small particles such as aerosols. The ratio of radar to lidar provides information on the particle size of atmospheric targets.

The Tropical Western Pacific site (TWP) has a comprehensive set of world-class instruments available to the global scientific community. They include Raman lidars, sky-imagers, wind-profilers, cloud radars (millimeter wavelength), atmospheric emitted radiance interferometer, C-Band ARM Precipitation Radar (for cloud properties identification), Cimel Sunphotometer (CSPHOT), Doppler lidar, and Ka-Band Scanning Cloud Radar.

The Cimel Sunphotometer is a multichannel, sun-and-sky scanning radiometer that measures the solar irradiance and sky radiance at the Earth's surface. The millimeter cloud radars (MMCR) are useful for remote sensing of meteorological phenomena such as investigating the degree and composition of clouds at millimeter wavelengths. The MMCR is a zenith-pointing radar that functions at a frequency of 35 GHz. The central function of this radar is the verification of cloud boundaries (for instance, the tops and bottoms of clouds). It also serves the purpose of reporting reflectivity (dBZ) up to twenty kilometers. The Micropulse Lidar (MPL) is utilized to determine cloud altitude. The instrument is an optical remote sensing system. The physical principle behind MPL is the same as for the radar. Some of the instruments available through ARM are shown in figure 9[3].

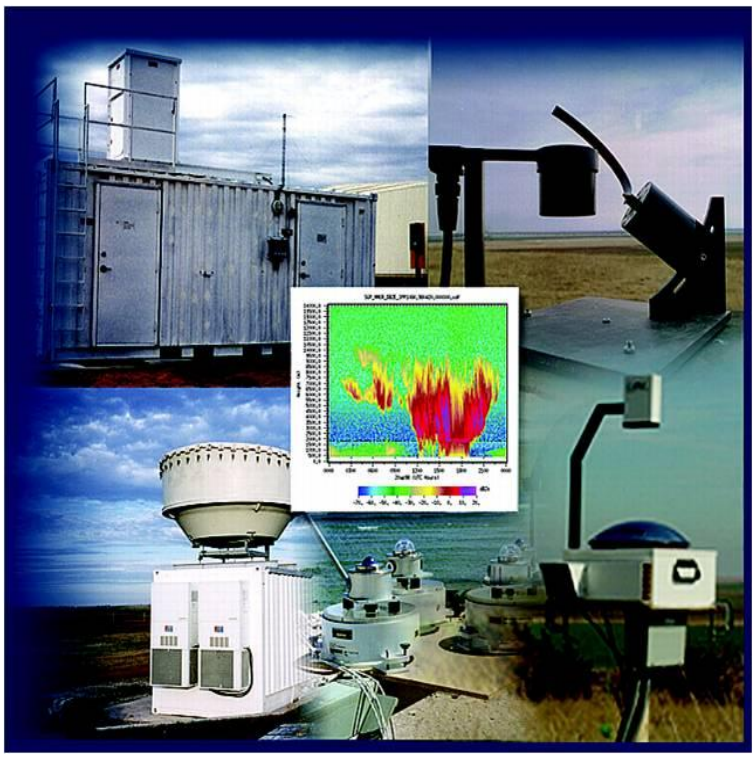

Figure 9: The instrumentation at the TWP site includes Raman Lidar, millimeter wave cloud radars, radar wind-profilers, total sky-imagers, Ka band cloud radar among others.

Research Objectives

One of the key goals of this research is the improvement of the application, and use of data available at the ARM TWP sites, and the development of retrieval algorithms, the parameterization of atmospheric targets, by developing the Climate Classification Preprocessing Algorithm (CPA), for the ARM Program. In addition a goal of this research is to make multi-sensor data easier for the climate physics scientific community as well as to investigate if data mining techniques are applicable to the analysis of ARM data. To that end, an analysis of over a decade worth of data provided from the TWP ARM site is performed.

Typically when research scientists attempt to identify targets in the atmosphere they utilize one frequency of radar and one frequency of lidar data. Though this method is a less time consuming method of identifying targets in the atmosphere, there are several frequencies of radars, lidars and other instrumentation that can be utilized to identify targets in the atmosphere. The difficulties involved in using several different instruments are numerous.

The first difficulty in exploiting the data from relevant instruments in the tropics is that the data for each instrument has its own time-height grid, and different units. Second, the amount of data quickly becomes enormous which can complicate the manipulation of the data. In the case of the radar data, the data points are on the order of 14 million a day. Third, all of the instruments are not used at the same time which provides another level of difficulty. Fourth, instrument sensitivity must be tracked and accounted. The CPA performs multi-sensor analysis by exploiting the data from millimeter cloud radars, lidars, radar wind profilers and various other relevant instruments at the ARM TWP sites. CPA produces reflectivity, velocity and spectral width graphs along with their corresponding distribution graphs, modified contour frequency by altitude diagrams (M-CFAD) for user defined periods of time, the condensed water content graphs in addition to classifying atmospheric targets in the TWP. CPA identifies atmospheric targets by utilizing neural fuzzy-logic data mining techniques and multiple instrument data. CPA standardizes units, and provides data quality flags, gas and liquid attenuation correction and instrument sensitivity which overall produces a truly robust classification algorithm. CPA advances the field of climate physics research by first analyzing multi-sensor data to identify targets in the TWP for large amounts of data as well as making multi-sensor data

easier to be utilized. CPA is the first step in achieving the long term goal of the Department of Energy's ARM program of the creation of a classification algorithm that is able to apply the an appropriate retrieval algorithm.

Due to uncertainties of the effect cirrus and mixed phased clouds have on the earth's radiative budget, there has been an increase interest in the analysis these cloud types. Throughout this process, it will be necessary to take specific atmospheric targets and advance the ability to describe their characteristics. This dissertation concerns the development of Climate Classification Preprocessing Algorithm (CPA) that uses the data from the TWP site which provides a series of graphs that are essential for the analysis of climate. CPA produces spectral width, reflectivity, Doppler velocity, contoured frequency by altitude diagrams, and their associated histograms, the condensed water content profiles which together aids in atmospheric target identification and classification. The accuracy of the diagrams is verified by comparison with ARM analysis for the same time-period. By using the data provided at the TWP site, each pixel is categorized through neural fuzzy-logic and a characterization mask filtering system. The result of the aforementioned algorithm is a graphical representation showing what each pixel represents. CPA provides standardization of units, and information to indicate if the signals are contaminated with ground clutter or if there is unknown radar attenuation in rain and other effects. CPA provides gaseous and liquid attenuation correction, the interpolation of lidar, rain rate, liquid water path (LWP), and ice water path (IWP) on the same time height scale as the radar which will result in target classification by using neural fuzzy-logic data mining techniques.

Outline of the Dissertation

The chapters in this dissertation are organized in the following manner:

Chapter I is the introduction to the Atmospheric Radiation and Measurement Program and facilities (ARM), ARM database, and the research objectives of the Climate Classification Preprocessing Algorithm (CPA). Chapter II encompasses the basic development and implementation of this algorithm. Chapter III contains the results of the CPA and error analysis. Chapter IV focuses on Conclusions and future research and development of CPA.

CHAPTER II:

Data Mining and The Climate Classification Preprocessing Algorithm (CPA)

In 2011, Science dedicated an entire special edition issue to the "Dealing with Data". This article by Overpeck and Meehl address the issue of data accumulation, distribution, and access of data in the climate research community. Climate data is increasing in volume and diversity. The issue of storage distribution and access of data as well as verification of the accuracy of the data are major issues for the climate community. The Department of Energy's ARM program has made significant steps toward solving these problems through the ARM web-accessible database. This database has updated prescreen remote as well as insitu data from ARM sites.[1,82,81]

Data mining is the process of searching large amounts of data for patterns and characteristics. In the case of CPA the patterns are the classification states of the atmospheric targets. Data mining techniques in the ARM program are supported by the ARM data archive, the ARM computer system and the various ARM algorithms. Another essential part of data mining process is addressing the accuracy of data also known as data cleansing. Data cleansing is achieved through the ARM Data Management Group. The ARM Data Management Group is discussed in more detail in the Chapter III.

Data mining has seven broad categories and five logical techniques applied to data archives. The categories of primary interest of CPA are classes, clusters and associations. Classes are the ability to efficiently find data in predetermined groups. A Cluster is the process in which data is organized according to a predetermined relationship. Associ-

ations are relationships found through analyzing the data. Other categories are forecasting and sequential patterns, which are mostly, associated with local or global climate models. The logical techniques are fuzzy logic, neural network, decision trees, rule induction and genetic algorithms. CPA uses a combination of neural and fuzzy logic techniques[1,2,3].

Due to the uncertainties of that the effects cirrus, mixed phased clouds, and other atmospheric targets have on the earth's radiative budget, there has been significant increase interest in parameterization of atmospheric targets. Throughout this process it will be necessary to take a specific atmospheric cloud type and advance our ability to describe its characteristics. This dissertation concerns the development of the Climate Classification Preprocessing algorithm (CPA). CPA utilizes the data and instrumentation available at the TWP and provides a series of graphs that are essential in the analysis of climate in the tropics. To that end, a general analysis of the data provided from the TWP ARM site located off the coast of Papua New Guinea is performed. This is being achieved by comparing Doppler Velocity, Spectral Width and Reflectivity in areas with/without mixed phased clouds. Classification occurs by utilizing the techniques of data mining to identify specific atmospheric patterns. Those patterns are Clear Sky, Warm Cloud, Warm Precipitation, ice, Melting ice, Super Cooled Liquid, drizzle and/or rain, aerosols, insects. CPA also indicates to the user if there is clutter in the radar or lidar echo as well as liquid attenuation, and ground clutter.

A graphical representation of the pattern occurrence is created showing what each pixel represents. The accuracy of the diagrams is verified through comparison with ARM VAPS analysis for the same time period. In addition error analysis is performed by regraphing the associated data with and without the error components. The phrase "data

without error" refers to the assumption that the data is accurate without taking into effect bias, mean error, instrument error, noise and other elements that contribute to error in the datastream. Next, a graph that displays the difference between the CPA atmospheric target identification graph without error and the CPA atmospheric target with error is created. By utilizing the data provided at the TWP site each pixel is categorized through neural-fuzzy data mining process.

The primary reason for the Department of Energy's ARM program's interested in cloud and atmospheric target classifications is to provide input to a decision tree. There are multiple cloud property retrievals that make use of different instruments (e.g. radars, lidars, and radiometers). The kind of retrieval used depends on the state of the atmosphere. If the atmosphere is saturated with drizzle/rain then a retrieval algorithm that specifically works in that specific atmospheric condition is applied. With this information, one can then build an atmospheric target identification system that appropriately chooses from among the available retrieval techniques. There are other applications of such an algorithm, but this has been of keen interest to the ARM program for some time. Until this point there has not been a great deal of progress in this area. CPA is the first crucial steps in creating a multi-retrieval algorithm.

Different clouds types are controlled by diverse cloud dynamic processes and posses diverse microphysical properties, which cause different cloud radiative forcings. Climate changes can result in changes in the frequency of occurrence and shifting characteristics of a given cloud type. When these changes are combined, they establish the changes in the function of clouds in the Earth water and energy. The climate research and modeling community faces many impediments to accurately predicting future climate

change. Unless the climate models are improved to efficiently embody the mechanisms of processes and feedbacks when managing properties of diverse cloud types, the climate physics community will continue facing obstacles that will interfere with accurate predictions. Categorizing clouds, and atmospheric targets in class types is crucial to undertaking in remote sensing of clouds and the study of global cloud climatology [50, 3, 52, 88, 91].

One of the objectives of this research is to improve atmospheric target identification by using multi-sensor data available from the ARM TWP sites, and application of retrieval algorithms. To that end, a general analysis of the data provided from the TWP ARM site located off the coast of Papua New Guinea is performed. In addition this project improves the parameterization of several atmospheric cloud types and improves the ability to describe their characteristics. This is achieved by comparing Doppler Velocity, Spectral Width and Reflectivity, and several other properties in areas with/without mixed phased clouds. Additionally, cloud classification occurs by providing characteristic mask classes such as Clear Sky, Warm Cloud, Warm Precipitation, Melting, Super Cooled Liquid, Ice and Mixed Phase. After the masks are applied and compared with 2-D reflectivity, velocity and spectral width plots to insure the classifications are accurate, a graphical representation is created showing what each pixel represents. The frequency distribution of the occurrence of each class is also demonstrated. The data was analyzed for any new identification markers of cloud types. The results can be applied toward development of a product that will seamlessly transition from one retrieval algorithm to another based on a given condition.

Introduction

The study of cloud formation processes, the classification of atmospheric targets and their influence on radiative transfer are key objectives of the ARM and this dissertation. Due to uncertainties of the effects cirrus and mixed phased clouds have on the earth's radiative budget, there has been significant increase in the analysis these cloud types and atmospheric targets. This dissertation concerns the development of CPA that utilizes the data and instrumentation available at the TWP that provides a series of graphs that are essential in the analysis of climate in the tropics. CPA produces the spectral width, reflectivity, Doppler velocity, Contoured Frequency by Altitudes diagrams, their associated histograms, and the condensed water content profile. The accuracy of the diagrams is verified by comparison with ARM VAPS analysis for the same time period. The accuracy is also verified through compassion of the classification with and without error.

After training CPA on TWP ARM data, it was also tested on additional data sets to ensure accuracy. By using the data provided at the TWP site each pixel is categorized through a neural fuzzy-logic filtering system. In CPA a graphical representation of the occurrence is created showing what each pixel represents. The algorithm will provide a standardization of units, data quality flags, instrument sensitivity flags, gaseous and liquid attenuation correction. These tasks are preformed through the interpolation of lidar, rain rate, liquid water path (LWP), and ice water path (IWP) on the same time height scale as the radar, which will result in target classification by utilizing combined neural fuzzy-logic.

ARM Instruments

The Atmospheric Radiation Measurement (ARM) program is the leading global climate change research facility funded by the Department of Energy. ARM was created to improve cloud and radiation physics and cloud simulation capabilities in global climate models. At the ARM sites are a comprehensive set of instruments that are available to the global scientific community. The key remote sensing instruments comprise Raman lidar, sky imagers, wind profilers and millimeter wavelength cloud radars and several micro-wave radiometers. Data measurements are stored and distributed via a data archive and scientists can research the feedback processes that are critical to understanding world-wide climate change. Data products from continuous field measurements to advance global climate models are available for analysis [3, 17, 4].

The instrumentation at the ARM Tropical Western Pacific site (TWP) is displayed in Table 1 and figure 10. The millimeter cloud 35 GHz zenith pointing radar (MMCR), is utilized to analyze the composition of clouds at millimeter wavelengths and determines cloud tops and bottoms, as well as radar reflectivity (dBZ) of the atmosphere up to 20 km. The MMCR also reports Doppler velocity, spectral widths, horizontal winds, and vertical velocity. The Micropulse Lidar (MPL) is an optical remote sensing system. Lidar remote sensors operate on the same tenet as radar sensors. Lidar pulses are trans-mitted into the sky as the pulses come in contact with targets. The energy is scattered back to a receiver and is a time resolved signal. As with radar, the time delay between the transmitted signal and the backscattered signal determines the distance the target is from the transmitter. In addition, MPL detects cloud base heights, aerosols extinction, cloud fraction and radar polarization. The MPL received signal is often used to characterize

aerosols. The Surface Meteorological Instrument (SMET) is an in-situ instrument that obtains one minute increment statistics on atmospheric moisture, pressure, temperature, and precipitation, horizontal wind, relative humidity and rain rates. The Vaisala Ceilometer (VCEIL) is an active remote sensor, laser ceilometer that measures cloudbase height, vertical visibility, and potential backscatter signal from aerosols. The VCEIL has a perpendicular range of 7700m which transmits in the range of infrared and receives scattered light from clouds and other hydrometeors. The Microwave Radiometer (MWR), which operates at 23.8 and 31.4 GHz, is a passive sensor that measures the microwave emission from water vapor and liquid water in the atmosphere. The MWR performs time series measurements of column integrated cloud liquid water, water vapor and liquid water path. The Raman Lidar (RL) is used to measure aerosol scattering, atmospheric moisture, and cloud base height. Additional instrumentation at the ARM TWP is shown in table 1 and figure 10.

Figure 10: Some of the instrumentation at the ARM site: From left to right is the Millimeter wave cloud radar (MMCR), Micropulse Lidar (MPL), Surface Meteorological Instruments (SMET), Vaisala Ceilometer (VCEIL), Raman Lidar (RL)

Table 1: TWP Site Instrumentation and the data retrieved from the instruments

Instrument	Data Descriptions
Millimeter Wave Cloud Radar (MMCR) 35 GHz	Reflectivity, Doppler Velocity, Spectral Width
Micropulse Lidar (MPL)	Vertical Profile of Hydrometeors, Cloud Base Heights
Surface Meteorological Instruments (SMET)	Atmospheric Moisture, Pressure, Temperature, Horizontal Wind, Precipitation
Vaisala Ceilometer (VCEIL)	Cloudbase Height, Vertical Visibility
Microwave Radiometer (MWR) 23.8-31.4 Ghz	Radiometric, Cloud Properties, Atmospheric Profiling
Raman Lidar (RL)	Vertical Profiles of Water-Vapor Mixing Ratio and Cloud and Aerosol-Related Quantities
Rain Gauges (RG) (1 minute intervals)	Precipitation
Sky Radiometers on Stand for Downwelling Radiation (SKYRAD)	Cloud Fraction Cover

Ka Band Scanning ARM Cloud Radar (KASACR)	Cross-polar radar reflectivity, Doppler velocity, spectra width
Doppler Lidar (DPL) (measures wind velocities (clear sky) at about 10 cm/sec	Range and time resolved measurements of radial velocity and attenuated backscatter The DL operates in the near-IR (1.5 microns) and is sensitive to backscatter from micron-sized aerosols.
Cimel Sunphotometer (CSPHOT)	Aerosol absorption, concentration, extinction, and optical properties, Particle number concentration and size distribution, Precipitable water.
Atmospheric Emitted Radiance Interferometer (AERI) Measurement range: 3300 to 520 wavenumbers (cm^{-1}) or 3-19.2 microns	Atmospheric moisture and temperature, Longwave spectral brightness temperature and radiance

The classification of clouds and atmospheric targets is achieved with reference to its height in the atmosphere, appearance, temperature and shape (Figure 4). The cloud formations easily seen include stratiform, cumuliform or large layered clouds, which occupy greater heights. However, some stratiform and cumulus clouds reside in lower altitudes of about two kilometers. The Troposphere contains clouds given the prefix cirro before their names for instance, cirrocumulus or cirrostratus. Intermediate altitude clouds have the prefix ‘alto’. While the cirrus cloud is only found in the highest parts of the troposphere (shaped like light brush strokes), the cumulonimbus cloud colonizes all the heights of the atmosphere from the ground to the tropopause. It is also responsible for the thunderstorms. [16, 17, 8, 22].

Hydrometeor, or precipitation, is defined as any form of water descending from the clouds to the ground. There are various forms of precipitation for example hail, rain, snow and sleet. Hydrometeor results from the process of cooling of warm moist air when it rises forming water vapor which then condense to form clouds. The precipitation will

either coalescence into rain droplets or ice. The Bagerone process entails the acquisition of water molecules from nearby super-cooled water droplets resulting in an increase in mass. It is the increase in mass that commences the process of falling. The falling ice may melt and become precipitation before contact with ground because of temperature differences[13, 12, 17, 16, 4, 8].

Atmospheric ice clouds strongly affect the radiant properties of the Earth. However, the process of homogeneous ice nucleation, the creation of ice particles in the atmosphere, is not fully characterized or analytically duplicated efficiently in global climate models. The reason for this lies in the fact that ice forms in aqueous aerosol droplets which can be composed of many other atmospheric targets of interest. The essential parameters vital to describing ice particle creation are temperature and relative humidity. [12, 3] By studying and developing characterization of clouds and atmospheric targets through the utilization of data at ARM sites in the TWP, vulnerabilities in numerical global climate models of the atmosphere can be analyzed and adjusted accordingly. The resulting characterization of targets in the atmosphere can also have significant implications for our understanding of the effects of different cloud types, and atmospheric pressure in a region have on the formation, duration and movement of other clouds. It can also indicate changes and effects of the liquid water paths (LWP) and ice water paths (IWP) in a region. The LWP and IWP are literally area of the sky or cloud that has water and or ice. It is used to adjust instrumentation for attenuation for radar and lidar measurements. Anvil clouds are ice clouds that form at the tops of deep thunderstorm clouds. By measuring the formation of anvil clouds, researchers investigate how these clouds

limit the amount of sunlight that reaches the Earth's surface, thereby raising temperatures and contributing to global warming. [12, 3, 17, 19]

Cloud and radiation measurements are then gathered from ground instruments, those attached to aircraft or placed on ships. Measurement data is then stored and distributed through the ARM data archive. Data from the ARM sites is taken 24 hours a day and approximately 345 days a year. This enables ARM to furnish the scientific community with decades of radar, lidar, ceilometer, and other equipment data that can be analyzed to research atmospheric radiation balance and cloud feedback processes, which are critical elements of global climate change. These data can then be utilized to research atmospheric radiation balance and cloud feedback processes critical to understanding global climate change. The measurement provided encompasses data essential to the analysis of everything from Aerosols and Atmospheric carbon to cloud properties. Even with extensive data retrieval at ARM sites, all parameters that are of interest to scientists cannot be economically or practically measured, this is another reason that VAP's are utilized by ARM. Once created, a VAP to analyze mixed-phased clouds for example, in the Tropical Western Pacific sites (TWP) is available to scientists worldwide. This type of data archival and data analysis eases the process of distribution of new characteristics and discovers in climate research and the verification of scientists results. Therefore, there are internal and external VAP's as well as special data precuts available to the scientific community through the ARM archive and website. Some of the most well known VAP's are the Active Remote Sensing Cloud Relocation (ARSCL), the Merge Sounding (MERGESONDE), the Microwave Radiometer Statistical Retrieval (MWRRET), and the Microphysical Baseline (MICROBASE). As with all VAPs at ARM, they are regularly

updated and modified based upon advancements in hydrometeor identifications [3, 18, 24, 44, 36, 3].

ARSCL, the Active Remote Sensing Cloud Relocation, value added product (VAP) is utilized in the analysis of cloud properties. ARSCL combines data from millimeter cloud radars (MMCR), laser ceilometers (LC), microwave radiometers (MR), and Micropulse lidars (ML). This VAP combines data resources to produce a purposeful determination of hydrometeor altitude distributions and approximations of their radar reflectivities, perpendicular velocities, and Doppler spectral widths. This VAP provides fundamental information for retrieving cloud microphysical characteristics of the clouds and the analysis of radiative effects of clouds on climate. Like all ARM VAPs updates and changes in ARSCL can are finalized if advancements or changes in site equipment, algorithm development, or error analysis are achieved. The last update to ARSCL algorithm was in 2005. Merge Sounding (MERGESONDE) is a value added product, VAP, which produces a best estimate of the atmospheric state of column above to the ARM research sites. It is a derivative of the operational amplifier product produce by [5] but was modified to conform to ARM Line by Line Radiative Transfer Model (LBLRTM) grid spacing. This VAP utilizes observations from Radiosondes sounding, microwave radiometers, surface meteorological instruments [3, 17, 4, 18, 19, 20].

Microwave Radiometer Statistical Retrieval (MWRRET) measures the atmospheric at 31.4 and 23.8 GHz. The 23.8 GHz frequency is most sensitive to liquid water emission. The converse is true for the 31.4 GHz. With these two microwave radiometers (MWR) observed emissions are converted into precipitable water vapor (PWV) and cloud liquid water path (LWP). These are crucial variables to understanding radiative transfer

in the atmosphere and clouds. These retrievals are made on the basis of a statistical methodology that employs site-dependent monthly retrieval coefficients developed by [45]. The statistical retrieval is constructed by taking for example years five through ten of the Radiosondes profiles of temperature and relative humidity (RH) and adding different amounts of the liquid water when the RH reaches a particular threshold, usually 95-98%. The resulting ensemble is used to compute brightness temperatures. The results of which are transformed into opacity, which has a more linear relationship with LWP and integrated water vapor. After the multiple linear regressions, the regression values are utilized to calculate LWP and integrated water content. As a consequence, if the observed atmospheric conditions vary greatly from the mean atmospheric conditions than the precipitable water vapor (PWV) and LWP retrievals will not give the user an accurate assessment. Compensation for the effect of the clear bias in the LWP calculations and that the bias has a monthly and site dependence was first noted by [46]. This effect is compensated for by the VAP by efforts to decrease the size of the LWP bias by removing small offsets from the observation of temperature. [3, 17, 12, 19, 13, 21].

The Microphysical Baseline (MICROBASE) VAP is a broadband heating rate profile project (BBHRP) conducted within ARM. The BBHRP produces two heat rate profiles, an instantaneous heat rate profile (PI) and an average heat rate profile for the site (PA). This VAP involves the continuous survey of the cloud microphysical properties above the column above the site and over the entire Cloud and Radiation Testbed. It provides detailed information of cloud ice water and cloud liquid water [3, 12, 22, 23].

Climate Classification Preprocessing Algorithm (CPA)

CPA is written in Matlab with memory management software to accommodate for shortages in memory for processing data. This is necessary because one day's worth of data is in excess of 40 million data points. These data points must be loaded, and classified into groups utilizing the logic system in CPA.

There are a variety of measurements that are beneficial to the categorization and classification of clouds phase, types, and hydrometeors. Though water and ice clouds are relatively unproblematic to identify utilizing ARM's ground based instrumentation. Clouds which have a mixture of ice and water content are much more difficult to identify. These types of clouds, which are known as mixed phase clouds are an area of intense study in the climate physics community. The level of strong interest in mixed phased cloud is based upon the scientific community's lack of knowledge of how or to what extent these type of clouds effect cloud formation or hydrometeors in the atmosphere. Mixed phase clouds, along with Cirrocumulus, Cirrus, Anvil, and various other types of clouds can be investigated via insitu measurements which can provide data that can be analyzed to obtain detailed microphysical properties. The act of accumulating large data sets in an adequate amount for analysis is costly. It is for this reason, along with the desire to provide the scientific community with large datasets to analyze the effects of global warming that the Atmospheric Radiation and Measurement program was created and funded by the United States.

Radar systems are sensitive to the shape, size and type of hydrometeor, cloud and particulates in the atmosphere. As a consequence considerable information is in the covariance matrix which can be utilized to extract microphysical properties. There are var-

ious methods that can be utilized for identification of particulates, hydrometeors and clouds in the Tropical Western Pacific (TWP) sites of Manus and Nauru. Decision algorithms based on a Boolean decision tree, a statistical decision theory, neural networks and fuzzy logic are but a few options available. The decision tree is not adequate because of its basis being essentially Boolean in nature. In some instances it is difficult to distinguish between atmospheric targets. Therefore, a Boolean logic system is inadequate for climate classification. In addition, Boolean logic decision scheme do not allow for measurement errors. Since the covariance matrix created is not exclusive to various hydrometeor or particulate types a neural fuzzy-logic approach is best. Neural fuzzy-logic algorithms have the ability to use simple rules to describe the system. Neural fuzzy-logic classification scheme can reach distinct decisions even though there is overlapping data.

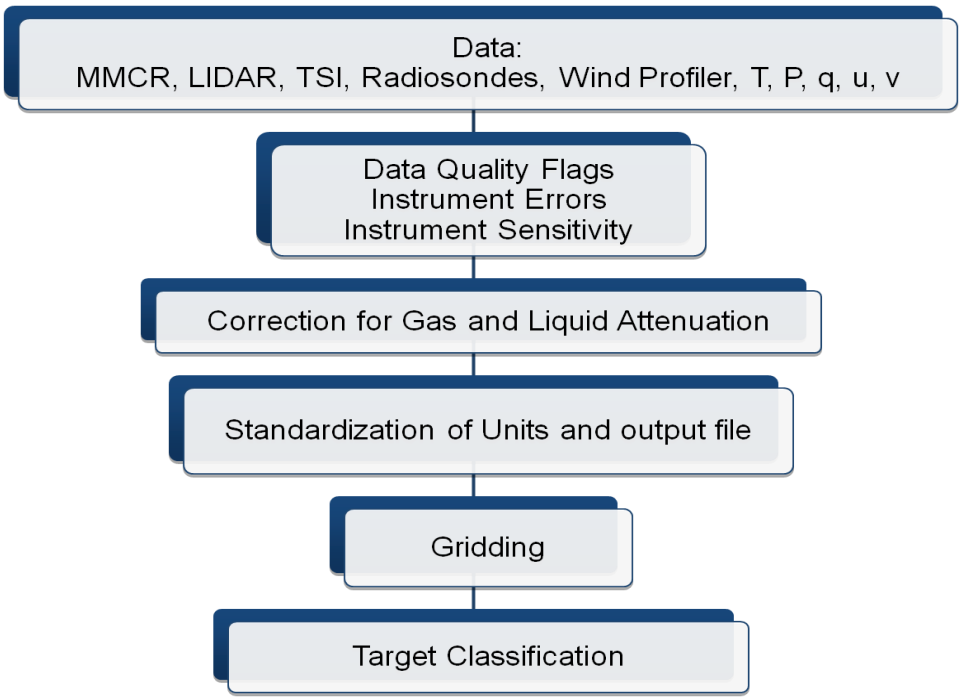

Figure 11: The simplified flow chart for the Climate Classification Preprocessing Algorithm. In this figure T, P, q, and v refer to temperature, pressure, horizontal and vertical wind

The CPA algorithm shown in Figure 11 demonstrates the flow of the algorithm. The data from MMCR, lidars, Ceilometers, Radiosondes, wind profilers along with temperature, pressure, is gathered through the ARM database. Data at the TWP sites are collected continuously throughout the day. In the case of this algorithm data was analyzed over several months of data from the Tropical Western Pacific sites (TWP) was analyzed for the purpose of classifying particulates, hydrometeors and other atmospheric targets. After the ingestion of the data, quality flags are set to enable the user to correct for any anomalies that may be in the data stream. These data quality flags indicate if the data is contaminated by clutter, or if attenuation is an issue. The data quality flags also indicate if liquid water attenuation has been modified utilizing microwave radiometer measurements of the liquid water path and the lidar estimation of the local of liquid clouds. Additionally there are flags that indicate if an echo is detected by the radar and lidar, or if the lidar echo indicates clear sky. The CPA algorithm also enables the user to correct for liquid or gas attenuation as needed.

The fuzzy logic system of identifying rain, drizzle, ice, supercooled ice, melting ice, cloud droplets, insects and aerosols is shown in figure 12. In the fuzzy identification system the inputs are reflectivity, Doppler velocity, IWP, LWP, temperature humidity, height and co-polar correction coefficient. The data provided to the fuzzy logic algorithm

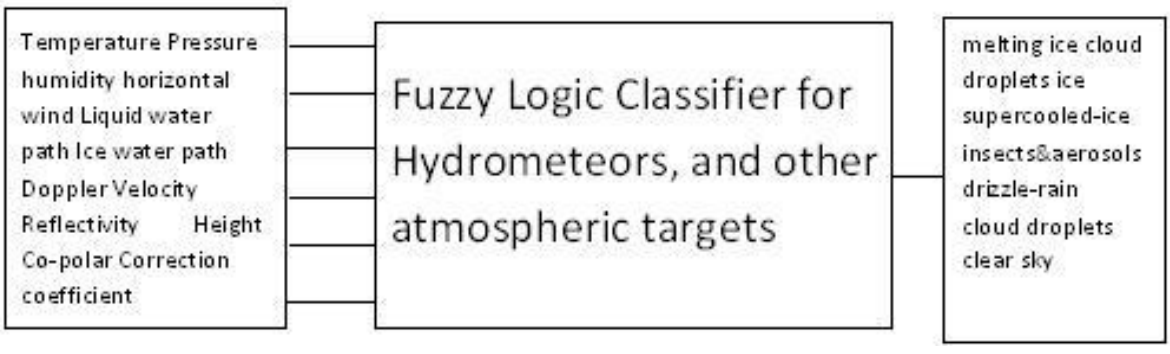

Figure 12: Fuzzy Logic Classifier for the TWP

is from the millimeter cloud radars (MMCR), laser ceilometers (LC), microwave radiometers (MR), Micropulse lidars (ML), Surface Meteorological Instruments (SMET), Raman lidar. The purpose of the fuzzification aspect of the algorithm is to convert the exact inputs into fuzzy sets with a corresponding membership. The necessity of this is apparent because some hydrometeors and other atmospheric targets are difficult to distinguish between, for example drizzle and rain, or cloud droplets and melting ice. By utilizing fuzzy logic the membership function describes to what degree a particular target is a member of a particular set. It also provides the connection between the data input and the fuzzy sets created. The fuzzy classifier, consisting of fuzzification, rule inference, aggregation and defuzzification, will deduce the hydrometer or other atmospheric target, Table 2, from the rule base from the input data from the ARM instruments. In addition all data is placed on the radar time-height grid, data quality flags are set to inform the user if the radar and lidar detected an echo, if there is clutter in the radar signal, liquid water attenuation (affects radar), clear sky air molecular scattering (affects lidar) and flag to indicate if radar reflectivity has been corrected for utilizing the radiometer data which gives liquid water path.

Table 2: The Classes of atmospheric targets identified by CPA

Classes (Masks)	Classifier Output
Clear Sky	1
Ice	2
Ice and Supercooled Droplets	3
Melting Ice	4
Melting Ice and Cloud Droplets	5
Drizzle and/or Rain	6
Drizzle and/or Rain and Cloud droplets	7
Aerosols and Insects	8
Insects	9

In figure 13 is a simplified block diagram for the atmospheric target classifier utilizing fuzzy logic. The input data of altitude, temperature, pressure, wind (horizontal and vertical), radar and lidar, rain data are converted to membership functions. The membership classes created correspond to the number of atmospheric target classes created, which in this case is nine. The nine classes, which are shown in Table 2, are Ice, Clear sky, Drizzle and/or Rain, Drizzle/Rain and Cloud droplets, supercooled droplets and Ice, Melting Ice, Melting Ice and Cloud droplets, Insects, Aerosols and Insects. There are nine membership functions for each of the input variables. After the fuzzification portion of the logic process is performed then the *If -then* statement aspect of the Rule Inference is carried out based upon the rule base for the classification system. Next, Rule Aggregation is performed to implement all of the Rule Inferences. The last step is the defuzzification which converts the Aggregation into a weighted atmospheric target type.

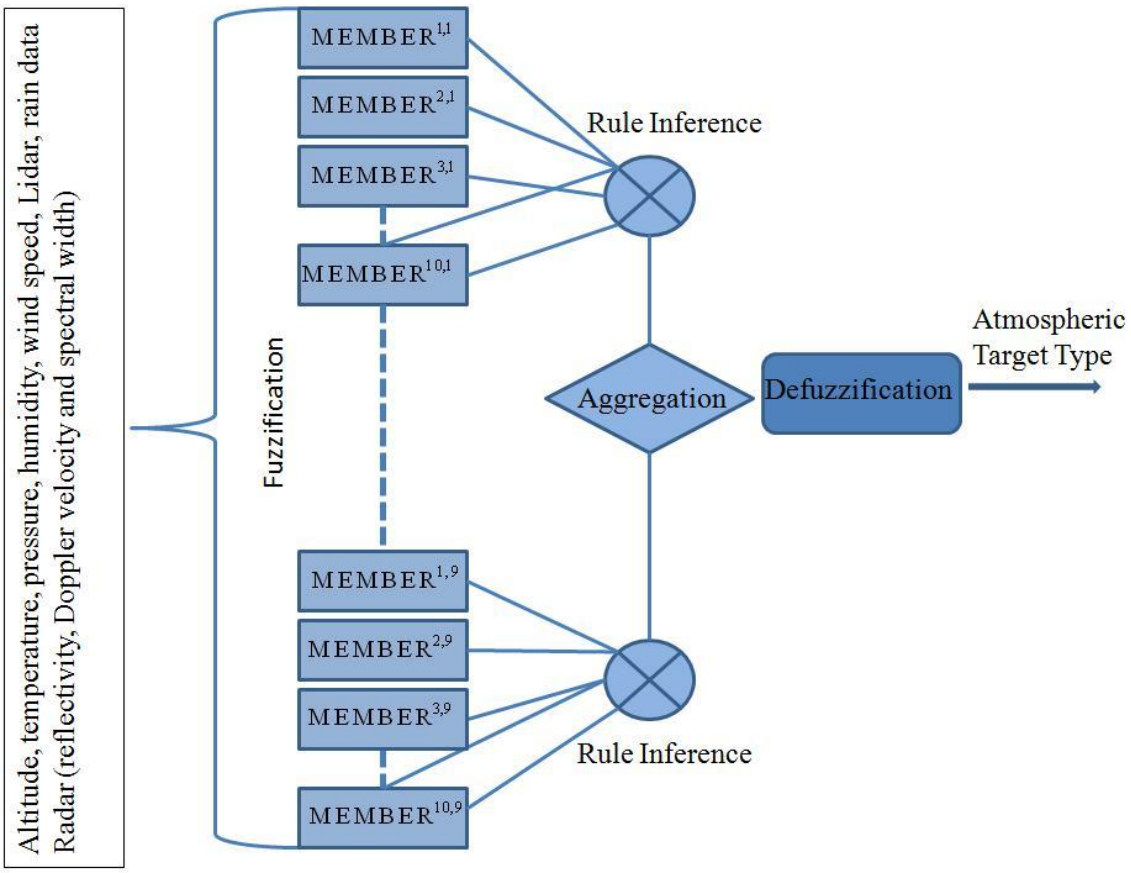

Figure 13: The fuzzy logic diagram for CPA. For the ten items of input data there are a corresponding nine member sets

Atmospheric Target Characteristics

Clouds in the tropics with temperatures of below -16°C are assumed to be ice clouds and above 0°C are considered to be liquid clouds. This parameter is also utilized in the classification masks. The nine classes are shown in Table 2.

The atmospheric targets can be described according to a set of characteristics that enables their identification. Clear sky is identified by a reflectivity less than 35 dBZ. A warm cloud occurs at an altitude below the melting level and has a reflectivity of less than 0 dBZ. Warm precipitation has also a reflectivity greater than 0dBZ and occurs at and below the melting level. The melting level is a band of high reflectivity below 0° iso-

therm where ice melts into raindrops. It appears in the radar as a band of enhanced reflectivity. Supercooled liquid has a reflectivity of less than 10 dBZ with a Doppler width of less than 1 m/s and an altitude of above the melting level but below 8 km with a temperature of about 20°C. Ice occurs most often at levels at 8 Km and above. It has a reflectivity greater than the liquid-ice threshold. Drizzle can be identified with a combination of lidar backscatter, Doppler velocity, spectral width, and radar reflectivity. The ratio of the radar to lidar gives the particle size.

Gridding or Mapping

The term gridding or mapping is when data with different grid systems are 'mapped' on the same map and or grid. In the case of CPA radar, lidar, rain rate, LWP, IWP and other relevant instrumentation data are place on the same height-time grid as the radar. In the case of rain rate, which is a one dimensional data, is added linearly on the radar time axis. Therefore you have two dimensional data and one dimension data on the same time height grid system as the radar.

Target classification

Reflectivity, Spectral Width, and Doppler Velocity

The objective of the Climate Classification Preprocessing Algorithm (CPA) is to provide a graphical representation of the classification of targets at the Atmospheric Radiation and Measurement Program (ARM) Tropical Western Pacific sites (TWP). In addition, CPA provides a standardization of units, instrumentation synergy, data quality flags, provide liquid and gas attenuation compensation, instrument sensitivity signal response,

instrument error indicators, and frameworks lidar, rain rate, liquid water path data on the included on the same time height scale as the radar. In order to develop CPA a familiarity with the ARM data files is developed. This is achieved through the analysis of some of the common information essential in the study of meteorological targets.

A first step in developing a classification of targets in the TWP is familiarization with ARM data and verification of the accurate interpretation of ARM data by CPA. The least problematic path of acquiring knowledge of ARM data, as well as performing some of the preprocessing essential to analysis in climate research is to compare the ARSCL VAP's, figure 11, ability to display the reflectivity, spectral width and Doppler velocity with the CPA interpretation of the same data. The analysis of the data from the TWP site, figure 10, in CPA is performed for the following reasons: 1) When analyzing clouds and other atmospheric targets, the reflectivity, spectral width and Doppler velocity graphs are usually the first set of data diagrams reviewed by scientists. 2) Reviewing the afore mentioned diagrams allows the user to identify the melting level, Figure 13, areas of increased vertical velocity, identification of cloud top and cloud bottom, and identify areas of increased spectral width. 3) The purpose is also to gain experience analyzing ARM data for the TWP sites which is easily verifiable through comparison with the ARSCL VAP. This process also provides experience in processing large sums of ARM data which is essential in creating the CPA algorithm. Reflectivity is a measure of the returned power. The reflectivity is sensitive to the size and the number of hydrometeors. The spectral width is a measure of the spread of the Doppler spectrum. The spectral width is sensitive to the spread in the particle size spectra. The Doppler velocity can be utilized to identify the melting level because the area of greatest Doppler velocity is usually the melting lev-

el. The importance of these figures in the analysis and identification of atmospheric targets is apparent. Moreover, a larger spectral width, which is a spread in the Doppler velocity, is indicative of the presence of the varying array of targets in the atmosphere.

The data that are gathered at the ARM TWP sites, which are utilized to create the aforementioned graphs, are a combination of millimeter cloud radar (MMCR), Micropulse lidars, laser ceilometers, and microwave radiometers are employed to produce a time height graphs of cloud particulates in the TWP. This data provides essential information for accessing the radiative effects of clouds on climate and determination of hydrometeor height distributions.

A comparison of figures 14 and 15, as well as figures 16 and 17, demonstrates that with the same data files, CPA is able to create graphical representations of the reflectivity, Doppler velocity and spectral width graphs that are virtually identical to those created by the ARSCL VAP from the TWP Manus site for March 13, 2000 and March 14, 2000 respectively. These graphs are utilized frequently as first step in analyzing atmospheric targets. The data files involved includes data from the MMCR, SMET, and VCEIL instrumentation. This is the first step in data fusion or synergy, where different data streams from different instrumentations are utilized to for analysis of the atmosphere. The next phase in the development of CPA is to identify the melting layer from the data files. Additional reflectivity, spectral width and Doppler velocity graphs can be found in the Appendix.

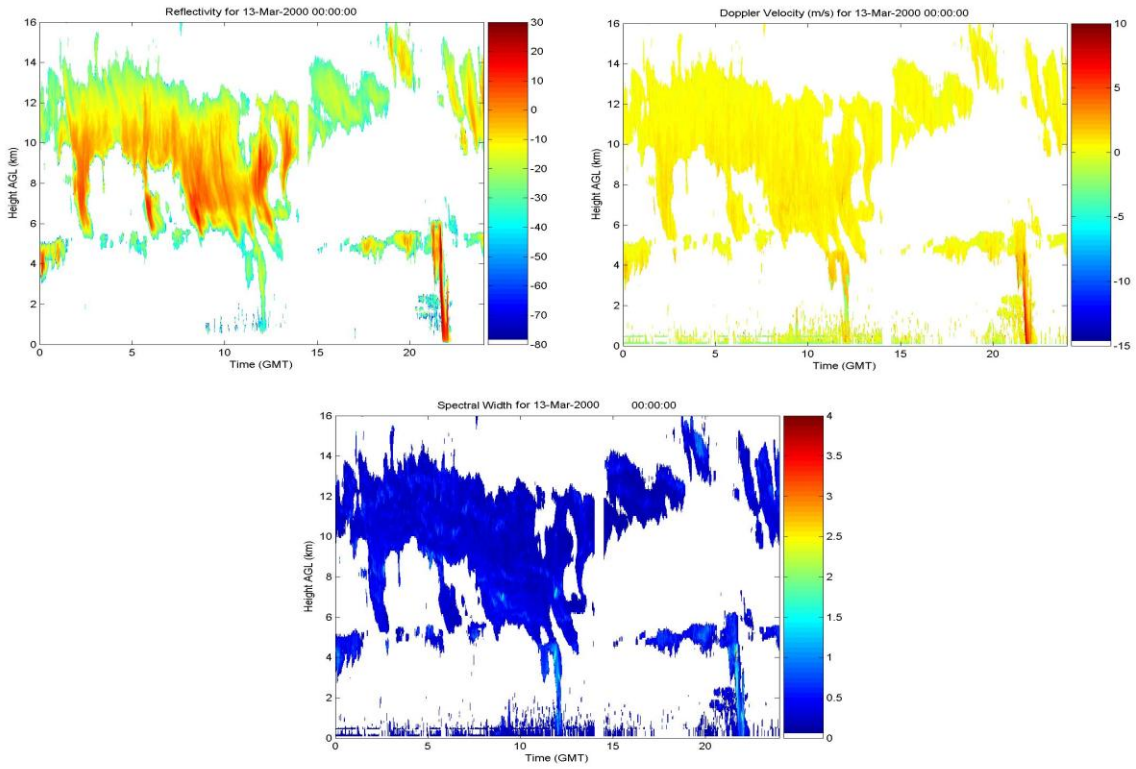

Figure 14: These are the reflectivity, velocity, and spectral width diagrams for March 13 2000 for the TWP site of Manus. These figures were created using CPA. In these diagrams there is an increase in reflectivity from 5km to 10 km. This area is mostly associated with mixed phased clouds. These graphs are the first essential diagrams utilized to identify cloud particulate and targets of interests. These were created from ARM data using a developed algorithm. This figure displays cumulus, altocumulus, altostratus, and cirrus clouds found in highly convective areas.

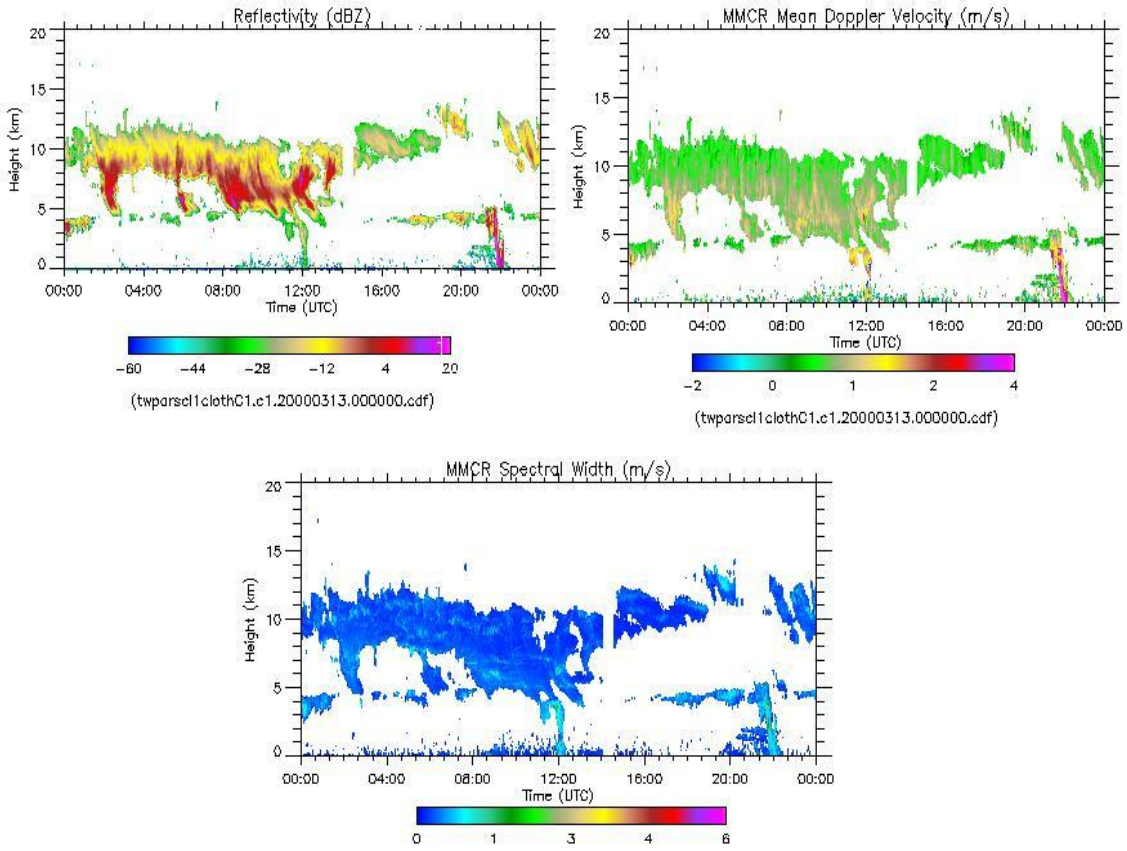

Figure 15: In this figure are the ARSCL VAP's Reflectivity, Doppler Velocity, and Spectral Width for March 13, 2000. These graphs are compared for verification of accuracy of algorithm to produce the same graphs that are part of CPA. The figures are essentially identical in there graphs[3]. Comparing figure 15 with figure 14 shows similarities in shape, height, time, and dimension of cloud formations as well as other atmospheric targets.

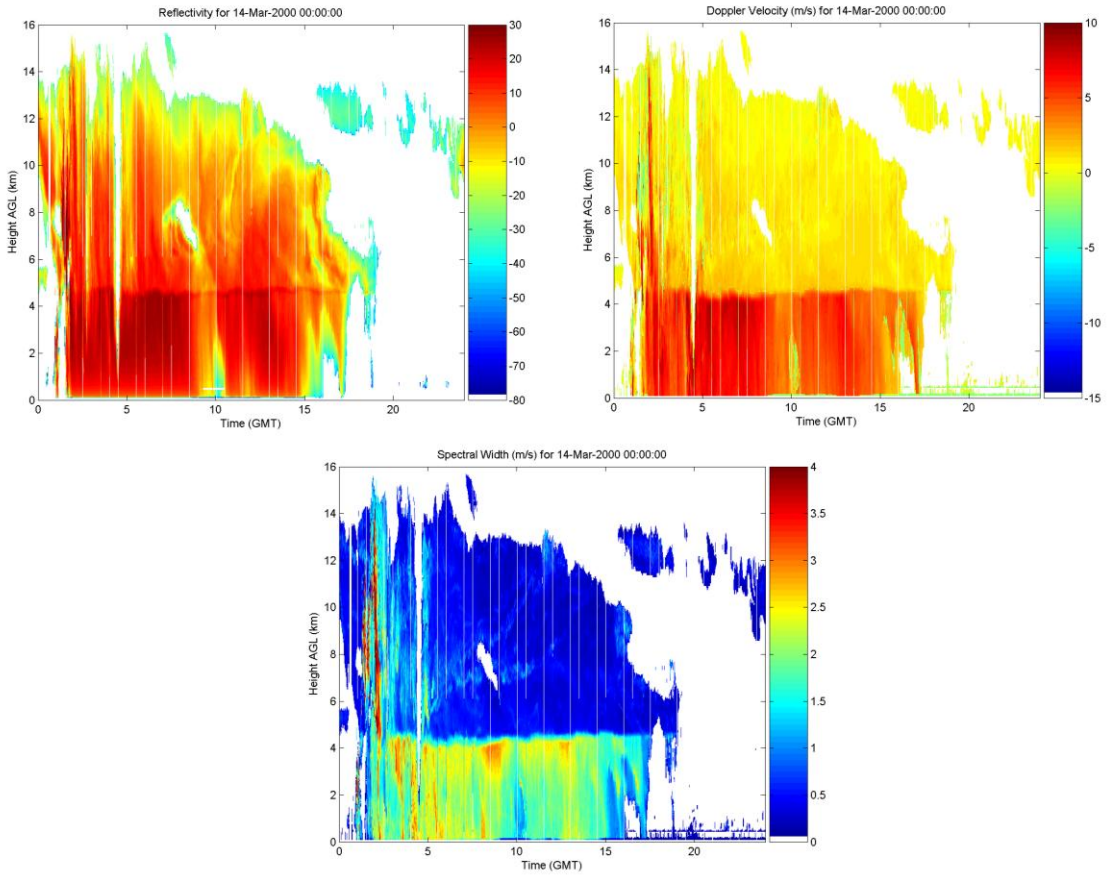

Figure 16: This is the reflectivity, spectral width and the Doppler velocity for the TWP Manus site on March 14 2000. These figures show an increase in reflectivity and Doppler velocity at approximately 4 km above ground level, identify the melting layer. These figures were created from ARM data utilizing the developed algorithm(CPA) and are compared to the same figures develop with the ARSCL VAP (figure 14) graphs for a verification of the correct interpretation of data from CPA.

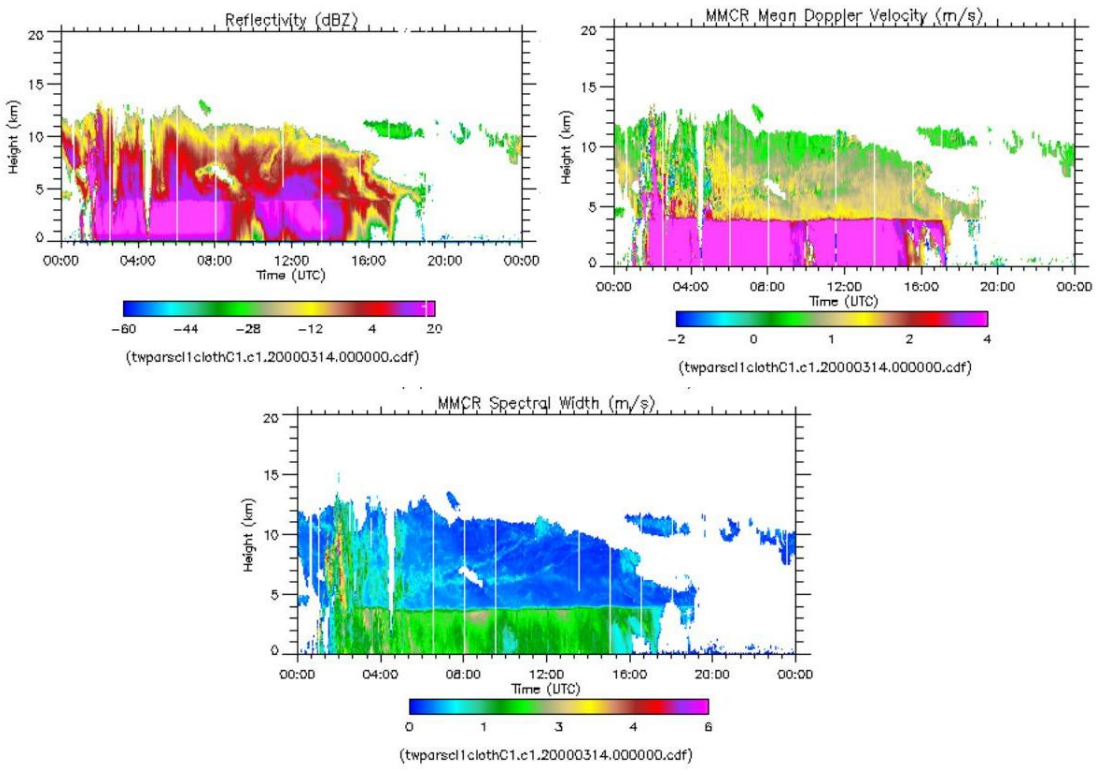

Figure 17: The ARSCL VAP's reflectivity, Doppler velocity and Spectral width for the ARM TWP Manus site for March 14 2000. These figures show an increase in reflectivity and Doppler velocity at approximately 4 km above ground level, identify the melting layer. These figures were created from ARM TWP data analyzed with the ARSCL VAP [3].

Melting Layer Identification

The melting layer is defined in general as the layer with the area of greatest divergence in Doppler velocity. In general the melting layer is approximately at 4km to 4.5km above ground level (AGL). It is often called the "bright band" due to the enhanced reflectivity in this region. The melting layer denotes the layer below 0°C isotherm where ice melts and turn into rain. The study of the melting layer is significant satellite research due to the melting layers degrading effect on satellite communications. The microphysics of the melting layer of precipitation is a significant attribute of stratiform precipitation. The melting layer can also be determined from the spectral width graphs as well. There is a

great increase in spectral region around 4km to 4.5km AGL. The spectral width can also be utilized to detect large sizes of hydrometeors that pass through the melting layer for example hail [3, 16, 5, 12, 15, 4, 17, 24].

In order to identify the melting layer in the datastream the first of many characterization masks was created for the CPA algorithm. Characterization masks or memberships are simply commonly known identification characteristics of a cloud of any atmospheric target of interest. In the case of the melting layer, it can be easily identified by the knowledge that the layer exists at 4 to 4.5km AGL. Another characteristic of the melting layer is enhanced reflectivity, as well as within the 5°C of 0°C isotherm and the area of greatest increase in Doppler velocity a characteristic of the melting layer. In figure 15 the combining of lidar and radar sensors both active and passive sensors enable the identification of the melting layer. These characteristics form a classification mask that allows the melting layer to be identified. When the CPA is discussed in detail the several characterization or classification masks are developed to aid in identification of the drizzle, ice, clear sky, precipitation, super cooled liquid, to name a few.

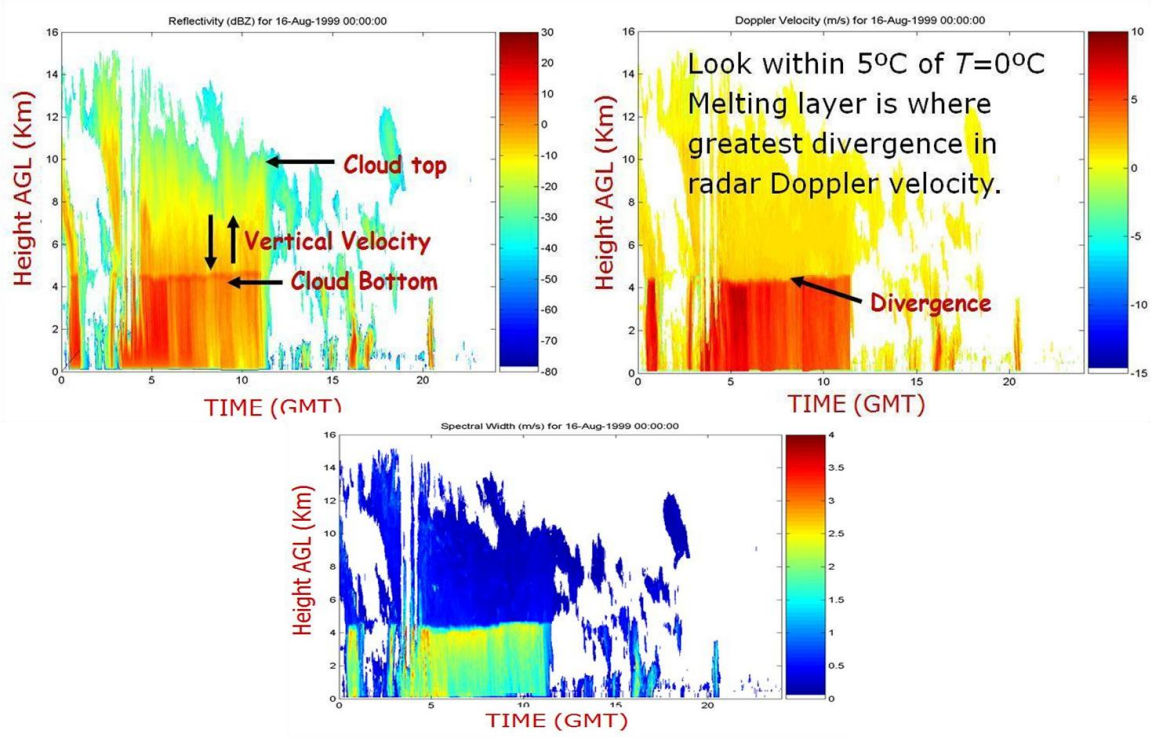

Figure 18: Melting Layer identification using the reflectivity, Doppler velocity, and spectral width data. From the MMCR, MPL, and VCEIL instruments at the TWP site enable the identification of the melting layer.

Figure 18 consists of the reflectivity, the Doppler velocity and the spectral width graphs from the millimeter wave cloud radar (MMCR). Cross referencing the MMCR data with the data from the Micropulse lidar (MPL) and the Vaisala Radiometer (VCEIL) the melting layer is identified. In Figure 18 the enhanced reflectivity along with the great divergence in Doppler velocity indicate the melting level at the TWP site of Manus. The cloud top and bottom are clear indicated with all three graphs when aided with the data from the VCEIL and the MPL. The spectral width is the spread of the Doppler spectrum. The yellow and red at the melting layer in the spectral width graph in figure indicates range of hydrometeors. The red in particular in the spectrum graph indicates particles that did not melt at the melting layer.

Modified Contour Frequency by Altitude Diagrams (M-CFAD)

Yuter and Houze in 1995 was the first to present contour frequency by altitude diagrams (CFAD). In Yuter and Houze's 1995 paper the CFAD is used as a statically method to examine the evolving properties of radar reflectivity, vertical velocity and spectral width over a storm event. The mathematics of CFAD's for a two dimensional histogram, where N is the frequency distribution function, the total number of points is defined as

$$N_t = \int_{-\infty}^{+\infty} \frac{\partial N(A)}{\partial A} dA = N_{t1} + N_{t2} + N_{t3} + \cdots \quad (1.1)$$

such that $\frac{\partial N(A)}{\partial A} dA$ is the number of observables of A in the range of A to $A + dA$ with a constant bin width of ΔA and the ordinate has values of frequency $N_{ti}(\Delta A)^{-1}$. The right hand side of equation 1.1 corresponds to the number of terms in the finite interval ΔA. The terms represent the area under one bar of the histogram:

$$N_{ti} = \int_{A}^{A+\Delta A} \frac{\partial N(A)}{\partial A} dA, \ i = 1,2,3, \ldots \quad (1.2)$$

In the case of a three dimensional plot, h is the height and $N(A, z)$ is the frequency distribution function such that $\frac{\partial N(A,z)}{\partial z \partial A} dz\, dA$ is the number of observations of A in the range of A to $A + dA$ at heights in the range of z to $z + dz$. Thus the total number of points in the volume is

$$N_T = \int_{-\infty}^{\infty} \int_{0}^{h} \frac{\partial^2 N(A,z)}{\partial z \partial A} dz dA \quad (1.3)$$

Consequently, the number of points in a bin is defined by z_j and A_i is

$$N_{Tij} = \int_{A_i}^{A_i+\Delta A} \int_{z_j}^{z_j+\Delta z} \frac{\partial^2 N(A,z)}{\partial z \partial A} dz dA, \ \ i = 1,2,3, \ldots, \ j = 1,2,3, \ldots \quad (1.4)$$

In the case of CFADs a constant vertical bin size of Δz is used that corresponds to the Cartesian volume grid spacing. Therefore since both ΔA and Δz are constants, the fre-

quency of occurrence of points per bin is $N_{Tij}(\Delta z \Delta A)^{-1}$. The normalization of the plot by the number of points at each level is often the next step in creation of CFADs. The total number of points in each bin, (1.4), is divided by N_{zj}, the number of points at each level z_j and then multiplied by 100 to express it in terms of percentage. Normalization by the number of points can have the effect of increasing the percentages at the top where there are fewer points, but it makes it easier to compare the diagrams [19, 25, 24].

In the CPA algorithm modified contour frequency by altitude diagrams (M-CFAD) are created that can be modified to sample the reflectivity, spectral width and Doppler velocity over various periods of time. M-CFAD's allow the specific stratification of data by height for specific time periods specified by the user. From these diagrams the identification, as a function of altitude and time, of regions of the atmosphere that contain hydrometeors can analyzed. The detection statistics of these attributes are quantified utilizing frequency distributions. The M-CFADs displays the probability of observation a radar reflectivity range for example at a given altitude. At each height the frequency of observing a given range of reflectivity values is illustrated by the color bar. M-CFAD's in the CPA program reveal statistically distribution of particles types of various periods of time which is specified by the user. The detection statistics of various cloud types and other atmospheric targets are quantified using frequency distribution contoured graphs by altitude. The graphs show the probability of observing a radar reflectivity value (Z) within a reflectivity range at a given height. At each height, the frequency of observing a given range of reflectivity values is illustrated by the color bar.

In figure 19 at a height of approximately 4.5 km above ground level (AGL) shows aspects of bimodality. The bimodality implies sharp gradients between dry and moist re-

gimes in space time. This is also an indicator of the melting layer. For the lower several kilometers the low reflectivity values of less than -10bBZ are indicators of liquid boundary layer clouds with maximum reflectivity increasing with altitude and peak relative humidity near 500 meters. From about 8.5 to 15km these values correspond to ice clouds particularly cirrus and anvil overflow from deep atmospheric convection. Clouds in this section display a decreased reflectivity with height. The decrease in reflectivity is possibly an indication of ice particles settling to the bottom of the cloud. The maximum frequency of occurrence of an ice cloud layer is about 12km. In figure 16 from -5 to 17dBZ is an area of high reflectivity. This feature may correspond to moist layers in the mean relative humidity profile. The values of reflectivity less than -60 dBZ are understood to be clear sky and are not displayed but they are incorporated in the calculation of the frequency distributions. The treatment of anything less than -60dBZ reflectivity being considered clear-sky is another characteristic mask developed that will be utilized in CPA. Below 5km there is an expanse of high reflectivity that is associated with precipitation. Although the millimeter cloud radar (MMCR) can see through drizzling clouds, it saturates in heavy precipitation.

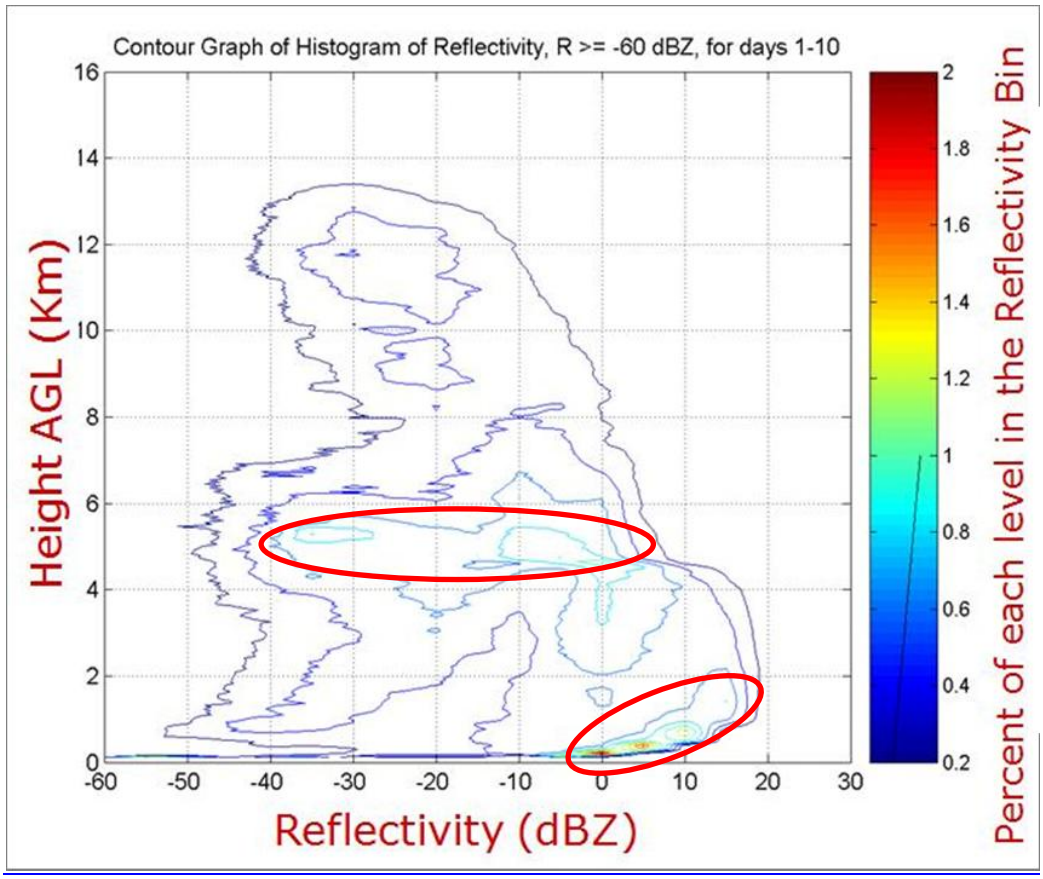

Figure 19: This modified contour frequency by altitude graph (M-CFAD) illustrates some of the types of clouds found in the tropics. In this case various types of cumulus and cirrus clouds. The detection statistics are displayed in terms of the M-CFADs. The M-CFAD displays the probability of observing a radar reflectivity within a given altitude. The lower several kilometers the low reflectivity values (< -10dBZ) are indicators of liquid boundary layer clouds. The top red ellipse demonstrates bimodality in the 10 days of data. The bimodality indicates sharp gradients between dry and moist regimes.

Figure 20 is the M-CFAD for the velocity corresponding to the same 10 days analyzed in figure 19. The Doppler velocity is the radial constituent of the velocity vector of a scattering object as observed by a remote sensor. The Doppler velocity from 2km AGL to ground level and Doppler velocity from approximately 0 to 8 m/s corresponds to the increase in reflectivity in figure 19 in the same region.

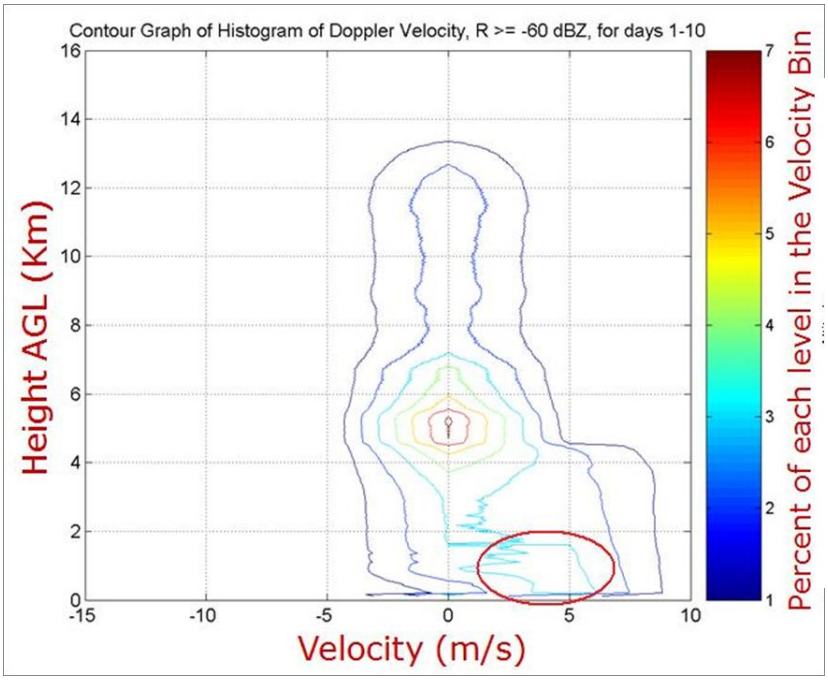

Figure 20: This is the M-CFAD for the velocity corresponding to the same 10 days analyzed in figure 16. The Doppler velocity is the radial component of the velocity vector of a scattering object as observed by a remote sensor. The Doppler velocity from 2km AGL to ground level and Doppler velocity from approximately 0 to 8 m/s corresponds to the increase in reflectivity in figure 16 in the same region.

In figure 20 is the M-CFAD of the spectral width for the same 10 days of data as figures 18 and 19. The spectral width depends upon the spread of the terminal fall speeds of the scatterers. This effect is more pronounced for rain than for snow. The spectral width also depends upon the turbulence of the air particularly upper levels in highly convective areas, and the vertical wind shear e.g., along a gust front. In figure 18 the flat area at the height of about 4 to 4.5 km AGL clearly indicates the melting layer. The top circle which is at about 4.5 to 8km AGL shows a spectral width of 1 to 1.5 which is a great increase in spectral width when compare to figure 19 which is essential flat in this same region. The increased spectral width in figure 18 for the 10 day period is an indicator of an expansive range of sizes of hydrometeors.

The M-CFAD figures can be created in CPA for various time periods such as 14 days, 30 days, 60 days, 90 days, 6 months, and 9 months, an example of which is in figures 18, 19, and 20. In figure 18, is the M-CFAD of the spectral width for ten days in 2000. It summarizes the frequency distribution of a target in a given radar echo volume. In figure 19 is the M-CFAD of the spectral width for 90 days in 2000. The focus of figure 19 is on the melting layer to about 9Km AGL which is the area most associated with mixed phase clouds. In figure 20, the focus is on the lower level particulates and hydrometeors. By analyzing this data along with velocity and reflectivity M-CFAD's for the region the frequency of occurrence of particulates can be identified. In the CPA algorithm the time period is specified by the user with the limitation that time periods must be consecutive. For example if the user wishes to perform a 14 day M-CFAD to analyze hydrometeor trends in a region the algorithm will not allow disjointed dates to be one M-CFAD, i.e. user must specify day 1-14, 2-15…etc.

In figures 21, 22, 23, 24 and 25 are MCFAD's for various time periods. In figure 21 is a modified contour frequency by altitude diagram (MCFAD) of the spectral width for the isle of Manus for days 1-10 of 2000. In this figure the diagram is stratified by altitude with filters for clear sky, aerosols (through there is little aerosols in the tropics) insects. By analyzing these types of graphs it can summarize the frequency distribution of a target in a given radar echo volume. In figure 22, the M-CFAD for the spectral width is stratified to focus on the data from the melting layer to about 9km AGL which is the area most associated with mixed phase clouds. By analyzing this data along with velocity and reflectivity M-CFAD's for the region, the frequency of occurrence of particulates can be identified. In figure 23 is a diagram of the reflectivity for days 1-120 for the year 2000. In

this figure the focus is only on the height below the melting level. The high reflectivity below 2 km AGL can be caused by hydrometeors falling through the melting layer. In figure 24, the melting level is clearly identified at 4 to 4.5 km AGL. The spectral width at the height of 4.5 to 8km AGL is a significant value. This indicates a wide spread of targets during the 10 days sampled. In figure 25 the spectral width for 10 days of data are displayed. The melting layer is clearly identified between 4 and 4.5 km AGL. The spectral width from 4.5 km AGL to 8Km AGL ranges from 1 to 1.2. This figure's spectral width is much smaller than the values for figure 18's spectral width in the same region. This indicates less hydrometeors and particulates during figure 19's 10 day sample.

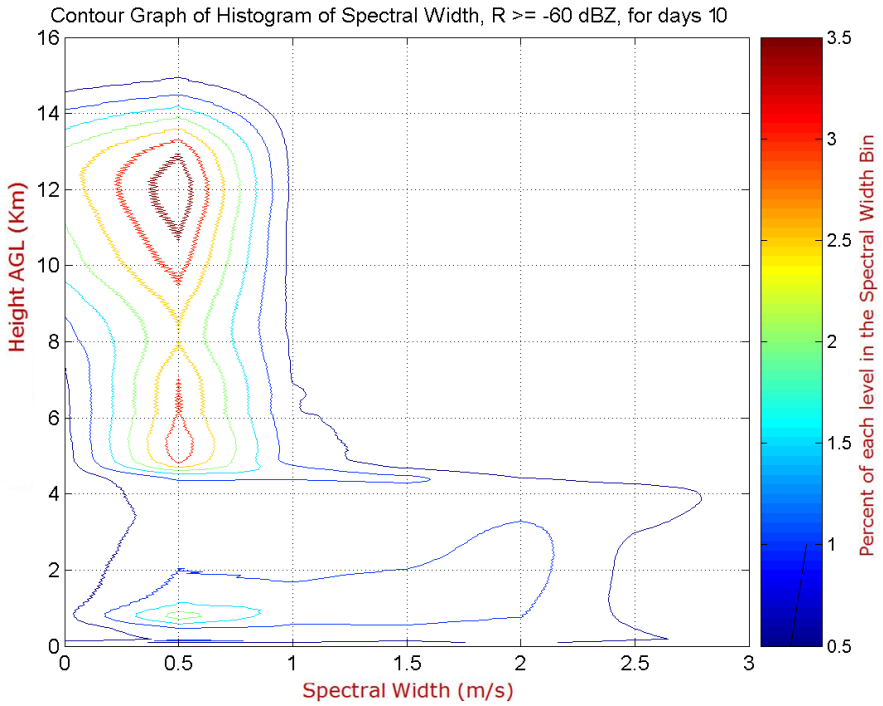

Figure 21: A Modified Contour Frequency by altitude diagram of the spectral width for the isle of Manus for days 1-10 of 2000. In this figure the diagram is stratified by altitude with filters for clear sky, aerosols (through there is little aerosols in the tropics) and insects. By analyzing these types of graphs it can summarize the frequency distribution of a target in a given radar echo volume.

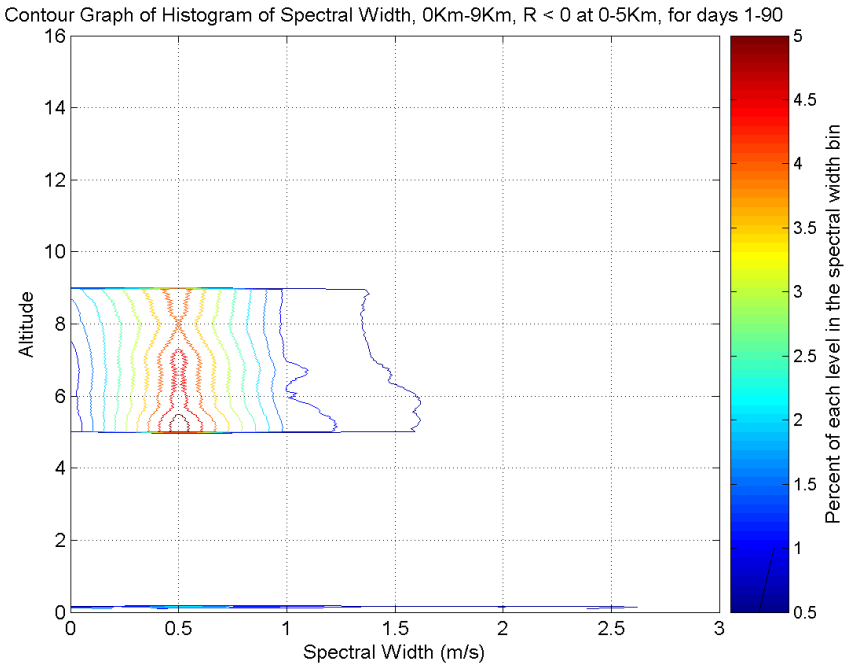

Figure 22: In this figure the M-CFAD for the spectral width is stratified to focus on the data from the melting layer to about 9Km AGL which is the area most associated with mixed phase clouds. By analyzing this data along with velocity and reflectivity M-CFAD's for the region the frequency of occurrence of particulates can be identified.

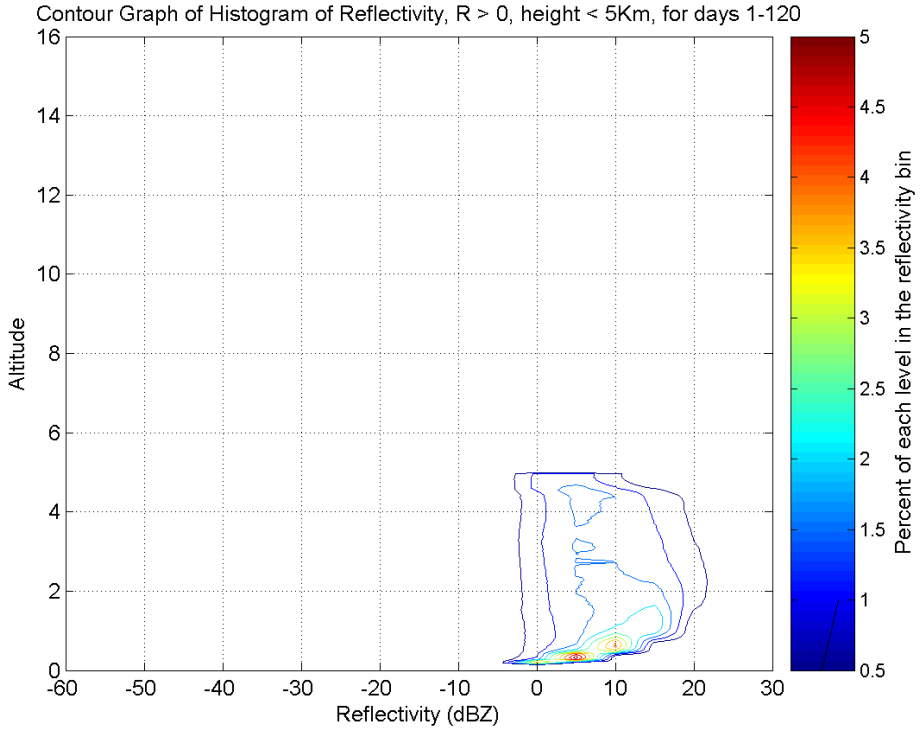

Figure 23: This is the M-CFAD diagram of the reflectivity for days 1-120 for the year 2000. In this figure the focus is only on the height below the melting level. The high reflectivity below 2 Km AGL is due to hydrometeors falling through the melting layer.

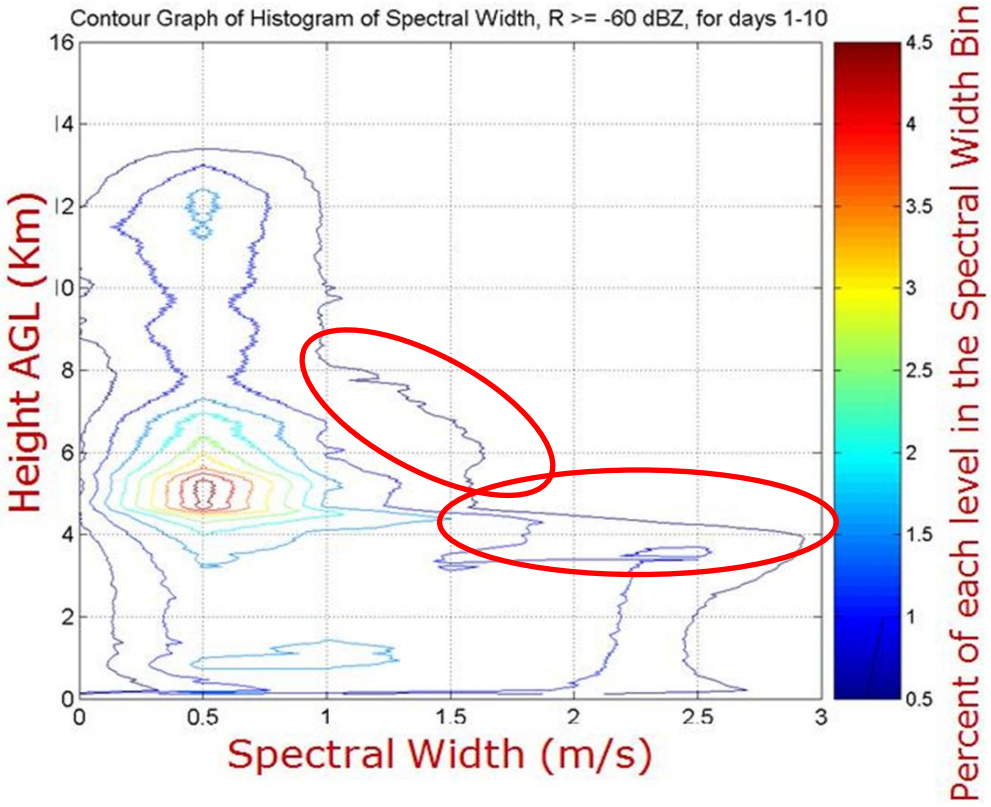

Figure 24: In this figure the melting level is clearly identified by the ellipse at 4 to 4.5 km AGL. The spectral width at the height of 4.5 to 8km AGL is a significant value. The ellipse at 4.5 to 8km indicates a wide spread of targets during the 10 days sampled.

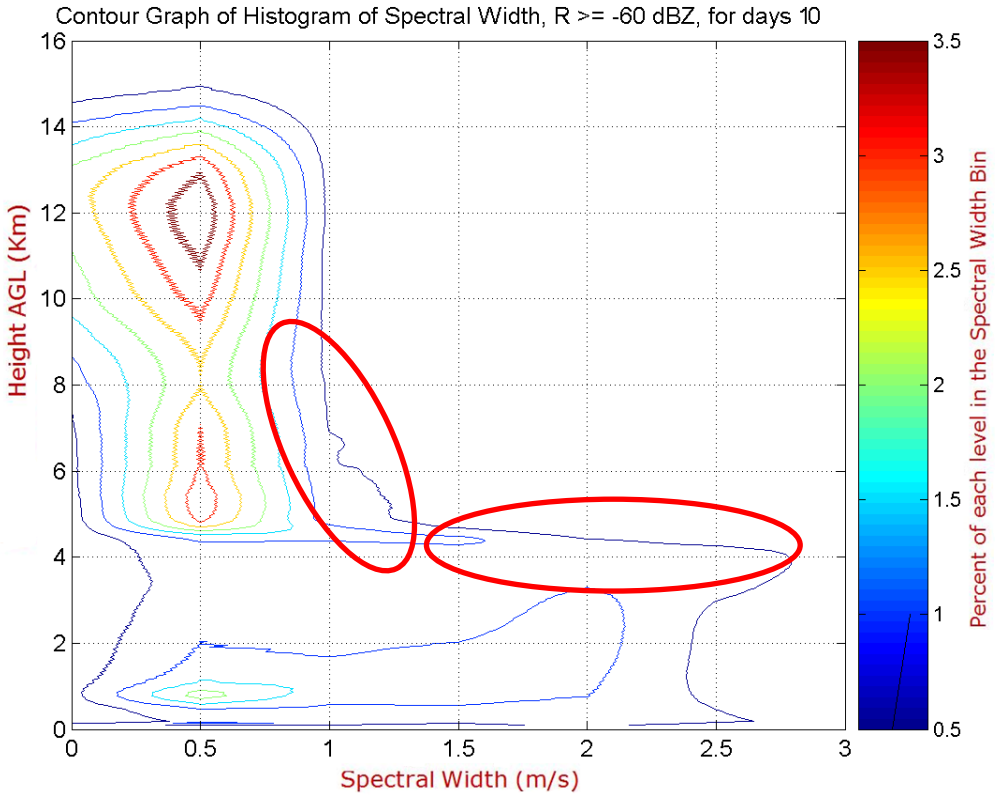

Figure 25: In this figure the spectral width for 10 days of data are displayed. The melting layer is clearly identified by the ellipse between 4 and 4.5 Km AGL. The spectral width from 4.5 Km AGL to 8Km AGL, indicated by an ellipse, ranges from 1 to 1.2. This figures spectral width is much smaller than the values for figure 18's spectral width in the same region. This indicates less hydrometeors and particulates during figure 19's 10 day sample.

Ice Water Content, Liquid Water Content, Condensed Water Content

The Department of Energy funded Atmospheric Radiation and Measurement Program (ARM) consists of on-site instrumentation measurements at several sites throughout the world with one mobile unit. The research in this dissertation focuses on the Tropical Western Pacific (TWP) sites of the islands of Manus and Nauru. The instruments at the TWP sites , Table 1, includes microwave radiometers (MWR), which provides measurements of column integrated water vapor, Radiosondes which are launched twice a day,

provide vertical distributions of temperature and water vapor, Micropulse lidar (MPL) and ceilometer provides vertical distributions of hydrometers, millimeter wavelength cloud radar (MMCR), which provides microphysical cloud properties and cloud location. In identification of targets in the atmosphere delineation of temperature, water vapor and pressure are essential in the identification. The radar reflectivity, figure 27, and temperature profiles are utilized to retrieve cloud water content. Clouds in the tropics with temperatures of below -16°C are assumed to ice clouds and above 0°C are considered liquid clouds. The clouds that are intermediate in temperature may be mixed phase. This parameter is also utilized in the classification masks.

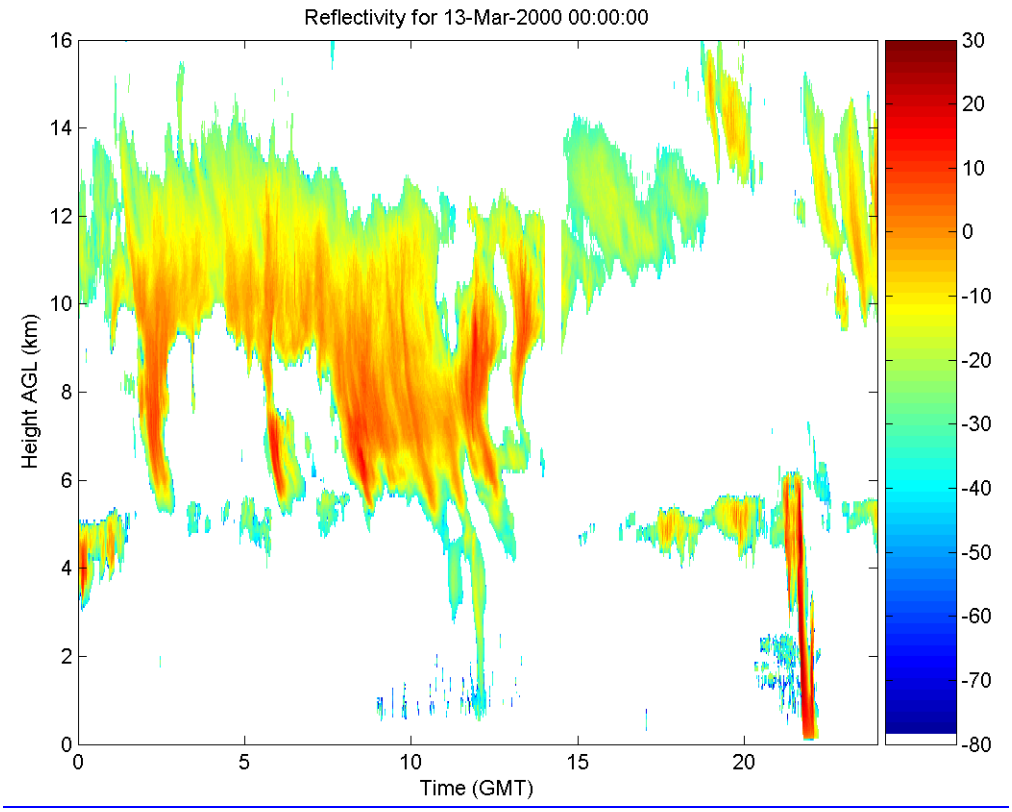

Figure 26: In this reflectivity graph for March 13 2000 displays clouds typical for the TWP site. There is drizzle at approximately 22 GMT. The drizzle is the bright red stream that reaches to the ground in the figure. Cirrus, Shallow cumulus, altocumulus and alto stratus clouds are also present in this figure.

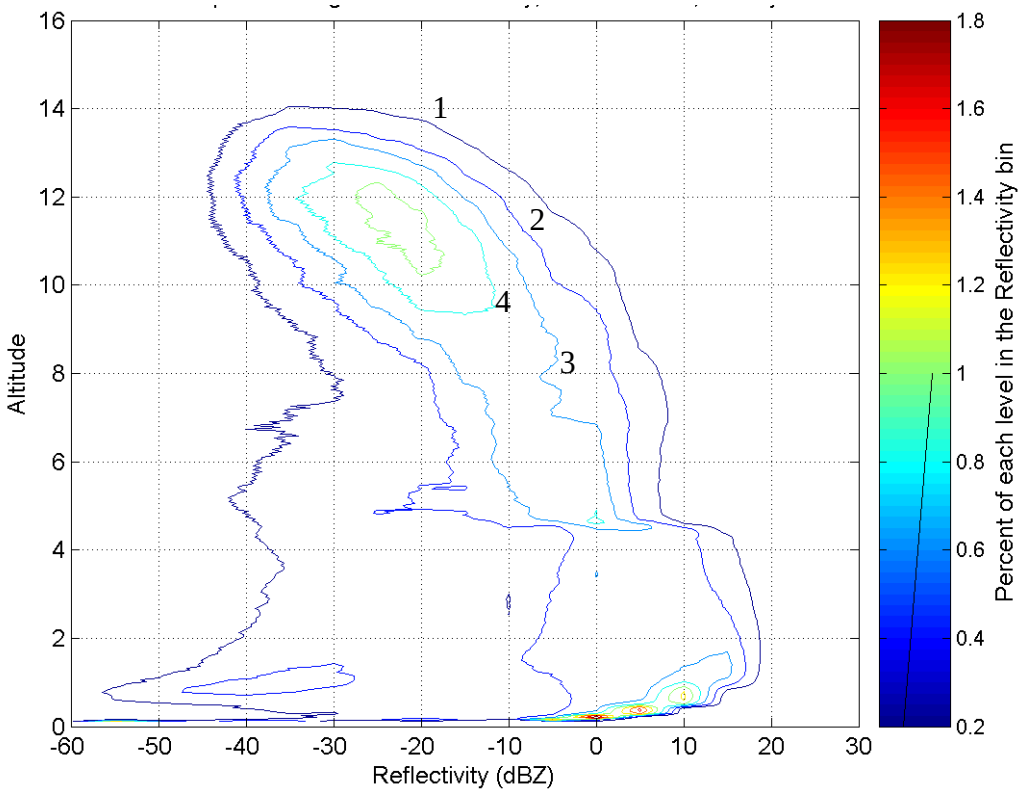

Figure 27: This is a figure of the reflectivity frequency distribution for Manus. Clear sky is set as reflectivity values less than -60dBZ. The graph reveals 4 distinct features, which are moist layers, in the cloud profile.

There are several ways to calculate liquid water content (LWC) and ice water content (IWC). The method utilized in this research is a combination of the adiabatic and linear regression approach created by Liao and Sassen with the density of water feature from the work of Frisch et al., 1995 and a modified number concentration of 74 cm^{-3} with a standard deviation of 45cm^{-3} $cm^{-3}$for stratocumulus and status clouds combined with radiometer and lidar observations. In the adiabatic method values of the liquid water content which varies with height in the cloud is a regression calculation where

$$LWC = \left(\frac{N_d Z}{3.6}\right)^{\frac{1}{1.8}} \quad (1.5)$$

and N_d $N_d$is the number concentration. The liquid clouds in this case are then the lognormal size distribution with width of σ = .35 $\sigma = .35$with mode radius $r_m = \left(\frac{3LWC}{4\pi\rho_w N_d\left(e^{9\sigma^2}\right)}\right)^{\frac{1}{3}}$, where ρ_w $\rho_w$is the density of water. The ice clouds have a regression equation of $IWC = (.097)Z^{.59}$ with an effective radius of $r_e = \left(\frac{75.3+.5895T}{2}\right)$. Although ice dominates the radar signal in mixed phase clouds, the liquid aspects of the mixed phase cloud dominates the radiative transfer due to the small particle size and the larger mass of the liquid. These calculations are performed based on the supplied reflectivity, and temperature. The combination of the liquid and ice content is the condensed water content (CWC). An improved value for IWC can be achieved by utilizing temperature along with reflectivity [19,111]. The calculation of IWC is a function of reflectivity and all atmospheric particulates have temperature dependence.

In figures 28, 29, and 30 are the CWC for March 8, 13 and 14 of 2000. In figure 28 there is an increase in CWC from 8 to 0 Km AGL. In figures 29 and 30 for the Manus Tropical Western Pacific (TWP) site are shown the kinds of clouds typically found in the tropics. Shallow Cumulus, altocumulus, altostratus, and cirrus are just a few of the cloud types shown in these graphs. As expected the main features of the CWC in figures 29 and 30 corresponds to their corresponding reflectivity graphs in figures 27 and 16, respective-ly.

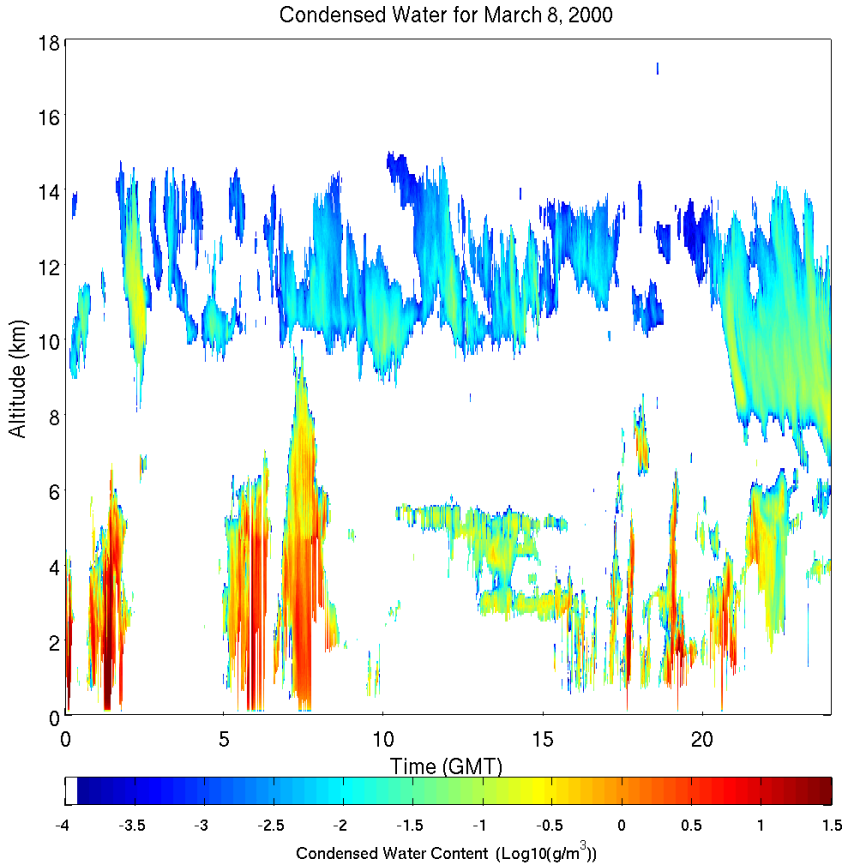

Figure 28: In this figure is the calculated Condensed Water Content from the insitu data at the TWP sites. The water content increases in the middle and lower levels of the atmosphere.

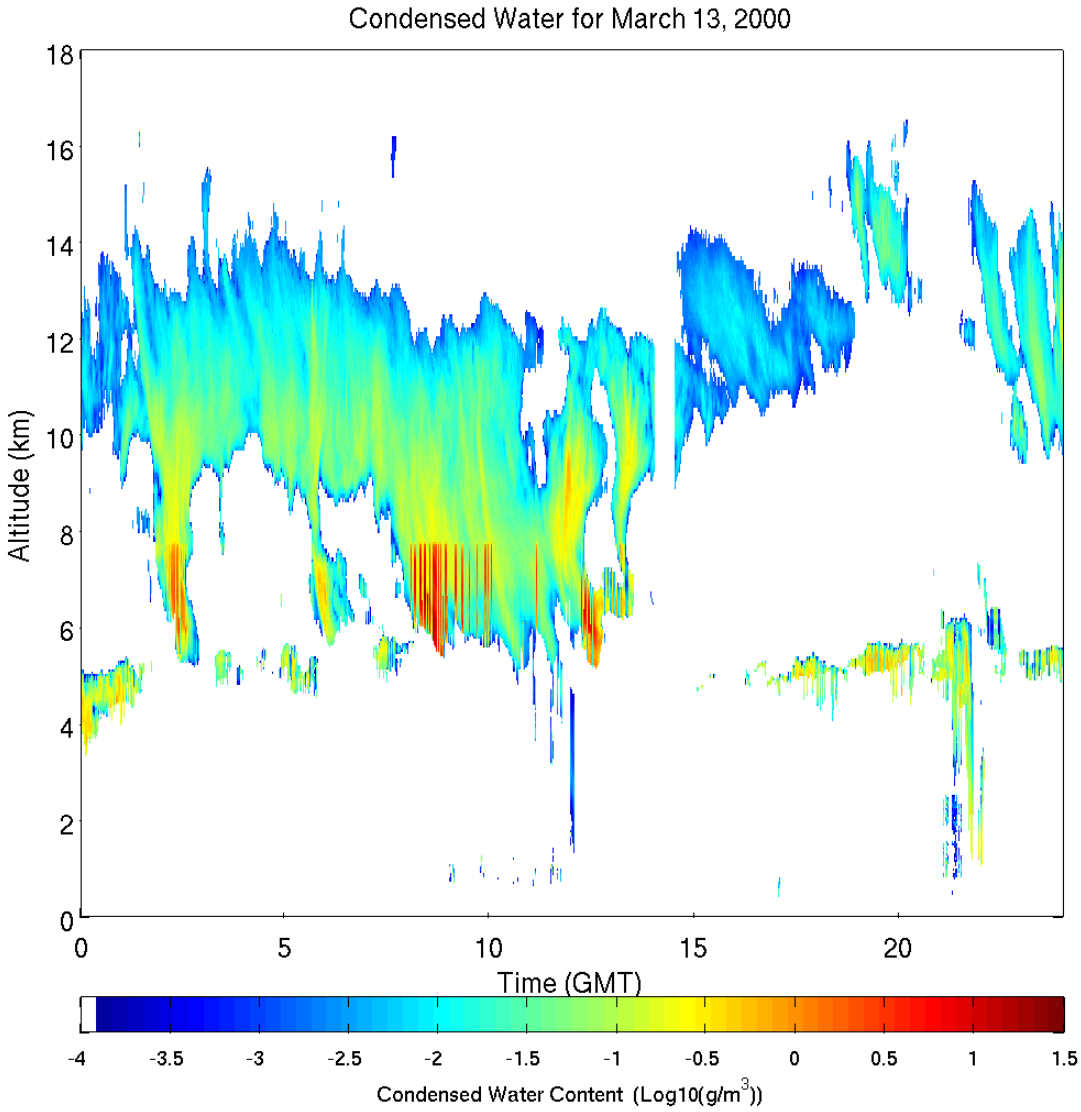

Figure 29: In this figure is the calculated Condensed Water Content from the insitu data at the TWP sites. This figure corresponds to the reflectivity figure 26. The deep yellow streaks from 10 Km to 6Km combined with the red streaks at 8 to 6 km indicate the presence of mixed phase clouds (cloud with ice and water content.

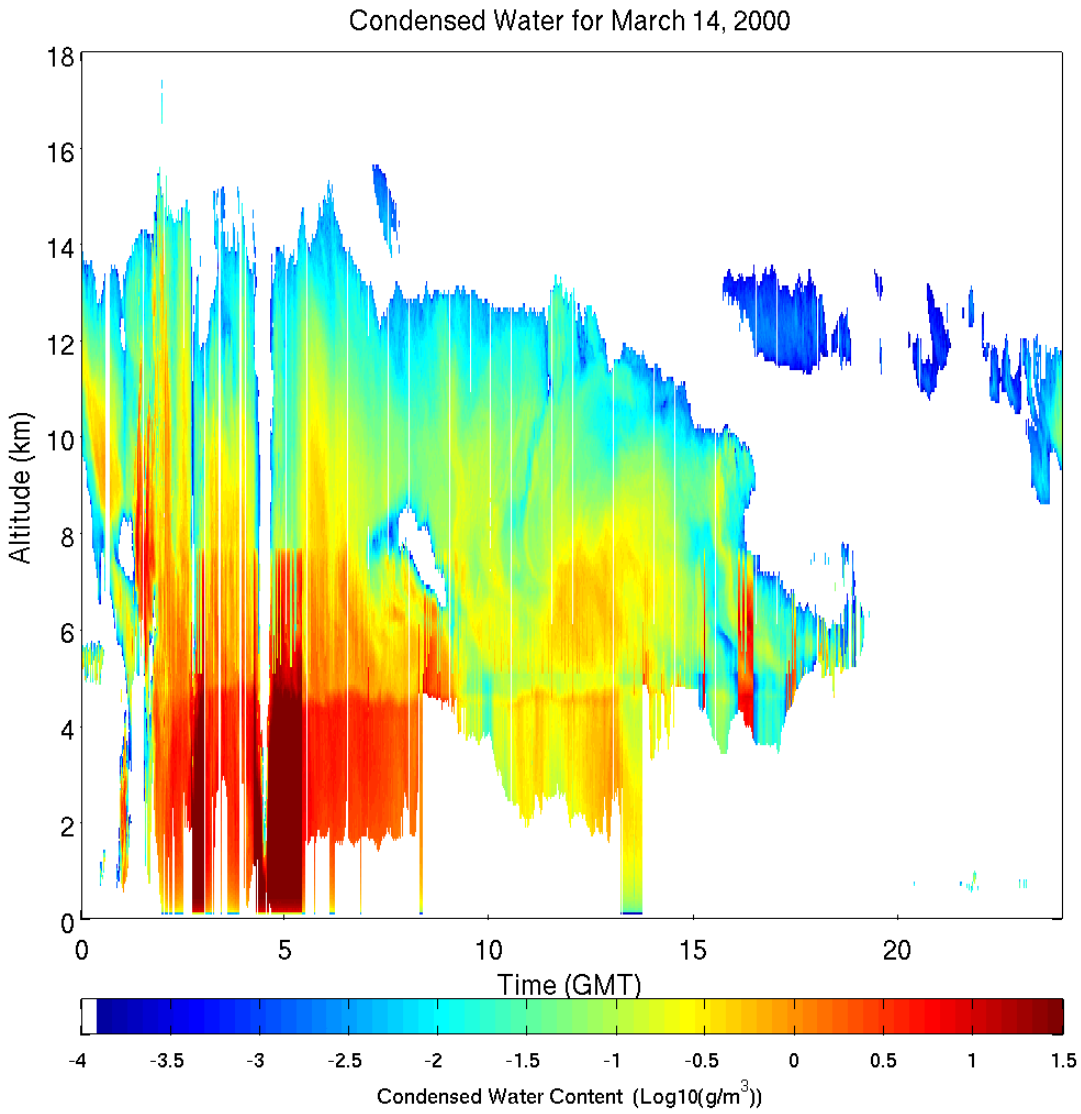

Figure 30: In this figure is the calculated Condensed Water Content from the insitu data at the TWP sites for March 14, 2000.

Each pixel of the image is classified in terms the membership created by the CPA. The classification determines through neural fuzzy-logic whether the there is the presence of ice, insects aerosols, and liquid droplets. Figure 31 is the classification of atmospheric target types for March 13, 2000 for the isle of Manus. There are supercooled droplets as well as ice indicating mixed phase clouds. There is also a trail of precipitation at 22hours.

Figure 32 is the classification for the island of Manus for March 14, 2000. In this figure there is heavy rain and the melting level is clearly indicated at approximately 5Km.

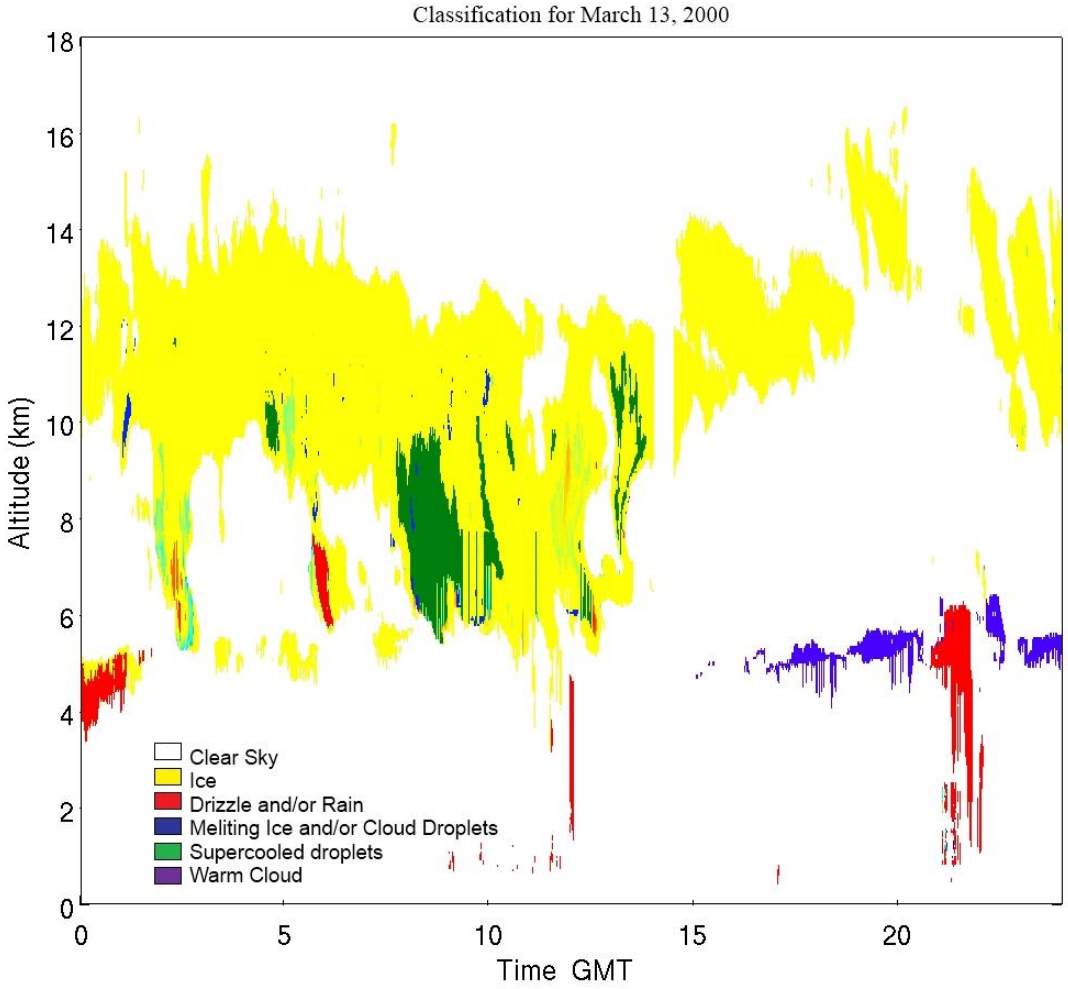

Figure 31:This is the classification of atmospheric target types for March 13, 2000 for the isle of Manus. There are supercooled droplets as well as ice indicating mixed phase clouds. There is also a trail of precipitation at 22hours.

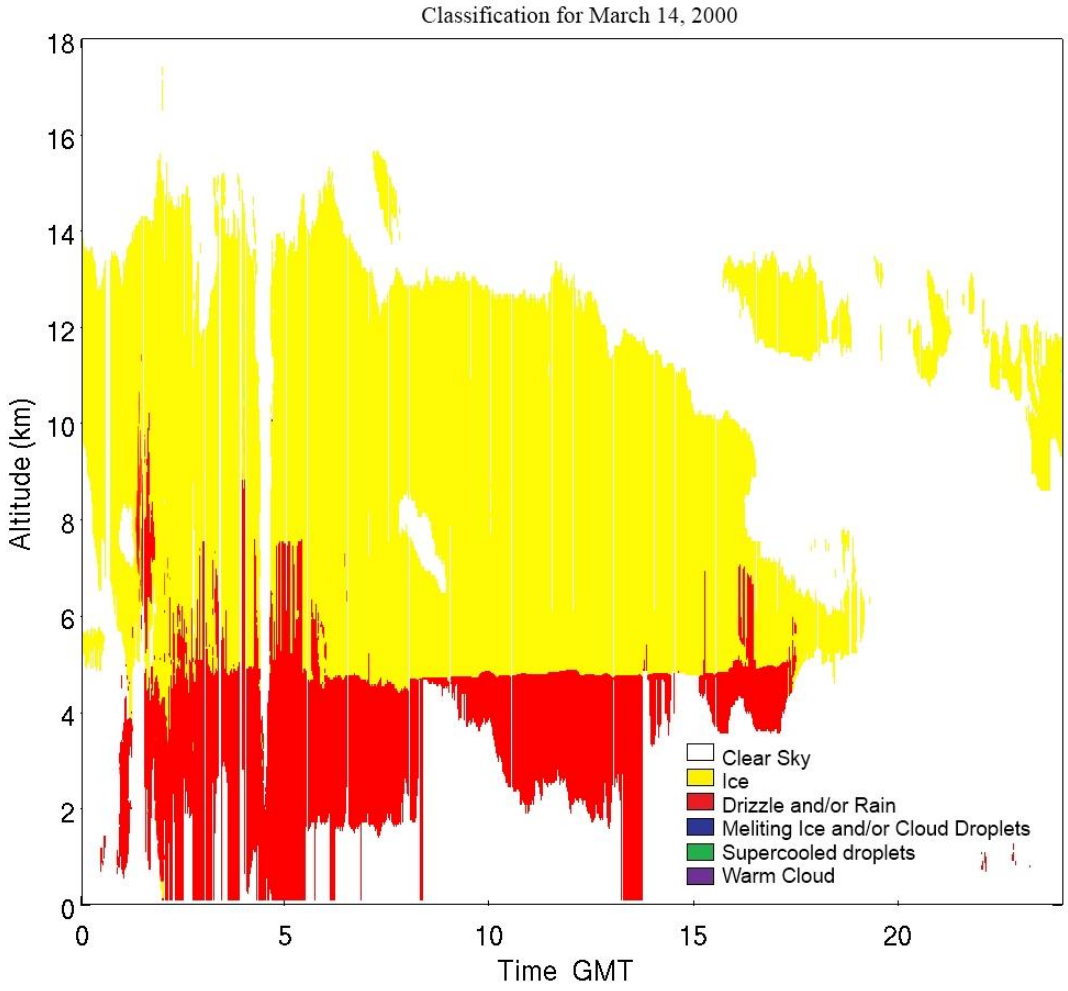

Figure 32: This is the classification for Manus for March 14, 2000. There is heavy rain and drizzle indicated. There is also various upper level ice clouds.

CHAPTER III: CPA and Error Analysis

The calculation of error and uncertainty in CPA is essential in determining the robustness of the algorithm. In creating a data archive from various instruments there are many aspects of error and uncertainty that must be accounted for with a data set. It is the role of the ARM Climate Research Facility (ACRF) data quality assurance program to track various errors and to make corrections to a datastream before said data is available to the climate community.

ACRF tracks uncertainty and error for all ARM instruments. ACRF defines uncertainty as the as the range of maximum change of a measured value from the true value within a 95% confidence interval. The root mean square error (RMSE) is a function of the variance, which is random error, and the mean error.

$$RMSE = (B^2 + \sigma^2)^{.5} \quad (1.6)$$

where B is the sum of all of the various errors that contribute to the mean error and σ^2 the sum of the variances of the contributors to the random errors. The 95% confidence interval is determined by using the t distribution where $t_{n,.025} = 2$ for a large ensemble. Therefore the uncertainty is twice the RMSE. The uncertainty for the millimeter wave cloud radar (MMCR) is in Table 3:

Table 3: The Uncertainty for the MMCR

MMCR Variable	Description	Uncertainty
Reflectivity	dBZ, (time, height)	.5dB
Spectral Width	m/s, (time, height)	.1 m/s
Doppler Velocity	m/s, (time, height)	.1 m/s

The micropulse lidar (MPL), which determines the cloud base height, will have an uncertainty due to timing electronics of about 2%. The microwave radiometer, which microwave emissions of liquid water and water vapor, has an uncertainty of .18K. The rain gauge has a 3% uncertainty in measurement. The uncertainty for the Surface Meteorological (SMET) the uncertainty is calculated using equation (1.6) for the RMSE. [9, 10, 11, 12, 13, 14,]

To account for the error in the data and to test the robustness of CPA, a simulation was created based upon the errors and uncertainty of the CPA instruments. The classification of atmospheric targets was processed without error, with error and a final graph displaying the differences between the graphs. The measurements are

$$M_j = M_i + rand(\quad) * sizeof\ the\ simulation * M_i \qquad (1.7)$$

where M_i is the measurement, $rand(\quad)$ is a random number generator. Therefore if an uncertainty for a particular day for a specific instrument is given by the ARCF then if the $rand(\quad) >$ the uncertainty, then the uncertainty is added to the measurement value, otherwise the uncertainty is subtracted from the measurement value. This calculation is per-

formed for a series of runs ($N_1 \ldots N_n$). The results are classifications of atmospheric targets (CPA) for March 13 and 14, 2000 without error, figures 31 and 32, and classification of atmospheric targets with error (CPA), figures 33 and 34. Two final graphs are created that display the changes in classification due to the addition of error. The last graphs produced are graphs that show the difference between CPA with error and CPA without error. These graphs, figures 35 and 36, are in black and white where black indicated a change in classification. For the March 13, 2000 there is a 10% change in classification and for March 14, 2000 there is approximately 3% change in classification. The classes that seem to switch are categories that tend to overlap.

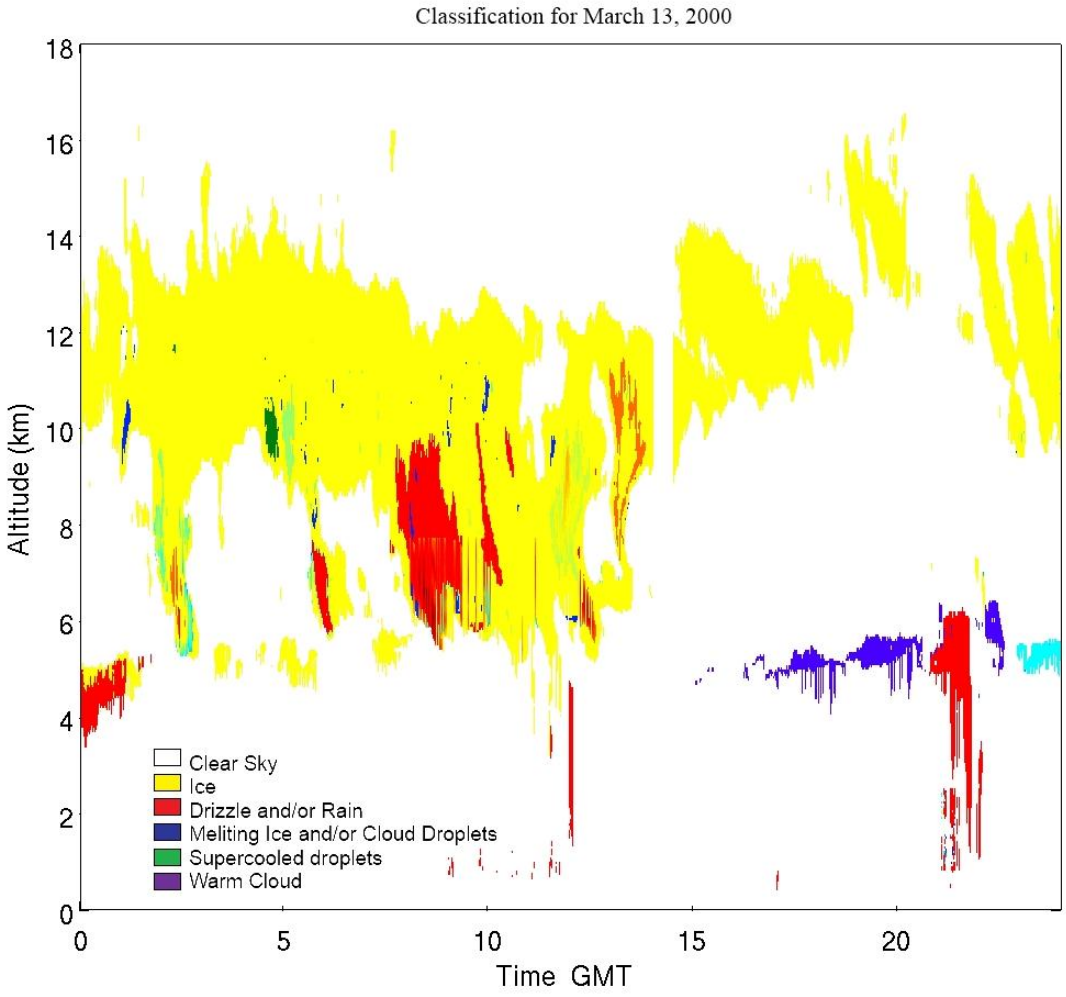

Figure 33: Classification of atmospheric targets using CPA with error added. The warm cloud and supercooled droplets classification changes to melting ice and/or cloud droplets and drizzle/rain due to addition of error.

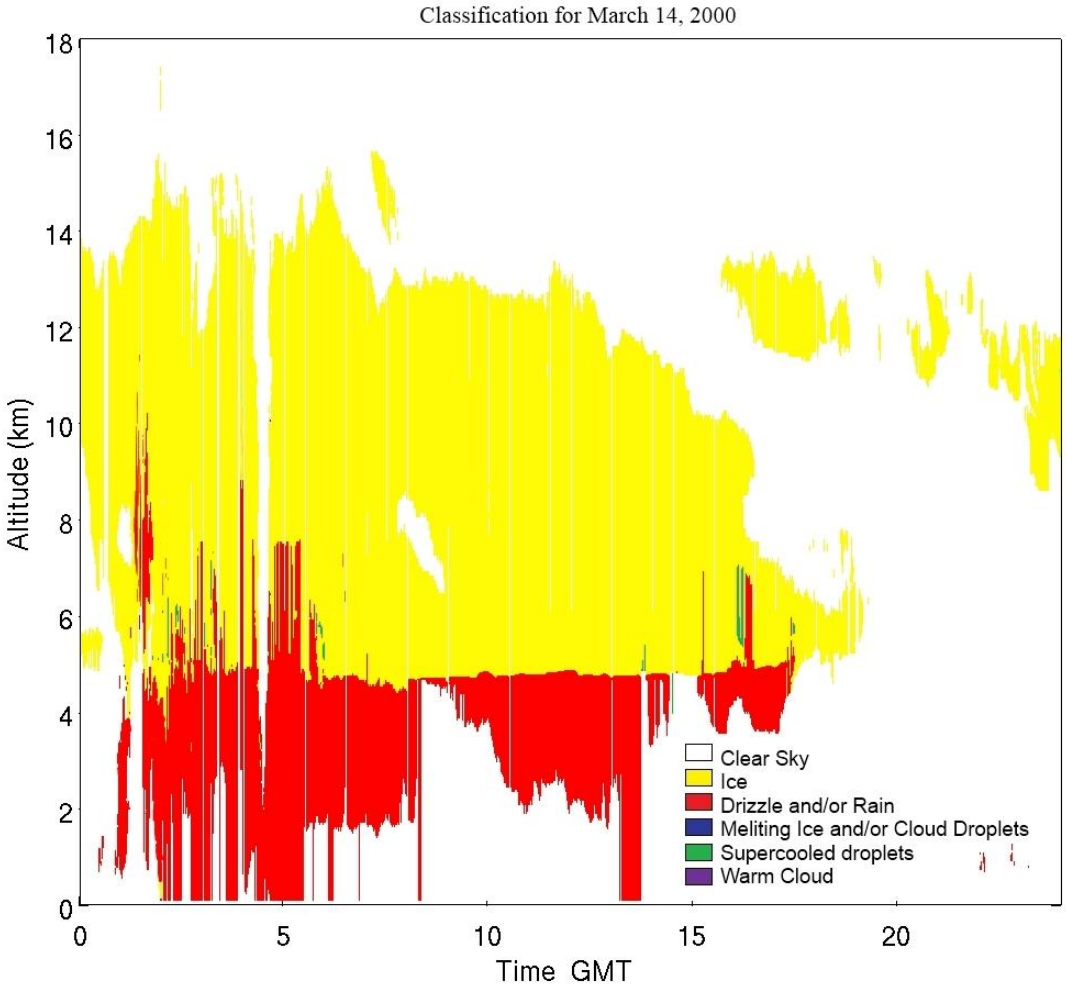

Figure 34: CPA classification with error. Some drizzle/rain classes switch to super-cooled droplets at 6Km AGL and above. The variations in temperature along with possible errors in calculation of IWC and LWC may be the cause.

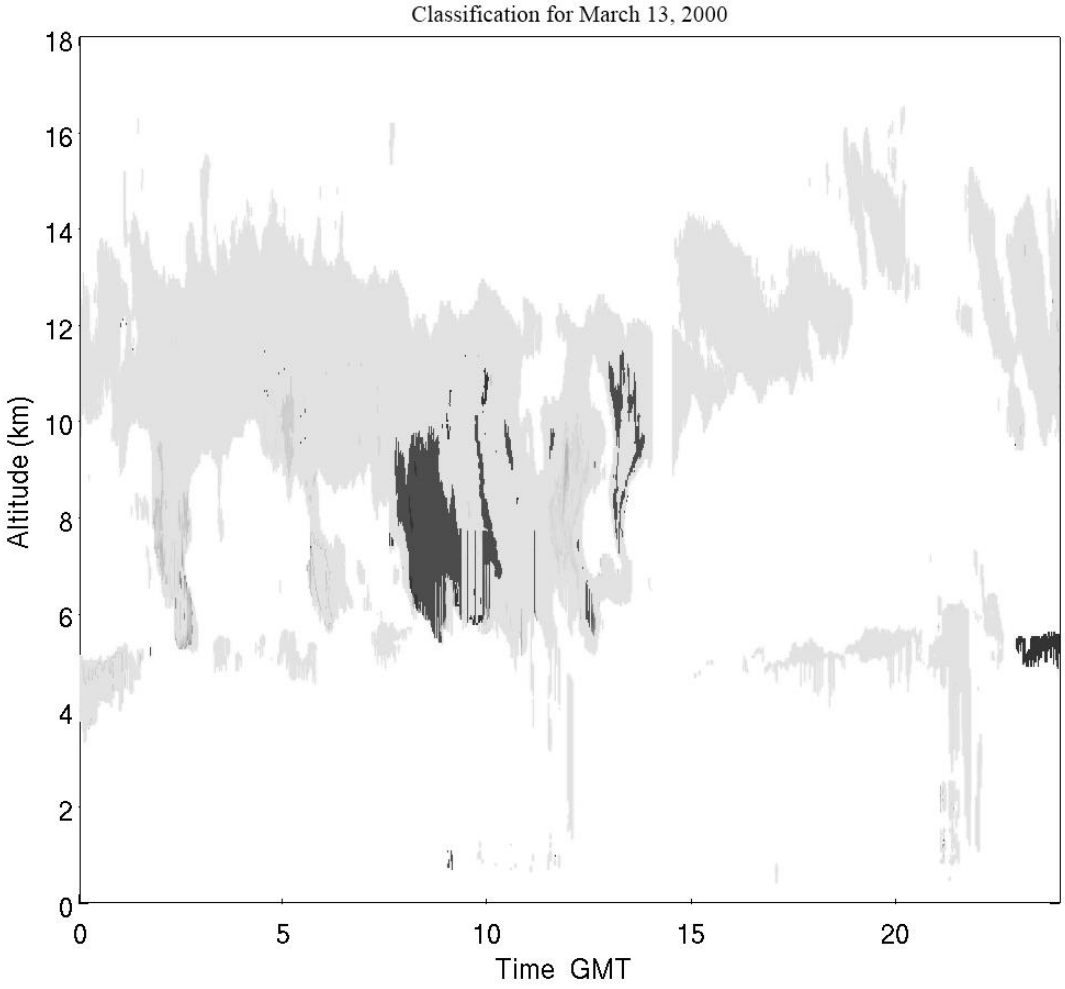

Figure 35: Difference between classification and classification with error. The black are the areas where the classifications change

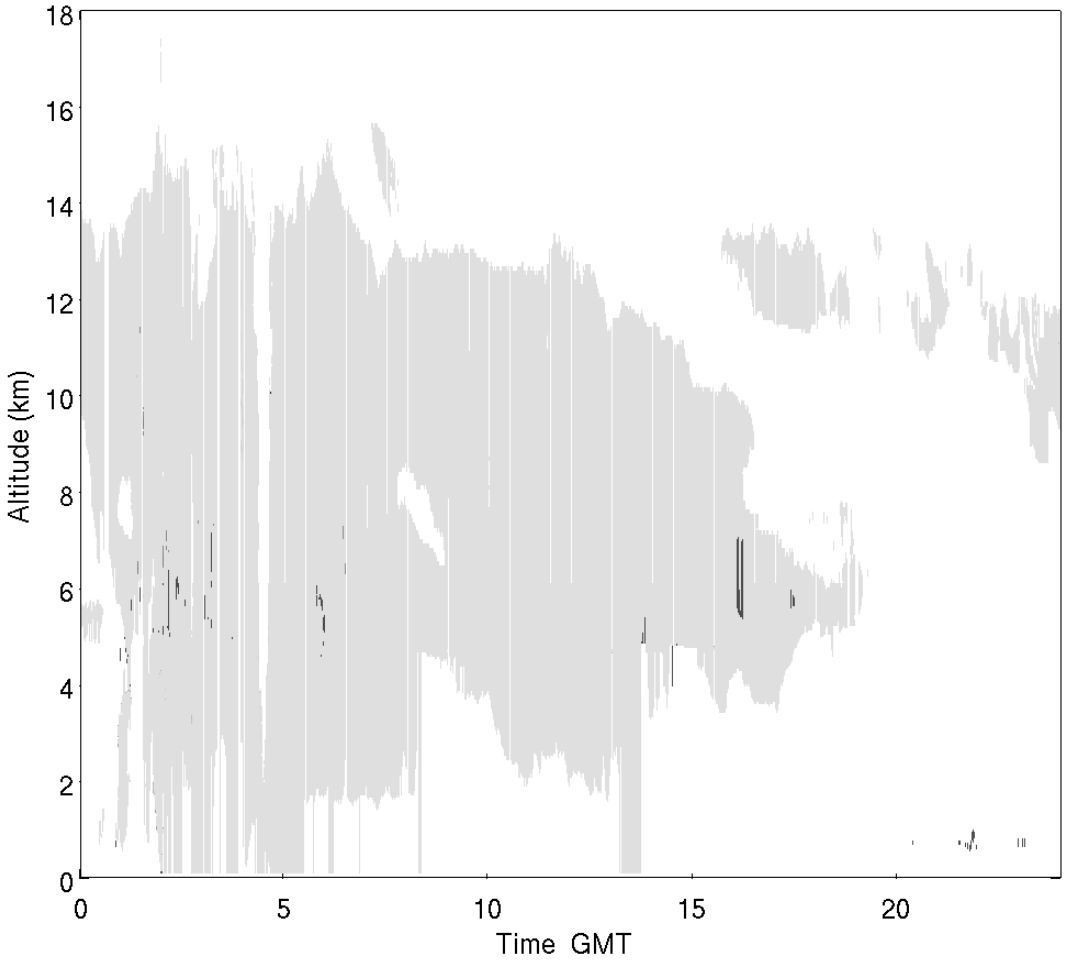

Figure 36: Difference between classification and classification with error. The black are the areas where the classifications change

CHAPTER VI: Conclusions and Future Research

.

CPA provides the scientific community with a multi-sensor algorithm that classifies atmospheric targets in at the ARM TWP sites through the utilization of a neural fuzzy logic data mining technique. This research explores multi-sensor responses to random and or complex targets such as atmospheric targets. Through the utilization of the CPA, the classification and characterization of atmospheric target properties at the ARM observation sites in the TWP is performed through the process of data mining. CPA processes approximately 14 million data points per radar and lidar sensor in addition to the several million data points for the additional instruments used to classify atmospheric targets.

Data mining is the process of finding patterns or relationships in large data sets. CPA provides and/or identifies gaseous and liquid attenuation, reflectivity, velocity and spectral width diagrams, Contour Frequency by Altitude Diagrams (M-CFAD), condensed water content, and standardization of units, by utilization of multiple instruments, which results in the graphical classification of atmospheric targets at ARM TWP site. Consequently, a fully robust classifier for targets based on several different instruments at the TWP site is achieved, thereby achieving the first step in achieving one of ARM's long term goals for the program.

The ARM program's primary interest in atmospheric target classifications is to provide input to a decision tree that will be able to choose the correct retrieval algorithm based on the atmospheric target identification. There are multiple cloud property retrievals that make use of various instruments such as radars, lidars, and radiometers. However, the state of the atmospheric pressure and other factors determines the suitable of a re-

trieval algorithm. With this information, one can build a data mining algorithm that appropriately chooses from among the available retrieval techniques. Other applications of the CPA are validation of global climate models, and atmospheric column model. The CPA is the first step in creating a multi-retrieval algorithm for the Department of Energy's ARM program. With error rates of as low as 5% and as high as 10% within areas of similar class type, CPA is a robust algorithm with many additional applications.

Future work includes the possibility of using a genetic algorithm as the core of CPA. Genetic algorithms are global optimizers that are robust that are named after the Darwin natural selection principle. Genetic algorithm optimization schemes are often used in military radar software and analysis packages. Since CPA is a multi-sensor algorithm, optimizations as well as robustness are key design factors. After the appropriate optimization scheme is added to CPA the additional work of building a truly multi-retrieval algorithm based on CPA can be achieved.

APPENDICES

APPENDIX A:

Additional Reflectivity, Spectral Width and Velocity Graphs

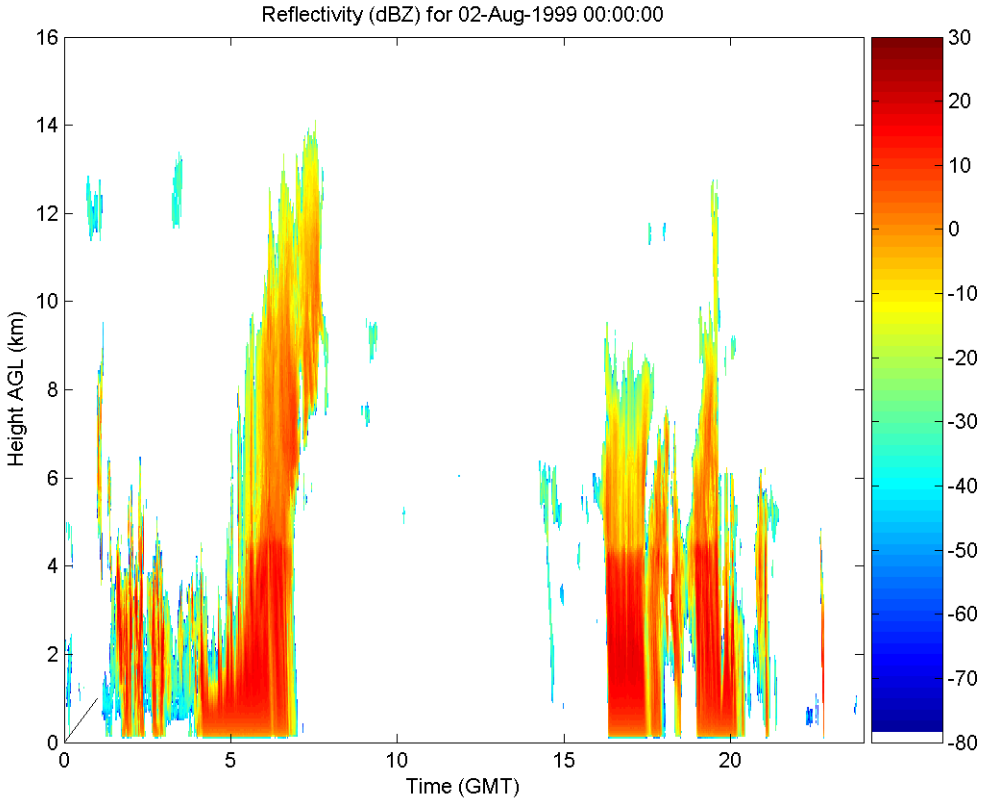

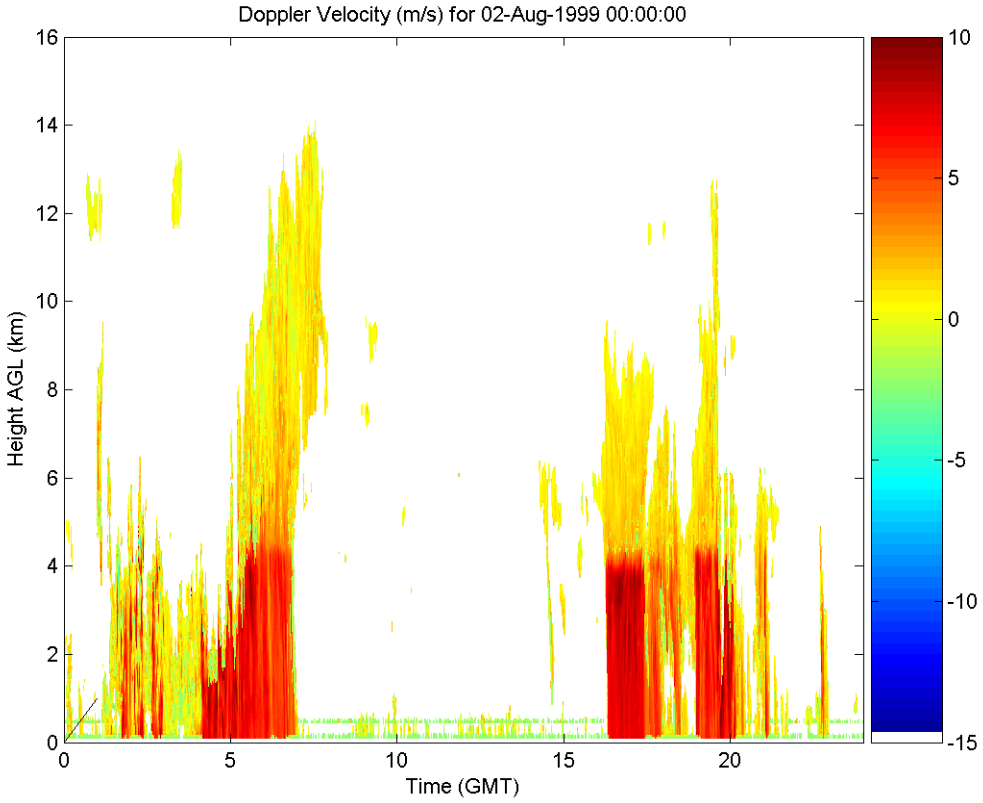
Doppler Velocity (m/s) for 02-Aug-1999 00:00:00
Height AGL (km)
Time (GMT)
0
2
4
6
8
10
12
14
16
0
5
10
15
20
10
5
0
-5
-10
-15

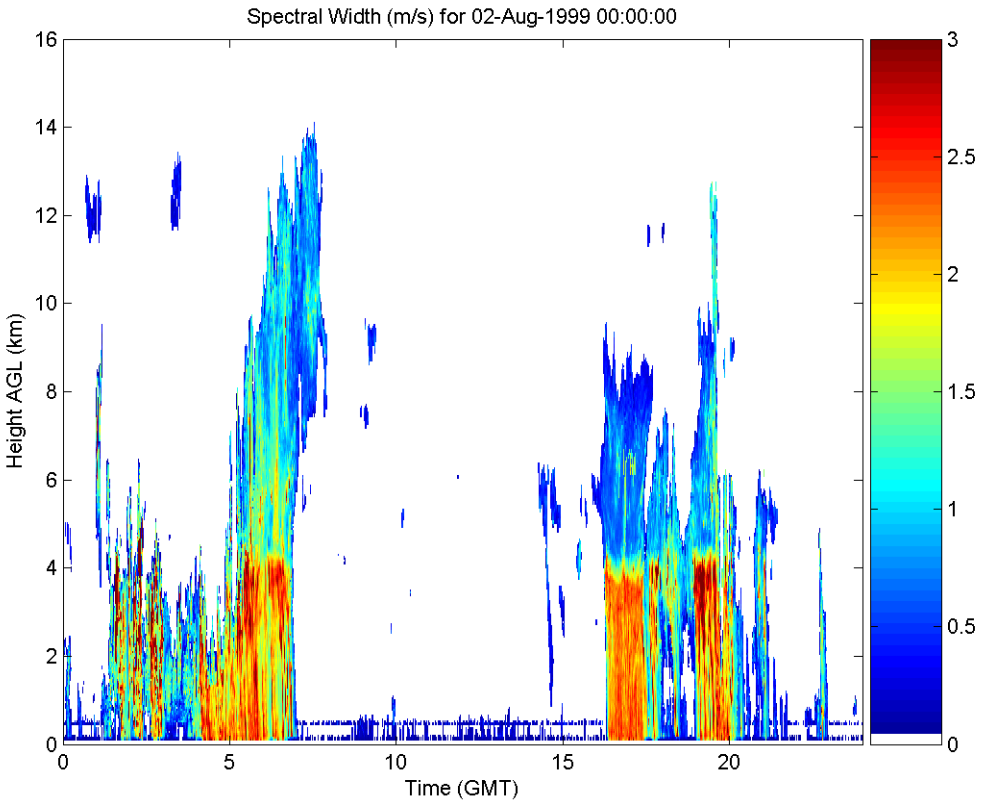
Spectral Width (m/s) for 02-Aug-1999 00:00:00
Height AGL (km)
Time (GMT)
0
2
4
6
8
10
12
14
16
0
5
10
15
20
0
0.5
1
1.5
2
2.5
3

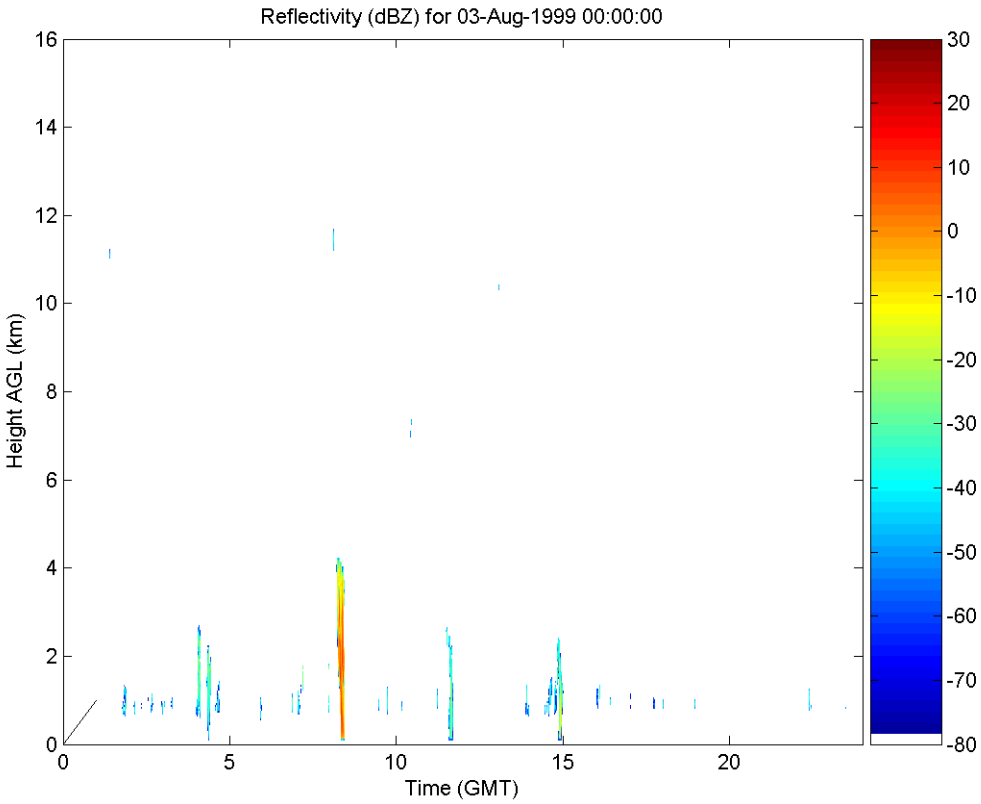
Reflectivity (dBZ) for 03-Aug-1999 00:00:00
Height AGL (km)
Time (GMT)
0
2
4
6
8
10
12
14
16
0
5
10
15
20
30
20
10
0
-10
-20
-30
-40
-50
-60
-70
-80

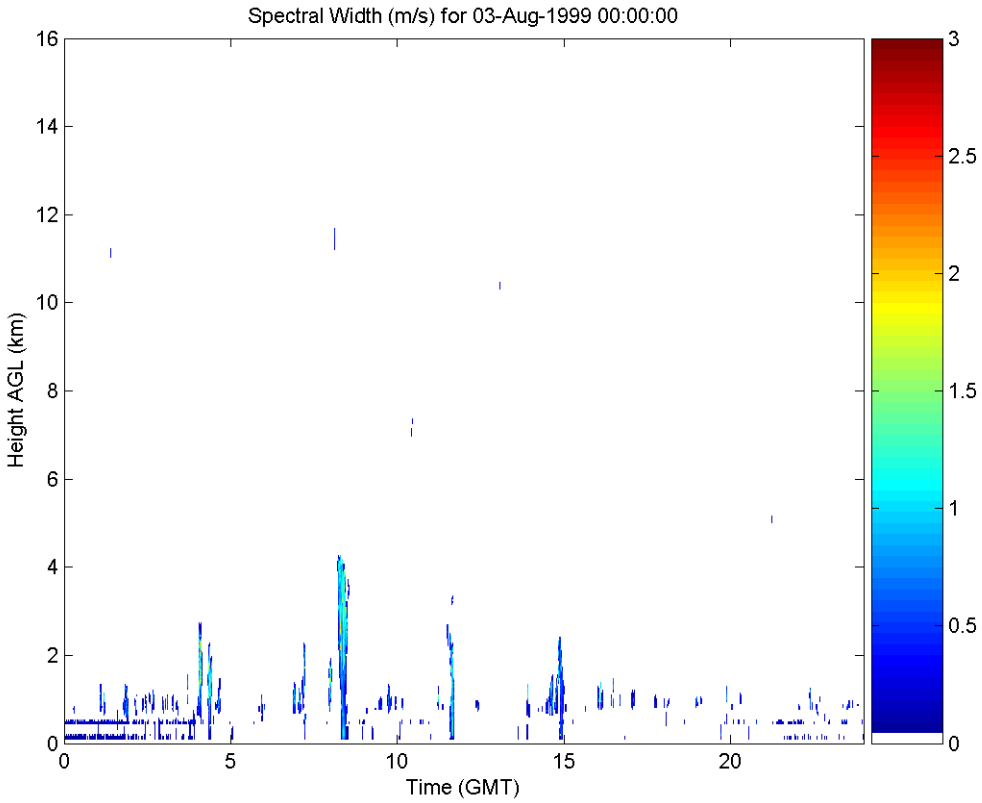
Spectral Width (m/s) for 03-Aug-1999 00:00:00
Height AGL (km)
Time (GMT)
0
2
4
6
8
10
12
14
16
0
5
10
15
20
0
0.5
1
1.5
2
2.5
3

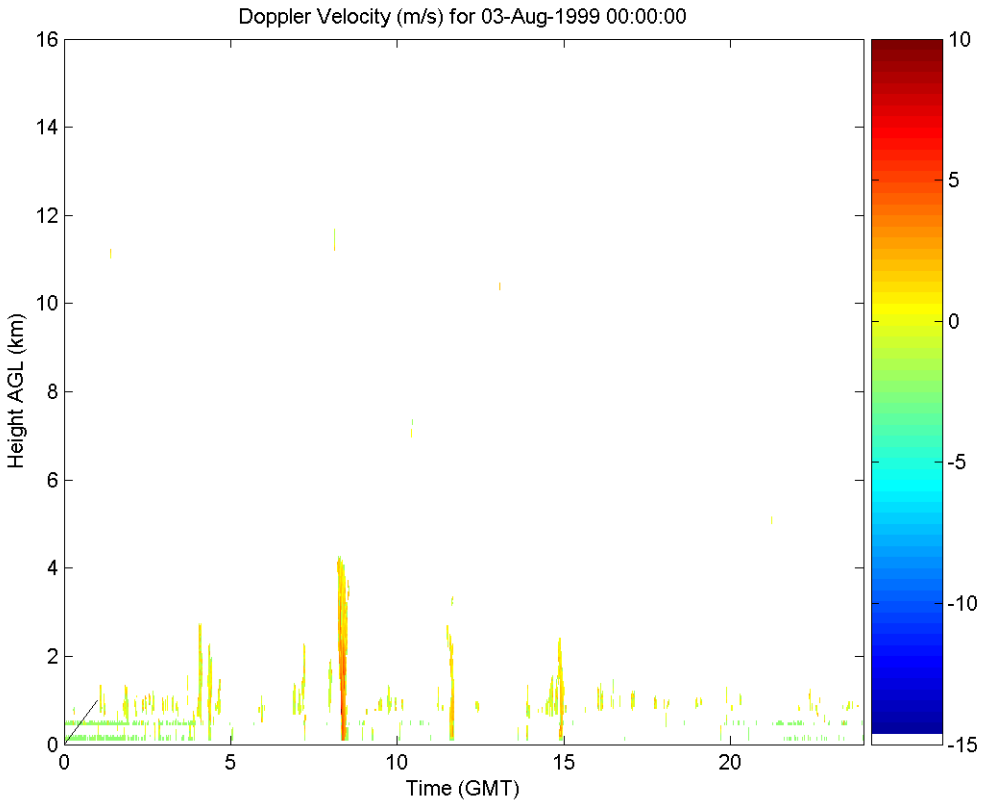
Doppler Velocity (m/s) for 03-Aug-1999 00:00:00
Height AGL (km)
Time (GMT)
0
2
4
6
8
10
12
14
16
0
5
10
15
20
10
5
0
-5
-10
-15

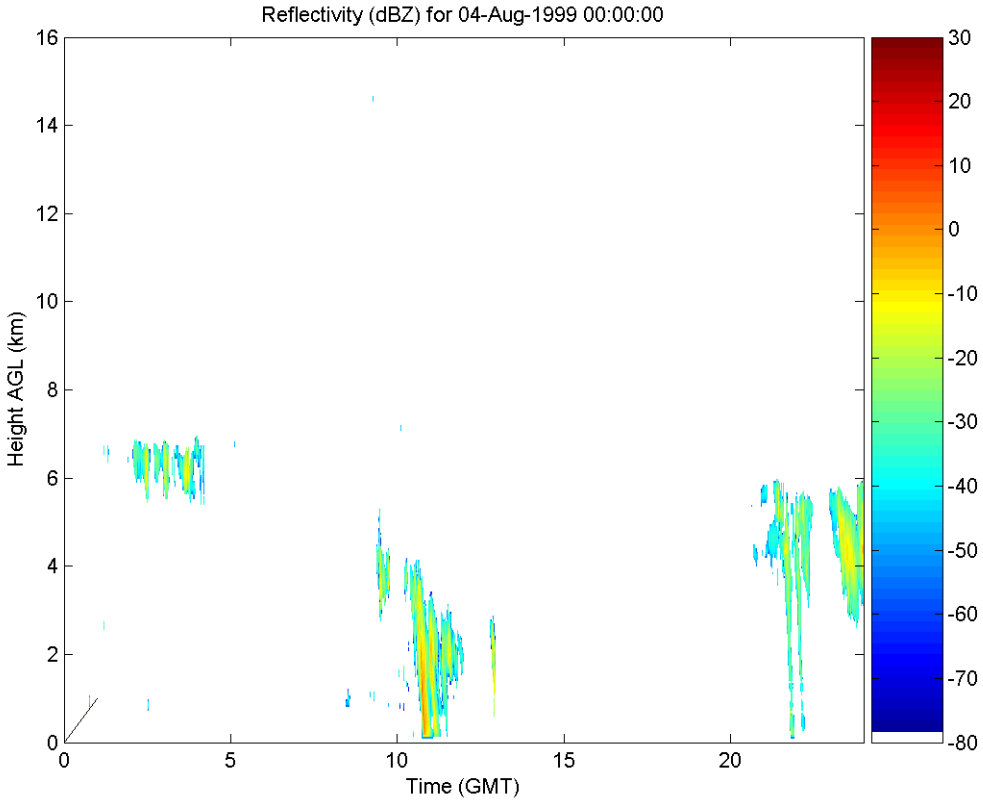
Reflectivity (dBZ) for 04-Aug-1999 00:00:00
Height AGL (km)
Time (GMT)
0
2
4
6
8
10
12
14
16
0
5
10
15
20
30
20
10
0
-10
-20
-30
-40
-50
-60
-70
-80

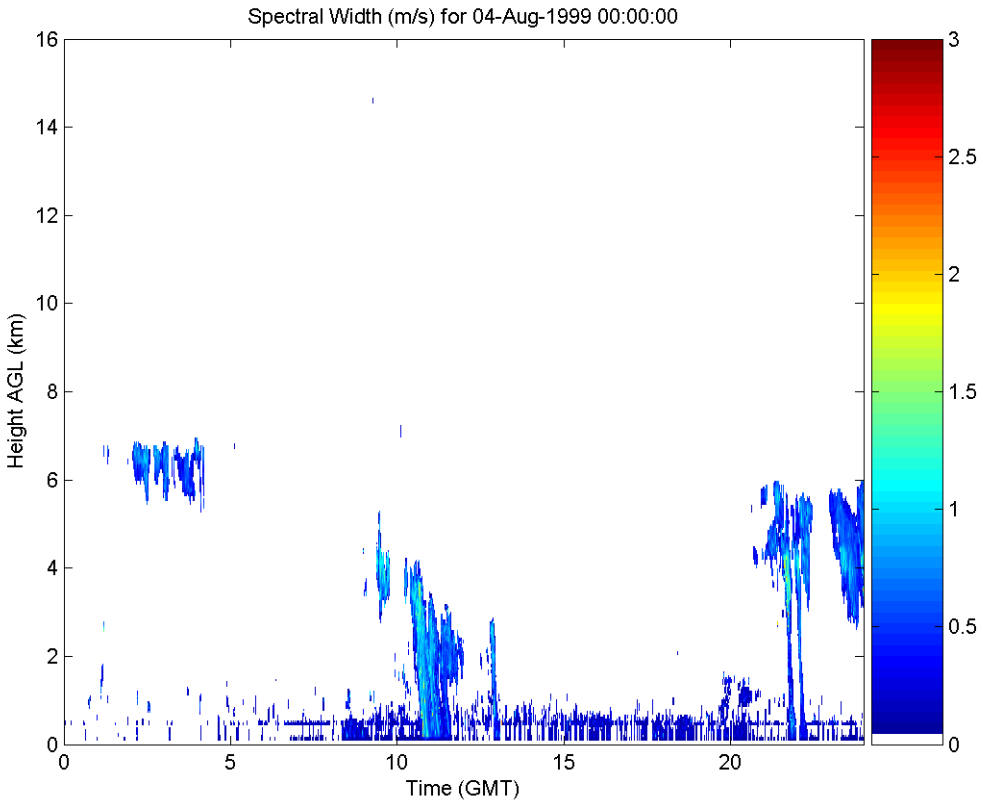
Spectral Width (m/s) for 04-Aug-1999 00:00:00
Height AGL (km)
Time (GMT)
0
2
4
6
8
10
12
14
16
0
5
10
15
20
0
0.5
1
1.5
2
2.5
3

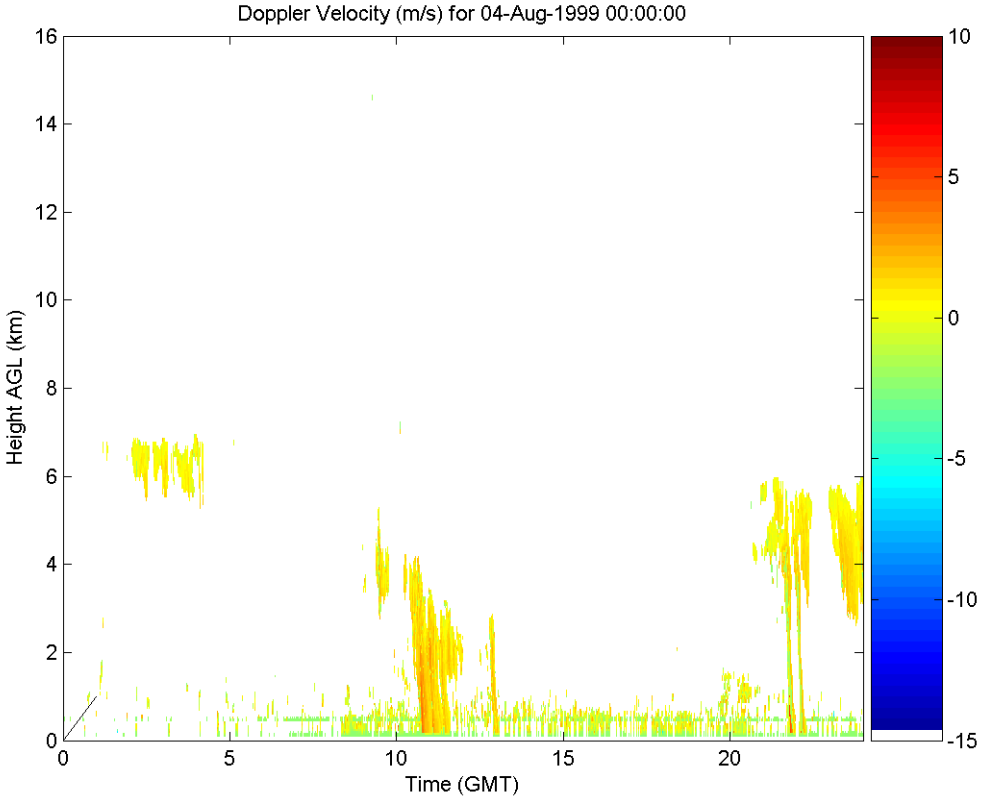
Doppler Velocity (m/s) for 04-Aug-1999 00:00:00
Height AGL (km)
Time (GMT)
0
2
4
6
8
10
12
14
16
0
5
10
15
20
10
5
0
-5
-10
-15

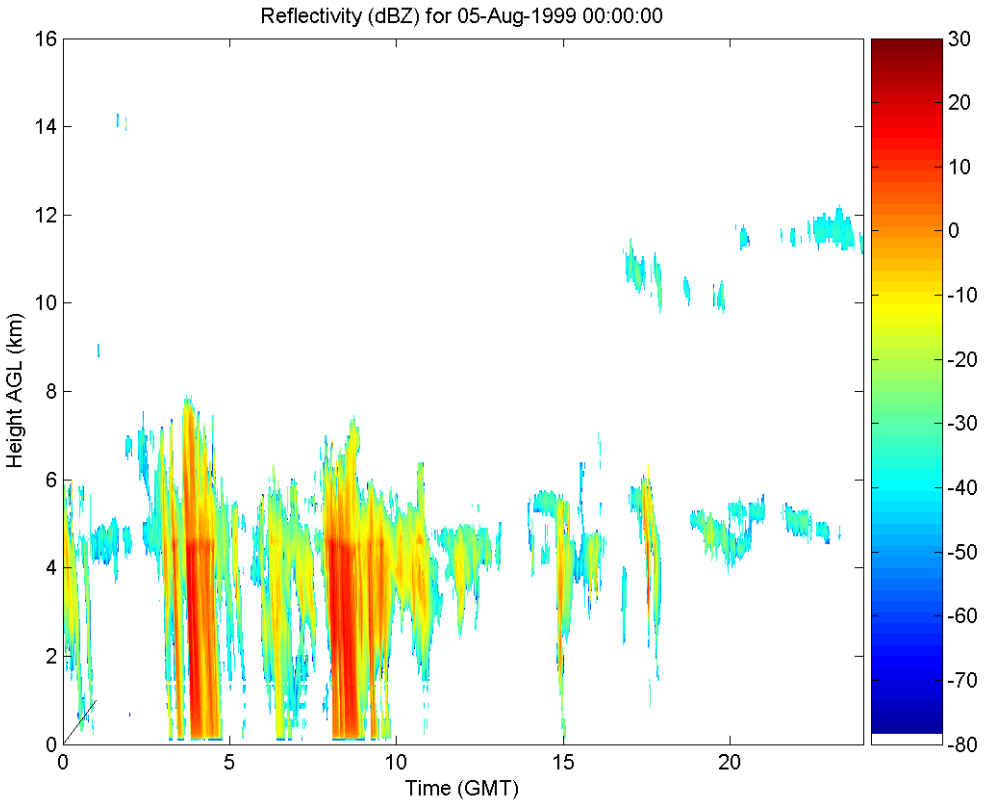
Reflectivity (dBZ) for 05-Aug-1999 00:00:00
Height AGL (km)
Time (GMT)
0
2
4
6
8
10
12
14
16
0
5
10
15
20
30
20
10
0
-10
-20
-30
-40
-50
-60
-70
-80

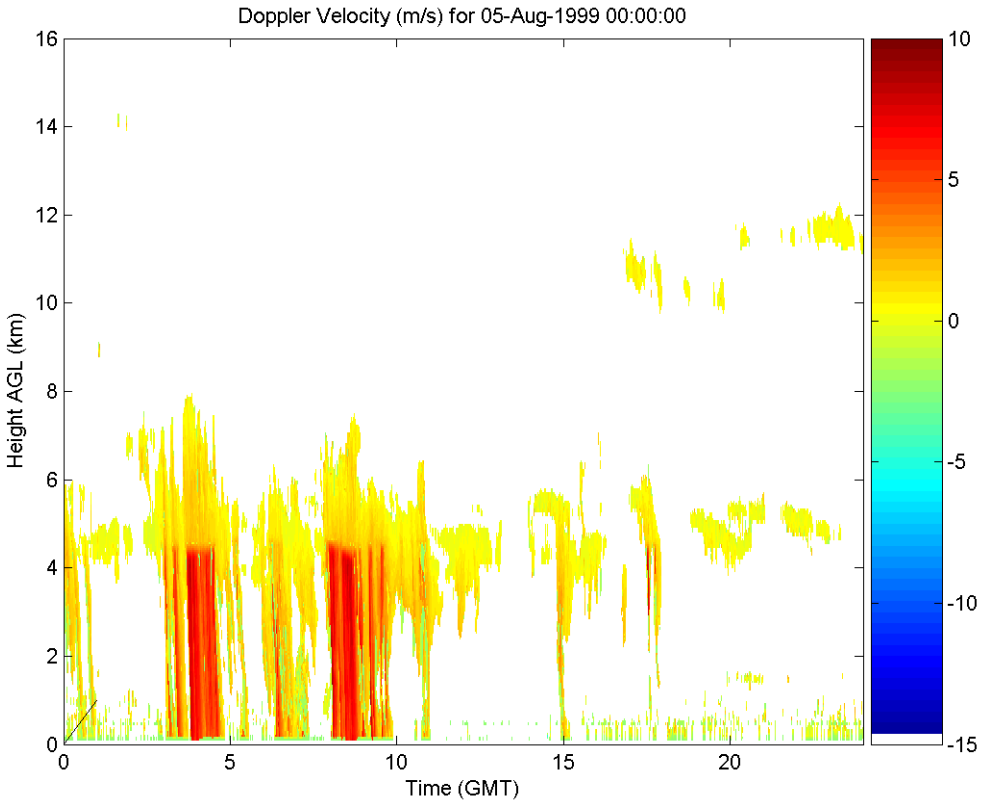
Doppler Velocity (m/s) for 05-Aug-1999 00:00:00
Height AGL (km)
Time (GMT)
0
2
4
6
8
10
12
14
16
0
5
10
15
20
10
5
0
-5
-10
-15

APPENDIX B:

Additional Contour Frequency by Altitude Diagrams

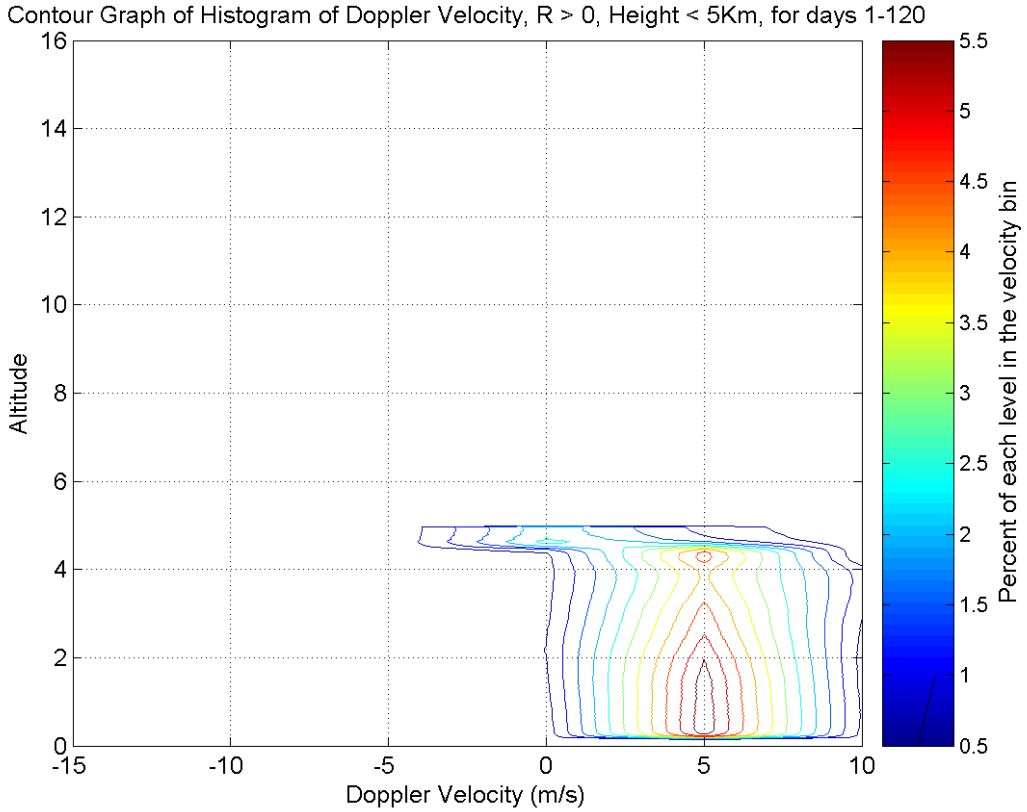

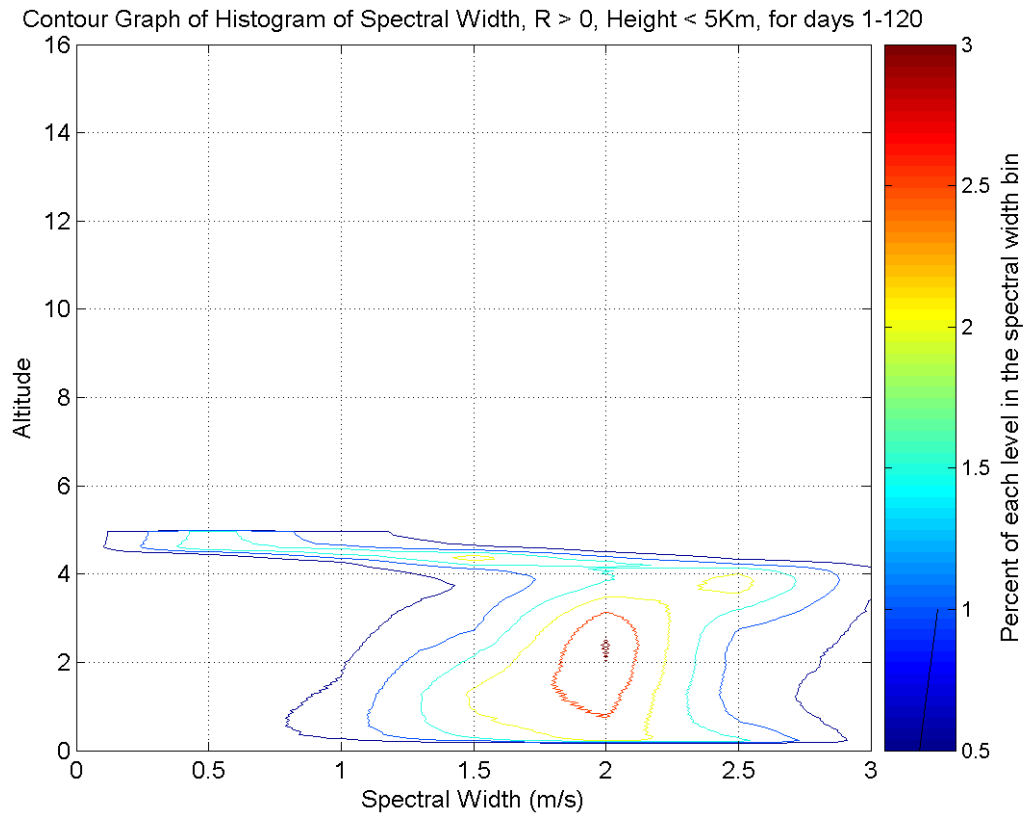
Contour Graph of Histogram of Spectral Width, R > 0, Height < 5Km, for days 1-120
Altitude
Spectral Width (m/s)
Percent of each level in the spectral width bin
0
2
4
6
8
10
12
14
16
0
0.5
1
1.5
2
2.5
3
0.5
1
1.5
2
2.5
3

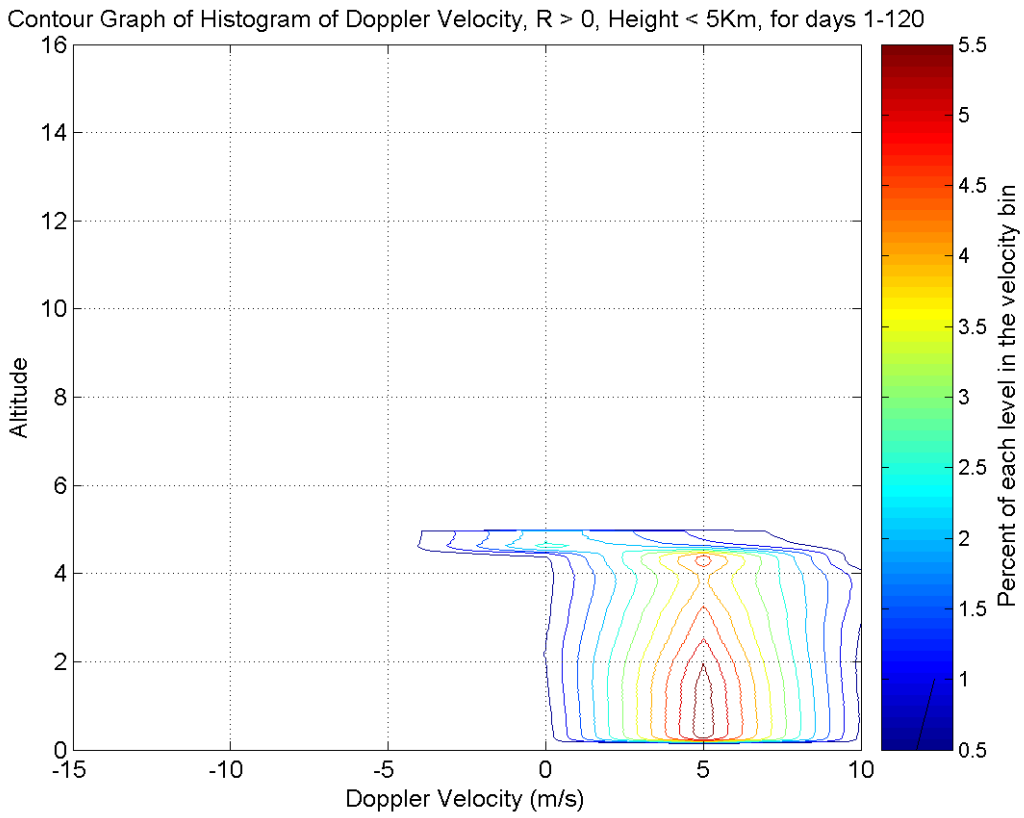
Contour Graph of Histogram of Doppler Velocity, R > 0, Height < 5Km, for days 1-120
Altitude
Doppler Velocity (m/s)
Percent of each level in the velocity bin
16
14
12
10
8
6
4
2
0
-15
-10
-5
0
5
10
5.5
5
4.5
4
3.5
3
2.5
2
1.5
1
0.5

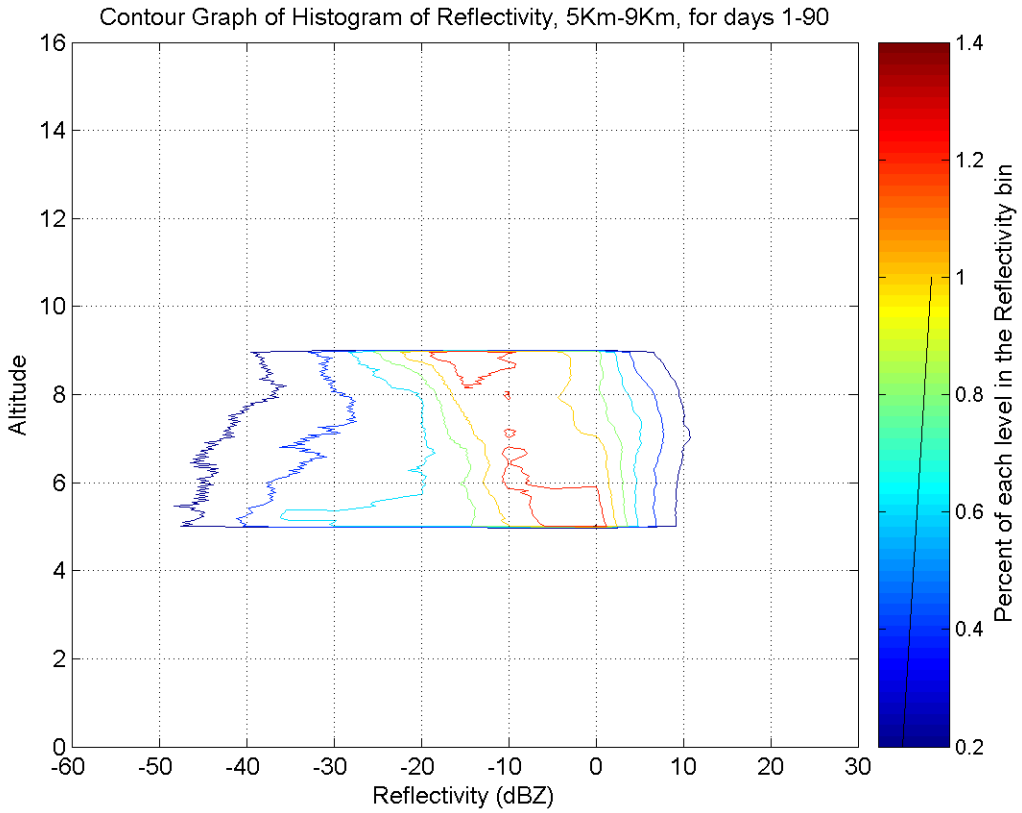
Contour Graph of Histogram of Reflectivity, 5Km-9Km, for days 1-90
Altitude
Reflectivity (dBZ)
Percent of each level in the Reflectivity bin
16
14
12
10
8
6
4
2
0
-60
-50
-40
-30
-20
-10
0
10
20
30
1.4
1.2
1
0.8
0.6
0.4
0.2

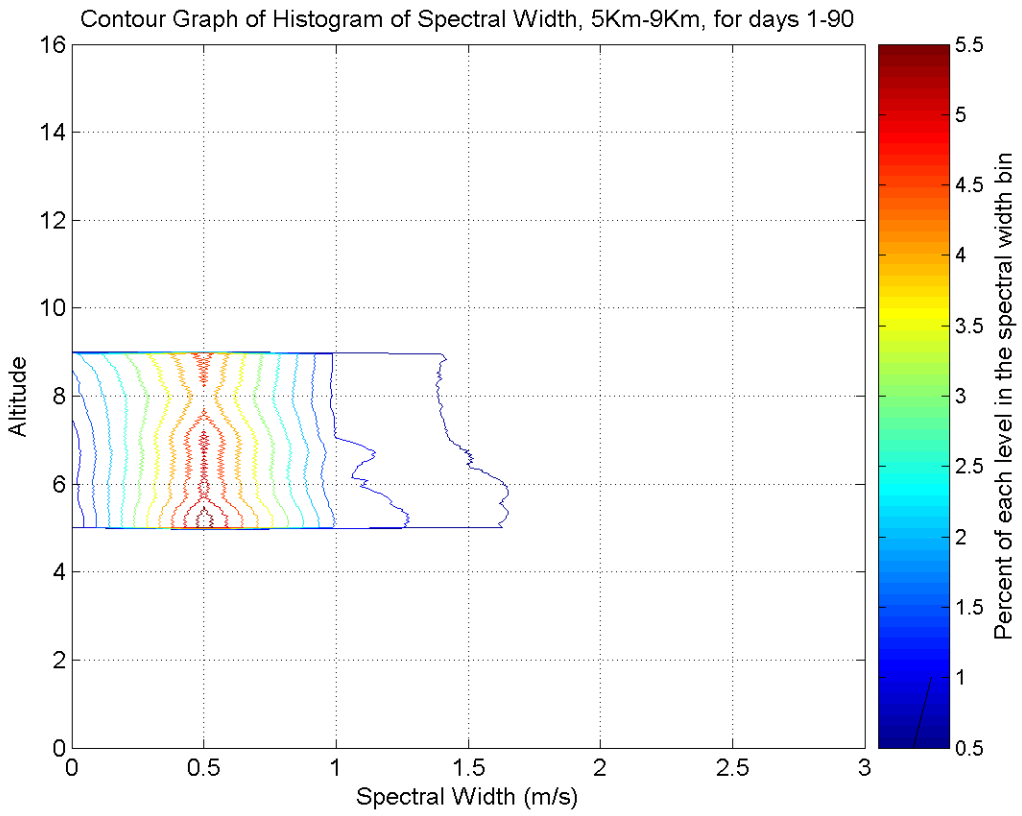
Contour Graph of Histogram of Spectral Width, 5Km-9Km, for days 1-90
Altitude
Spectral Width (m/s)
Percent of each level in the spectral width bin
0
2
4
6
8
10
12
14
16
0
0.5
1
1.5
2
2.5
3
0.5
1
1.5
2
2.5
3
3.5
4
4.5
5
5.5

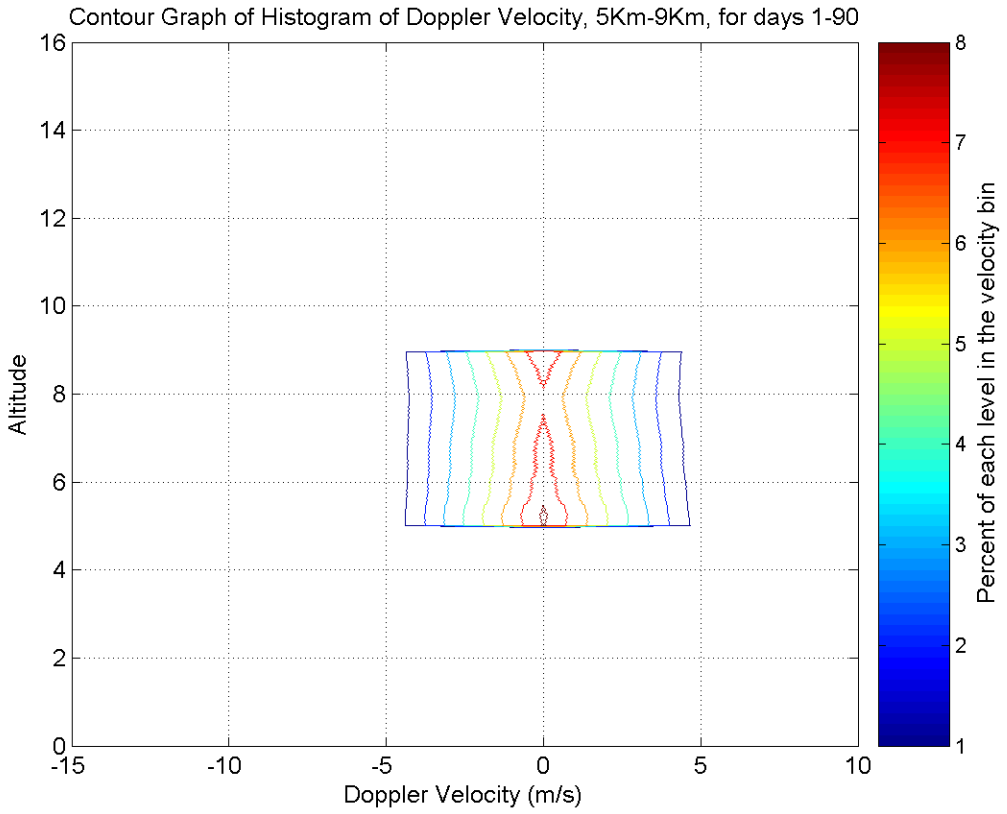
Contour Graph of Histogram of Doppler Velocity, 5Km-9Km, for days 1-90
Altitude
Doppler Velocity (m/s)
Percent of each level in the velocity bin
16
14
12
10
8
6
4
2
0
-15
-10
-5
0
5
10
8
7
6
5
4
3
2
1

APPENDIX C: Condensed Water Content Figures

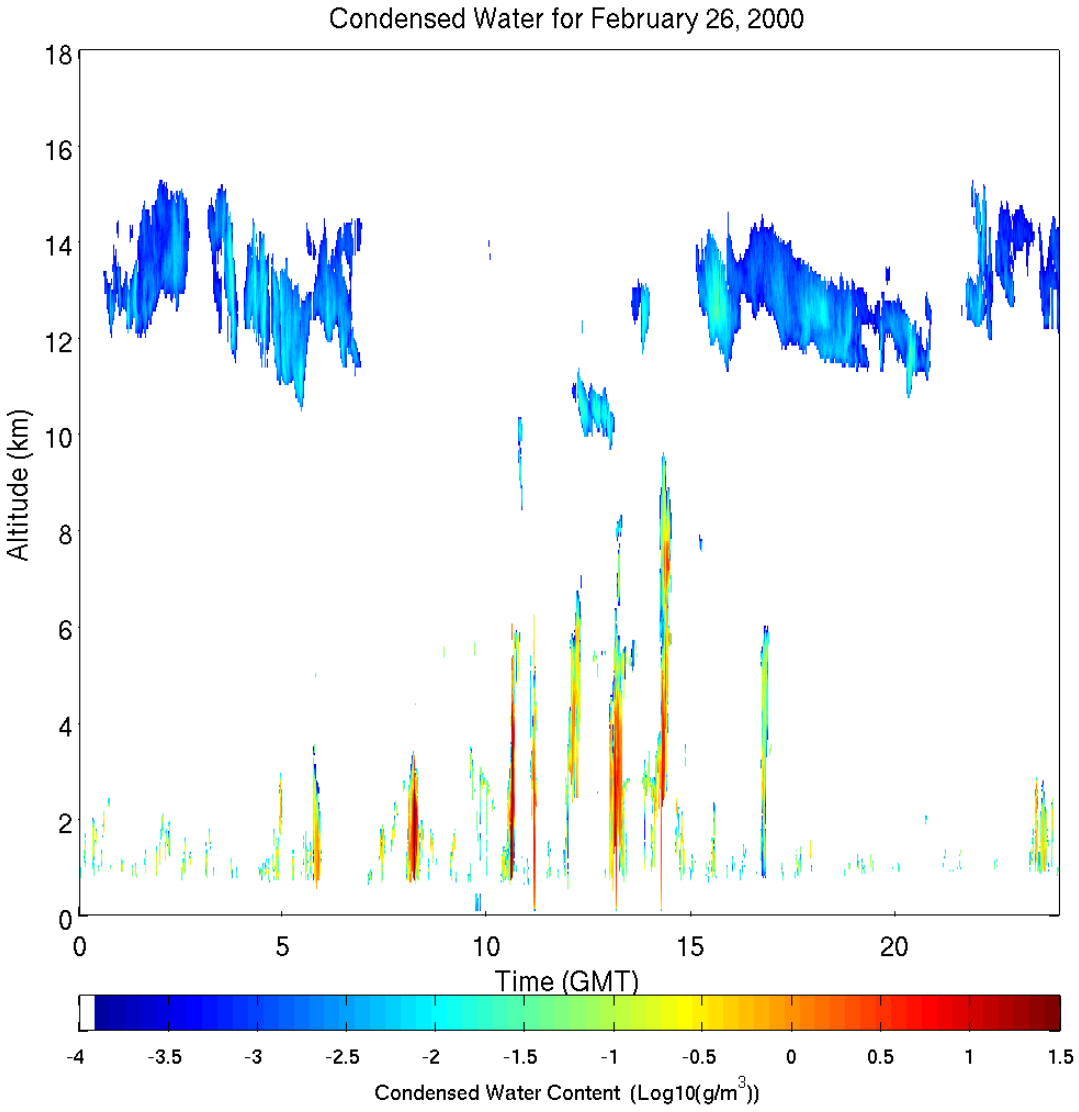

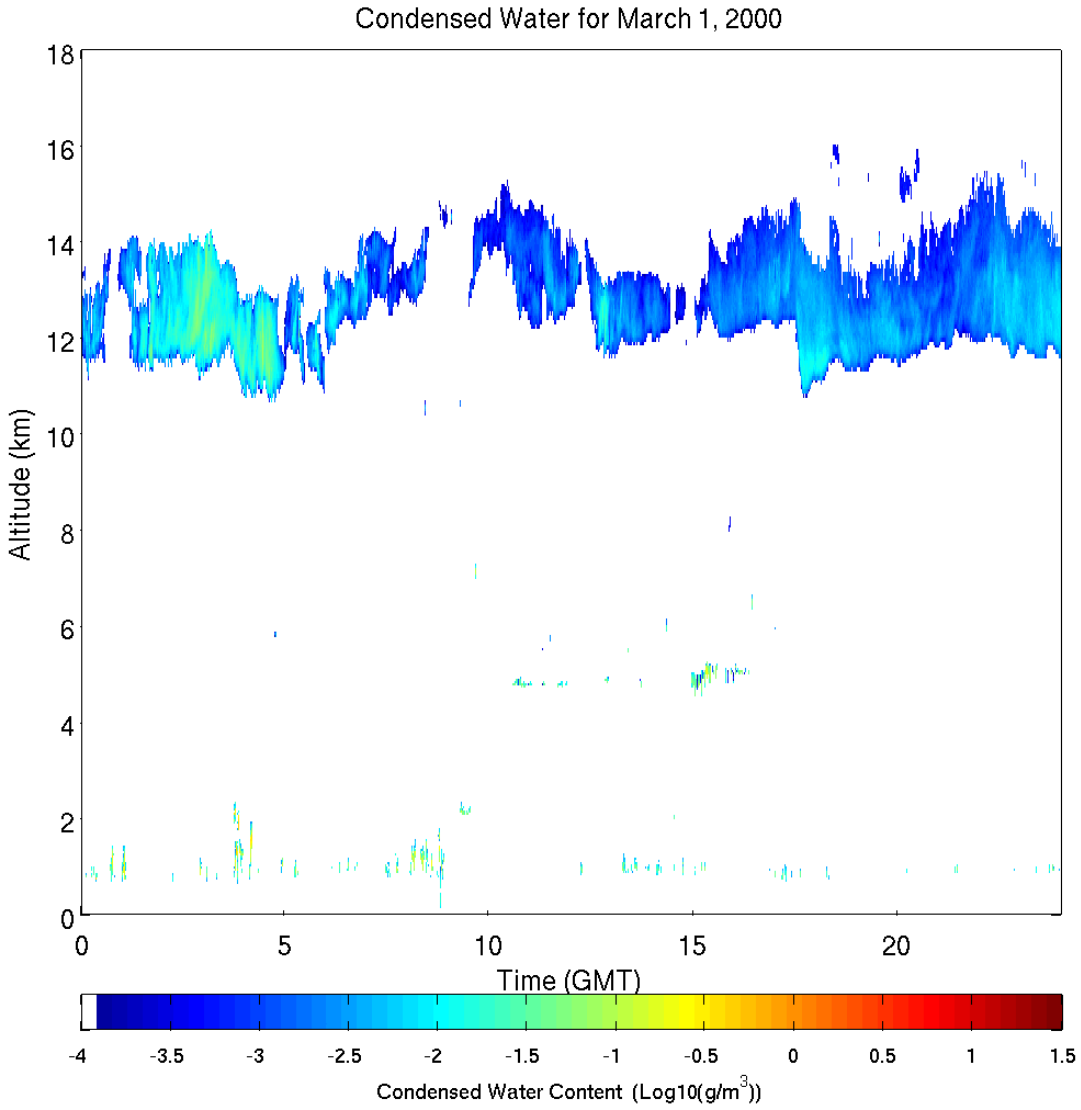
Condensed Water for March 1, 2000
Altitude (km)
0
2
4
6
8
10
12
14
16
18
0
5
10
15
20
Time (GMT)
-4
-3.5
-3
-2.5
-2
-1.5
-1
-0.5
0
0.5
1
1.5
Condensed Water Content (Log10(g/m3))

BIBLIOGRAPHY

[1] Overpeck, J., Meehl, G., Bony, S., Easterling, D., "Climate Data Challenges in the 21st Century." *Science* 11 February 2011: Vol. 331 no. 6018 pp. 700-702 DOI: 10.1126/science.1197869

[2] Fox, P., and Hendler, J., "Changing the Equation on Scientific Data Visualization" *Science* **331**, 705 2011. DOI: 10.1126/science.1197654.

[3] Atmospheric Radiation and Measurement Program www.arm.gov

[4] Shi, Y and Miller, M. 2003: ARSCL Cloud Statistics - A Value Added Product, *Thirteenth ARM Science Team Meeting Proceedings*, 1-9.

[5] Mace, G. Heymsfield, A. and Poellot, M., 2002: On Retrieving the microphysical properties of Cirrus Clouds using the moments of the Millimeter Wavelength Doppler Spectrum. *J. Geophy. Res.* 1-26.

[6] Riihimaki, Laura D., McFarlane, S. and Comstock., J. "Climatology and Formation of Tropical Mid-level Clouds at the Darwin ARM Site", Journal of Climate, 2012.

[7] Wang, J. "Observation of ambient aerosol particle growth due to in-cloud processes within boundary layers", Journal of Geophysical Research, 07/25/2007

[8] National Aeronautics and Space Administration, Science Mission Directorate. (2010). *The Earth's Radiation Budget*. Retrieved March 19, 2012, from Mission: Science website: http://missionscience.nasa.gov/ems/13_radiationbudget.html

[9] Buch, K., Sun, C. and Thorne, L. Cloud Classification Using Whole-Sky Imager Data *Proceedings of the Fifth Atmospheric Radiation Measurement (ARM) Science Team Meeting.* DOE CONF-9503140, March 1995.

[10] Wang, Zhuo. "Thermodynamic Aspects of Tropical Cyclone Formation", Journal of the Atmospheric Sciences, 2012.

[11] Fueglistaler, S. "Impact of clouds on radiative heating rates in the tropical lower stratosphere", Journal of Geophysical Research, 2006.

[12] Shi, Y and Miller, M. 2003: ARSCL Cloud Statistics - A Value Added Product, Thirteenth ARM Science Team Meeting Proceedings, 1-9.

[13] Zhien, Wang, and Sassen, K. Cloud Type and Macrophysical Property Retrieval Using Multiple Remote Sensors. Journal of Applied Meteorology Vol.40 October 2001.

[14] Hajime, Okamoto. "Vertical cloud properties in the tropical western Pacific Ocean: Validation of the CCSR/NIES/FRCGC GCM by shipborne radar and lidar", Journal

of Geophysical Research, 2008

[15] Giangrande, S and Babb, D. 2001: Processing Millimeter Wave Profile Radar Spectra. *Amer. Meteor*. Soc., 1577-1583.

[16] Korolev, AV, Issac, GA and Cober,S 2003: Microphysical Characterization of Mixed Phased Clouds. *Quarterly J. of the R. Meteor. Soc*. 129:39-65.

[17] Mather, J. S. McFarlane. 2006: Cloud Properties and Associated Heating Rates in the Tropical Western Pacific. *Journ. Geophy. Research*, Vol. 112. 2007.

[18] Clothiaux, E., Mace, G., Ackerman, T., Kane, T. Spinhirne, J and Scott, V. 1998: An automated algorithm for detection of hydrometer returns in micropulse lidar data. *J. Atmos. Oceanic Technol.*, **15,** 1035–1042.

[19] Yuter, S. and House, R. 1995: Three-Dimensional Kinematics and Microphysical Evolution of Florida Cumulonimbus. Part II: Frequency Distribution of Vertical Velocity, Reflectivity and Differential Reflectivity. *Amer. Meteor. Soc.*,1941-1963.

[20] Campbell, N. "The Climate Preprocessing Algorithm" XSEDE13: Extreme Science and Engineering Discovery Environment Conference Publication (pending).

[21] Mather, J. "Cloud properties and associated radiative heating rates in the tropical western Pacific", Journal of Geophysical Research, 2007

[22] Manabe, Syukuro and Stouffer, R. July 1999: Century-Scale Effects of Increased Atmospheric C02 on the Ocean Atmosphere System. Nature. 364, 215-218.

[23] Lawrence D. Carey. "Lightning location relative to storm structure in a leading-line, trailing stratiform mesoscale convective system", Journal of Geophysical Research, 2005

[24] Wang, Z. and Sassen, K. “An Improved Cloud Classification Algorithm Based on the SGP CART Site Observations”. *Fourteenth ARM Science Team Meeting Proceedings*, Albuquerque, New Mexico, March 22-26, 2004.

[25] Penaloza, M. A., and R. M. Welch, 1996: Feature selection for classification of polar regions using a fuzzy expert system. *Remote Sens. Environ.*, **58,** 81–100.

[26] Doran, J. "A comparison of cloud properties at a coastal and inland site at the North Slope of Alaska", Journal of Geophysical Research, 2002

[27] Delanoë, J. "A variational scheme for retrieving ice cloud properties from combined radar, lidar, and infrared radiometer", Journal of Geophysical Research, 2008

[28] Widner, K. and Johnson, K. "Millimeter Wave Cloud Radar Handbook"

www.arm.gov

[29] Coulter, R. "Micropulse Lidar Handbook" www.arm.gov

[30] Morris, V. "Microwave Radiometer" www.arm.gov

[31] Newsome, R. "The Raman Lidar Handbook". www,arm.gov

[32] Bartholomew, M. "Disdrometer and Tipping Bucket Rain Gauge Handbook". www.arm.gov

[33] Ritsche, M., "Surface Meteorological Handbook (SMET)" www.arm.gov

[34] Liu,C and Illingworth. 2000: Toward More Accurate Retrievals of Ice Water Content from Radar Measurements of Clouds: *Journ. Appl. Meteor.* 39:1130-1146.

[35] Hogan, R, Francis, P. Flentje, H. Illingworth, A. Quante, M. and Pelon, J. 2003: Characteristics of Mixed-Phase Clouds Part I: Lidar, Radar and Aircraft Observations from CLARE'98. *Q. J. R. Meteorol. Soc.* 129.

[36] Hogan, R, Illingworth, A. O'Connor, J and Poiares, J. Baptistat. 2003: Characteristics of Mixed-Phase Clouds Part II: A Climatology from Ground-Based Lidar. *Q. J. R. Meteorol. Soc.* 129

[37] Liljegren, J. C., and B. M. Lesht, Measurements of integrated water vapor and cloud liquid water from microwave radiometers at the DOE ARM cloud and radiation testbed in the U.S. Southern Great Plains. *Proceedings of the International Geoscience and Remote Sensing Symposium (IGARSS)*, Lincoln, Nebraska.1996.

[38] Turner, D.D., S.A. Clough, J.C. Liljegren, E.E. Clothiaux, K. Cady-Pereira, and K.L. Gaustad, 2007: Retrieving liquid water path and precipitable water vapor from Atmospheric Radiation Measurement (ARM) microwave radiometers. *IEEE Trans. Geosci. Remote Sens.*, 45, 3680-3690, doi:10.1109/TGRS.2007.903703.

[39] Zhien, Wang, Sassen, K., Whiteman, D. Arctic Mixed-Phase Cloud Microphysical Properties Retrieved From Ground Based Active and Passive Remote Sensing. *8th Conference on Polar Meteorology and Oceanography.* January 2005

[40] Zhien, Wang, and Sassen, K. Cirrus Cloud Microphysical Property Retrieval Using Lidar and Radar Measurements. Part I: Algorithm Description and Comparison with In Situ Data. *Journal of Applied Meteorology.* March 2002 Vol. 41. Pg. 218-229.

[41] Müller, D., Wandinger, U. and Ansmann, A. Microphysical Particle Parameters from Extinction and Backscatter Lidar Data by Inversion with Regularization: Theory. *Applied Optics.* Vol. 38, No. 12. April 1999.

[42] Dong, X., and Mace, G., Profiles of Low-Level Stratus Cloud Microphysics Deduced from Ground-Based Measurements. *Journal of Atmospheric and Oceanic Technology*. Vol. 20 June 2002.

[43] Wielicki, D. Climate Model Test Discussion An Observation Perspective. *CERES Science Team Meeting NCAR*, March 2004.

[44] May, P., Jakob, C., and Mather, J. Tropical Warm Pool International Cloud Experiment (TWP-ICE): Cloud and Rain Characteristics in the Australian Monsoon. DOE/ER/ARM-0401 May 2004.

[45] Ackerman, T., Mace, K., Moran, P., Marchand, R., Miller, M., and Martner, B., 2000: Objective determination of cloud heights and radar reflectivities using a combination of active remote sensors at the ARM CART sites. *J. Appl. Meteor.*, **39,** 645–665.

[46] Miloshevich, LM, et al. 2009. "Accuracy assessment and correction of Vaisala RS92 radiosonde water vapor measurements." *Journal of Geophysical Research* 114: D11305, doi:10.1029/2008JD011565.2009.

[47] Troyan, D. 2011. Sonde Adjust Value-Added Product Technical Report. U.S. Department of Energy. DOE/SC-ARM-TR-102.

http://www.arm.gov/publications/tech_reports/doe-sc-arm-tr-102.pdf.

[48] Wang, DY, et al. 2005. "Validation of stratospheric temperatures measured by Michelson Interferometer for Passive Atmospheric Sounding (MIPAS) on Envisat." *Journal of Geophysical Research* 110(D8): D08301.

[49] Clough , SA , and coauthors. 2005. "Atmospheric radiative transfer modeling: a summary of the AER codes, short communication." *Journal of Quantitative Spectroscopy & Radiative Transfer*, 91 , 233-244.

[50] Grant, EH, J Buchanan, and HF Cook. 1957. "Dielectric behavior of water at microwave frequencies." *Journal of Chemical Physics*, 26, 641-651.

[51] Liebe, HJ, and DH Layton. 1987. "Millimeter-wave properties of the atmosphere: Laboratory studies and propagation modeling." *National Telecommunications Information Administration*, Boulder, CO, NTIA Rep.87-24.

[52] Liebe, HJ, GA Hufford, and T Manabe. 1991. "A model for the complex permittivity of water at frequencies below 1 THz." *International Journal of Infrared Millimeter Waves*, 12, 659-675.

[53] Liljegren, JC, and BM Lesht. 1996. "Measurements of integrated water vapor and

cloud liquid water from microwave radiometers at the DOE ARM cloud and radiation testbed in the U.S. Southern Great Plains." *Proceedings of the International Geoscience and Remote Sensing Symposium (IGARSS)*, Lincoln , NE , 1675-1677.

[54] Liljegren, JC, and coauthors. 2001. "A new retrieval for cloud liquid water path using a ground-based microwave radiometer and measurements of cloud temperature." *Journal of Geophysical Research*, 106, 14485-14500.

[55] Marchand, R, and coauthors. 2003. "An assessment of microwave absorption models and retrievals of cloud liquid water using clear-sky data." *Journal of Geophysical Research*, 108, 4773, doi:10.1029/2003JD003843.

[56] Rosenkranz, PW. 1998. "Water vapor microwave continuum absorption: A comparison of measurements and models." *Radio Science*. 33, 919-928

[57] Turner, DD, and KL Gaustad. 2004. "Improved PWV and LWP Retrievals from the Microwave Radiometer for ARM." *Proceedings of the Fourteenth, Atomspheric Radiation Measurement Science (ARM) Team Meeting*. U.S. Department of Energy, Richland, Washington.

[58] Van Meijgaard, E, and S Crewell. 2005. "Comparison of model predicted liquid water path with ground-based measurements during CLIWA-NET." *Journal of Atmospheric Research*. 75, 201-226.

[59] Westwater, ER, and coauthors. 2001. "Analysis of integrated cloud liquid and precipitable water vapor retrievals from microwave radiometers during the Surface Heat Budget of the Arctic Ocean Project." *Journal of Geophysical Research*, 106, 32019-32030.

[60] Acquista, C., "Light scattering by tenuous particles: a generalization of the Rayleigh-Gans-Rocard approach," *Applied Optics*, Vol. 15, 2932–2936, 1976

[61] Wang, Z., Sassen, K., Whiteman, D., and Demoz, B., "The Analysis of Multi Year Low Level and Midlevel Mixed Phase Clouds Observed at the North Slope of Alaska Cloud and Radiation Testbed" *Fifteenth ARM Science Team Meeting Proceedings*, Dayton Beach, Fl. March 14-18, 2005.

[62] Mace, G., Ackerman, T., Minnis, P., and Young, D., "Cirrus Layer Microphysical Properties Derived from Surface-Based Millimeter Radar and Infrared Interferometer Data." *Journal of Geophysical Research, Vol. 103, No. D18, September 27, 1998.*

[63] Bishop, C. M. Neural Networks for Pattern Recognition, Oxford University Press, 1995.

[64] Gurney, K. An Introduction to Neural Networks, CRC Press, 1997.

[65] Clothiaux, E., Ackerman, E., Thomas, P. "Objective Determination of Cloud Heights and Radar Reflectivities Using a Combination of Active Remo", Journal of Applied Meteorology, May 2000 Issue

[66] Van Diedenhoven., B "An evaluation of ice formation in large-eddy simulations of supercooled Arctic stratocumulus using ground-based lidar and cloud radar", Journal of Geophysical Research, 2007.

[67] Hajime Okamoto. "Vertical cloud structure observed from shipborne radar and lidar: Midlatitude case study during the MR01/K02 cruise of the research vessel Mirai", Journal of Geophysical Research 2007.

[68] Green, P. D., S. M. Newman, R. J. Beeby, J. E. Murray, J. C. Pickering, and J. E. Harries."Recent advances in measurement of the water vapour continuum in the far-infrared spectral region", Philosophical Transactions of The Royal Society A Mathematical Physical and Engineering Sciences 2012

[69] Hugh Morrison. "Sensitivity of modeled arctic mixed-phase stratocumulus to cloud condensation and ice nuclei over regionally varying surface conditions", Journal of Geophysical Research,

[70] Isaac Moradi. "Comparing upper tropospheric humidity data from microwave satellite instruments and tropical radiosondes", Journal of Geophysical Research, 2010.

[71] Min Deng. "Cirrus cloud microphysical properties and air motion statistics using cloud radar Doppler moments: Water content, particle size, and sedimentation relationships", Geophysical Research Letters, 2008

[72] McFarlane, S. "Effect of clouds on the calculated vertical distribution of shortwave absorption in the tropics", Journal of Geophysical Research, 2008.

[73] Chandrasekar, V. "Potential Role Of Dual- Polarization Radar In The Validation Of Satellite Precipitation Measurements: Rationale and Opportunities", Bulletin of the American Meteorological Society, 2008

[74] Toshiro, Inoue. "Comparison of high-level clouds represented in a global cloud system–resolving model with CALIPSO/CloudSat and geostationary satellite observations", Journal of Geophysical Research, 2010.

[75] Shaocheng, Xie. "CLOUDS AND MORE: ARM Climate Modeling Best Estimate Data : A New Data Product for Climate Studies", Bulletin of the American Meteorological Society, 2010.

[76] Bourdages, L. "Physical properties of High Arctic tropospheric particles during winter",Atmospheric Chemistry and Physics Discussions, 2009

[77] Hajime, Okamoto. "An algorithm for retrieval of cloud microphysics using 95-GHz cloud radar and lidar", Journal of Geophysical Research, 2003

[78] Mace, G. "Cloud radiative forcing at the Atmospheric Radiation Measurement Program Climate Research Facility: 1. Technique, validation, and comparison to satellite-derived diagnostic quantities", Journal of Geophysical Research, 2006

[79] Chidong Zhang. "Bimodality in tropical water vapour", Quarterly Journal of the Royal Meteorological Society, 2003

[80] Madonna, F. "CIAO: the CNR-IMAA advanced observatory for atmospheric research", Atmospheric Measurement Techniques Discussions, 2010

[81] Hennemuth, B. "Quality assessment of water cycle parameters in REMO by Radar-Lidar synergy", Atmospheric Chemistry and Physics Discussions, 2007

[82] Delanoë, J. "A variational scheme for retrieving ice cloud properties from combined radar, lidar, and infrared radiometer", Journal of Geophysical Research, 2008

[83] Mather, J. "Cloud properties and associated radiative heating rates in the tropical western Pacific", Journal of Geophysical Research, 2007

[84] Doran, J. "A comparison of cloud properties at a coastal and inland site at the North Slope of Alaska", Journal of Geophysical Research, 2002

[85] Lawrence D. Carey. "Lightning location relative to storm structure in a leading-line, trailing stratiform mesoscale convective system", Journal of Geophysical Research, 2005

[86] Neel, M. "Predicative Data Mining and Discoveries Hidden Values of Data Warehouse"., ARPN Journal of Systems and Software 2010.

[87] Tsang, L., Kong, J., and Ding, K. Scattering of Electromagnetic Waves Theories: and Application. Wiley Series in Remote Sensing. Wiley-Interscience Publication. John Wiley and Sons., Inc. New York. 2000.

[88] Tsang, L., Kong, J., Ding, K. and Ao, C., Scattering of Electromagnetic Waves: Numerical Solutions Wiley Series in Remote Sensing. Wiley Interscience Publication. John Wiley and Sons., Inc. New York. 2001.

[89] Ulaby, F. and Dobson, M. Handbook of Radar Scattering Statistics for Terrain Artech House, Inc. Norwood, MA. 1989.

[90] Gibson, W. The Method of Moments in Electromagnetics. Chapman and Hall/CRC Publishers; 1st Edition November 2007.

[91] Balanis, C. Advanced Engineering Electromagnetics. John Wiley & Sons. 1989.

[92] Kong, J. Electromagnetic Wave Theory. Wiley-Interscience. 2nd Edition October 1990.

[93] Ruck, G., Barrick, D., Stuart, W., and Krichbaum, C. The Radar Cross Section Handbook 1970

[94] Furutsu, K., "On the theory of radio wave propagation over inhomogeneous earth," *J. Research, National Bureau of Standards, Radio Propagation*, vol. 67D, Jan–Feb 1963.

[95] Levy, M., Parabolic Equation Methods for Electromagnetic Wave Propagation, ser. *IEE electromagnetic waves series 45*, 2000.

[96] Tzaras, C. and Saunders, S. "An improved heuristic UTD solution or multiple-edge transition zone diffraction," *IEEE Trans. Antennas Propag*., vol. 49, pp. 1678–1682, Dec. 2001.

[97] Holms, P., "A new heuristic diffraction coefficient for non-perfectly conducting wedges," *IEEE Trans. Antennas Propag*., vol. 48, no. 8, pp. 1211–1219, Aug. 2000.

[98] Luebbers, R., "A heuristic UTD slope diffraction coefficient for rough lossy wedges," *IEEE Trans. Antennas Propag*., vol. 37, no. 2, pp. 206–211, Feb. 1989.

[99] El-Sallabi, H., Rekanos, I., and Vainikanen, P., "A new heuristic diffraction coefficient for lossy dielectric wedges at normal incidence," *IEEE Antennas Wireless Propag. Lett.*, vol. 1, pp. 165–168, 2002.

[100] Holms, P., "UTD diffraction coefficients for higher order wedge diffracted fields," *IEEE Trans. Antennas Propag*., vol. 44, no. 6, pp. 879–888, Jun. 1996.

[101] Srikanth, S., Pathak, P., Chuang, C. "Hybrid UTD-MM Analysis of Scattering by a Perfectly Conducting Semiconductor Cylinder" *IEEE Antennas and Propag*. Vol. AP-34 No. 10, pp. 1250-1257.

[102] Tseng, C., Hsien-Kwei, H., Tsung-Ying, C., "A Discrete-Time Uniform Geometrical Theory of Diffraction for the Fast Transient Analysis of Scattering from Curved Wedges", *IEEE Transactions on Antennas and Propagation* Volume 53, Issue 11, Nov. 2005, pp. 3633 – 3643.

[103] Tokgoz, C.; Marhefka, R.J.; "A UTD based asymptotic solution for the surface magnetic field on a source excited circular cylinder with an impedance boundary

condition." *IEEE Transactions on Antennas and Propagation*,Volume 54, Issue 6, June 2006 Page(s):1750 – 1757

[104] Durden, S.; Van Zyl, J.; Zebker, H. "Modeling and Observation of Radar Polarization Signature of Forested Areas". *IEEE Transactions on Geosciences and Remote Sensing Volume*. 27. No.3 May 1989.

[105] Keller, J. "One hundred years of diffraction theory" *IEEE Transactions on Antennas and Propagation, [legacy, pre - 1988]* Volume 33, Issue 2, Feb 1985 Page(s):123 – 126

[106] Stratis, G.; Anantha, V.; Taflove, A.; "Numerical calculation of diffraction coefficients of generic conducting and dielectric wedges using FDTD", *IEEE Transactions on Antennas and Propagation* Volume 45, Issue 10, Oct. 1997 Page(s):1525 – 1529

[107] Tzoulis, A.; Eibert, T.F.; "A hybrid FEBI-MLFMM-UTD method for numerical solutions of electromagnetic problems including arbitrarily shaped and electrically large objects" *IEEE Transactions on Antennas and Propagation*, Volume 53, Issue 10, Oct. 2005 Page(s):3358 – 3366

[108] Ellingson, S.W.; Gupta, I.J.; Burnside, W.D.; "Analysis of blended rolled edge reflectors using numerical UTD" *IEEE Transactions on Antennas and Propagation*, Volume 38, Issue 12, Dec. 1990 Page(s):1969 – 1971

[109] Roturier, B.; Souny, B.; "Numerical UTD diffraction coefficients with hybrid topologic method" *Antennas and Propagation Society International Symposium*, 1996. AP-S.Digest Volume 1, 21-26 July 1996 Page(s):660 - 663 vol.1

[110] www.deepseawaters.com

[111] Liao, L., and K. Sassen, 1994: Investigation of relationships between K_-band radar reflectivity and ice and liquid water content. *Atmos. Res.,* **34,** 299–313.